University of Glasgow
DEPARTMENT OF
AEROSPACE
ENGINEERING

Development of a Generic Helicopter Mathematical Model for Application to Inverse Simulation

Dr Douglas G. Thomson*

Internal Report No. 9216
June 1992

Development of a Generic Helicopter Mathematical Model for Application to Inverse Simulation

Dr Douglas G. Thomson*

Internal Report No. 9216
June 1992

*Royal Society University Research Fellow

Department of Aerospace Engineering
University of Glasgow
Glasgow
G12 8QQ

Summary

This paper describes the development of a non-linear, generic mathematical model of a single main and tail rotor helicopter suitable for use in an inverse simulation. Multiblade representations of the main and tail rotors are used, each blade being assumed rigid and to have constant chord and profile. The flow around the blades is assumed to be steady and incompressible allowing two-dimensional aerodynamic theory to be applied in calculating the blade aerodynamic loads. Main rotor flapping is modelled by use of a centre-spring representation of the rotor disc. The fuselage, tailplane and fin aerodynamic forces and moments from were obtained from "look-up" tables supplied by the Defence Research Agency (Bedford). The rotor model was derived using the computer algebra package, Mathematica that has allowed many of the terms normally disregarded for simplicity, to be retained. The derivation of the rotor model is dealt with in detail. Results are given for vehicle trim calculations and non-linear time responses to control input as well as some inverse simulations.

Contents

Nomenclature

a	translational acceleration	(m/s^2)
a_{H_x}, a_{H_y}, a_{H_z}	components of main rotor hub acceleration	(m/s^2)
$a_{x_{bl}}$, $a_{y_{bl}}$, $a_{z_{bl}}$	acceleration components of a main rotor blade element	(m/s^2)
a_0	main rotor blade lift curve slope	(/rad)
$a_{0_{TR}}$	tail rotor blade lift curve slope	(/rad)
b	number of blades in main rotor	
c	main rotor blade chord	(m)
C	force or moment coefficient	
c_{TR}	tail rotor blade chord	(m)
d	drag of blade element per unit span	(N/m)
e	length of main rotor blade root cut out as a fraction of total span	
e_{TR}	length of tail rotor blade root cut out as a fraction of total span	
$F_{P_{bl}}$	force on blade element per unit span	(N/m)
$f_{y_{bl}}$, $f_{z_{bl}}$	components of aerodynamic force per unit span on a blade element	(N/m)
g	acceleration due to gravity	(m/s^2)
h	height of obstacle in pop-up manoeuvre	
h_{Fin}	height of fin above centre of gravity	(m)
h_R	height of rotor hub above centre of gravity	(m)
h_{TP}	height of tailplane above centre of gravity	(m)
h_{TR}	height of tail rotor hub above centre of gravity	(m)
I_R	inertia of main rotor	$(kg\ m^2)$
I_{tr}	effective inertia of transmission and gearing	$(kg\ m^2)$
I_{xx}, I_{yy}, I_{zz}	helicopter moments of inertia about centre of gravity	$(kg\ m^2)$
I_{xz}	helicopter product of inertia about centre of gravity	$(kg\ m^2)$
I_β	blade moment of inertia about centre of rotation	$(kg\ m^2)$
K_3	overall gain of engine/rotorspeed governer	(Nm/rad/s)
K_β	flapping stiffness of blade	(Nm/rad)
l	lift of blade element per unit span	(N/m)
l_{Fin}	distance of fin behind fuselage reference point	(m)
l_{TP}	distance of tailplane behind fuselage reference point	(m)
l_{TR}	distance of tail rotor hub behind fuselage reference point	(m)
l_1, ..., n_3	direction cosines for Euler transformation	
L, M, N	components of external moments on vehicle	(Nm)
m	helicopter mass	(kg)
m_b	mass of main rotor blade	(kg)
m_0	blade mass per unit span	(kg/m)
$M_{P_{bl}}$	moment on blade element per unit span	(N)

$M_{Flap_{bl}}$	flapping moment of single blade	(Nm)
$M_{Hub_{bl}}$	total hub moment due to a single blade	(Nm)
M_β	blade mass distribution	(kg m)
n_β	rotor stiffness number	
p, q, r	components of helicopter angular velocity at centre of gravity	(rad/s)
p_H, q_H, r_H	angular velocity components of main rotor hub axes set	(rad/s)
$\bar{p}_H$, $\bar{q}_H$	normalised hub axes angular velocity components ($\bar{p}_H = p_H/\Omega$, etc.)	
Q	torque	(Nm)
r	position vector	(m)
r_b	distance of blade element from centre of rotor	(m)
$\bar{r}_b$	normalised position of blade element ($\bar{r}_b = (r_b - eR)/R$)	
R	total span of main rotor blade	(m)
R_{TR}	total span of tail rotor blade	(m)
s	main rotor solidity	
s_{TR}	tail rotor solidity	
S_{Fin}	area of fin surface	(m^2)
S_{TP}	area of tailplane surface	(m^2)
u, v, w	translational velocity components of helicopter centre of gravity	(m/s)
u_H, v_H, w_H	components of main rotor hub velocity	(m/s)
U_T, U_P	tangential and normal components of airflow at blade element	(m/s)
$\bar{U}_T$,$\bar{U}_P$	normalised velocity components ($\bar{U}_T = U_T/\Omega R$, etc.)	
v_i	induced velocity of flow at main rotor	(m/s)
v_0	uniform component of induced velocity at main rotor	(m/s)
$v1_c$, $v1_s$	harmonic components of induced velocity at main rotor	(m/s)
$v0_{TR}$	uniform component of induced velocity at tail rotor	(m/s)
$v1_{cTR}$, $v1_{sTR}$	harmonic components of induced velocity at tail rotor	(m/s)
V_f	helicopter flight velocity	(m/s)
$V_{x_{bl}}$, $V_{y_{bl}}$, $V_{z_{bl}}$	velocity components of a main rotor blade element	(m/s)
X, Y, Z	components of external force on vehicle	(N)
x_{cg}	position of rotor hub behind centre of gravity	(m)

Greek Symbols

α	angular acceleration of an axes set	(rad/s^2)
α_{bl}	angle of incidence of blade element	(rad)
α_{Fus}	angle of incidence the fuselage	(rad)
α_T	fixed angle of incidence the tailplane	(rad)

α_{TP}	angle of incidence the tailplane	(rad)
β	main rotor blade flapping angle	(rad)
β'	derivative of flapping angle w.r.t. blade azimuth position ($d\beta/d\psi$)	
β_{Fus}	angle of sideslip the fuselage	(rad)
β_F	fixed sideslip angle of the fin	(rad)
β_{Fin}	angle of sideslip the fin	(rad)
β_0	rotor coning angle	(rad)
β_{1_c}, β_{1_s}	rotor longitudinal and lateral flapping angles	(rad)
γ_s	forward tilt of main rotor shaft	(rad)
δ	blade profile drag coefficient	
η_x, η_y, η_z	normalised rotor hub acceleration ($\eta_x = a_{H_x}/\Omega^2 R$, etc.)	
θ	blade pitch angle	(rad)
θ_0	main rotor collective pitch angle	(rad)
θ_{1_s}, θ_{1_c}	main rotor longitudinal and lateral cyclic pitch angles	(rad)
θ_{tw}	main rotor blade twist at tip	(rad)
$\theta_{tw_{TR}}$	tail rotor blade twist at tip	(rad)
λ_0, λ_{1_c}, λ_{1_s}	normalised induced flow components (= $v_0/\Omega R$, etc.)	
λ_β	blade flapping frequency ratio	
μ	normalised in plane rotor hub velocity (= $\sqrt{\mu_x^2 + \mu_y^2}$)	
μ_x, μ_y, μ_z	normalised rotor hub velocities ($\mu_x = u_H/\Omega R$, etc.)	
ρ	density of air	(kg/m^3)
τ_{e_1}, τ_{e_2}, τ_{e_3}	engine and rotorspeed governer time constants	(s)
ϕ, θ, ψ	body roll, pitch and sideslip attitude angles	(rad)
ϕ	angle of attack of the blade element	(rad)
$\dot{\chi}_m$	maximum turn rate in a transient turn manoeuvre	(rad/s)
χ_w	rotor wake angle	(rad)
ψ	azimuth position of main rotor blade	(rad)
ω	angular velocity of an axes set	(rad/s)
ω_x, ω_y, ω_z	components of the angular velocity of a main rotor blade element	(rad/s)
Ω	angular velocity of main rotor	(rad/s)
Ω_i	angular velocity of main rotor at idle	(rad/s)
Ω_{TR}	angular velocity of tail rotor	(rad/s)

Subscripts

A	aerodynamic
b	body fixed axes set
bl	main rotor blade fixed axre set

C	centre of gravity
e	earth fixed axes set
Fin	fin
Fus	fuselage
h	main rotor hub fixed axes set
H	main rotor hub
I	inertial
I, M	individual and multiblade representations of flapping
R	main rotor
s	main rotor shaft fixed axes set
TP	tailplane
TR	tail rotor
tr	transmission
TRH	tail rotor hub
trh	axes set fixed in tail rotor hub
trbl	tail rotor blade fixed axes set
w	hub wind axes set

1. Introduction

The helicopter inverse simulation package, Helinv, which is used to calculate the control inputs necessary to fly a defined manoeuvre, was developed in the period 1983 - 1986 with the initial aim of quantifying agility [1, 2]. An early version of the Royal Aircraft Establishment's Helistab model [3] was used to drive the simulation. At this time Helinv was the only existing helicopter inverse simulation and so much effort was devoted to developing the inverse algorithm [4, 5] and the manoeuvre defining routines [6, 7]. The helicopter model recieved only small upgrades and, although it was kept relatively simple, it still maintained good validity [8, 9]. The model simplicity was important as the vehicle equations of motion were implicit in the numerical algorithm [4] which meant that enhancement of the model necessitated changes to the algorithm, and vice-versa.

More recently it has become apparent that if Helinv is to be applied to problems involving severe manoeuvring flight then a more comprehensive model is required. Further, it is clear that to ease future modification of the new model, and of the Helinv algorthim, it would be of advantage to structure the new model in a modular form. A new model has been created and named Helicopter Generic Simulation (HGS). As a by-product of its development, it has been possible to create a conventional helicopter simulation package containing trim, time response and eigenvalue calculations using the same model. The algorithms used in both the inverse and conventional simulation packages are discussed elsewhere, this report will concentrate on the development of the HGS model, and present some results for both conventional flight mechanics calculations (trim, and response to controls) as well as inverse simulations.

2. An Overview of the Model

The basis of creating any mathematical model is to develop the equations of motion of the system to be simulated. In common with many other aerospace simulations the HGS model adopts the familiar Euler rigid body equations for the fuselage:

$$\dot{u} = -(w\,q - v\,r) + \frac{X}{m} - g\sin\theta \tag{1a}$$

$$\dot{v} = -(u\,r - w\,p) + \frac{Y}{m} + g\cos\theta\sin\phi \tag{1b}$$

$$\dot{w} = -(v\,p - u\,q) + \frac{Z}{m} + g\cos\theta\cos\phi \tag{1c}$$

$$I_{xx}\,\dot{p} = (I_{yy} - I_{zz})\,q\,r + I_{xz}\,(\dot{r} + p\,q) + L \tag{1d}$$

$$I_{yy}\,\dot{q} = (I_{zz} - I_{xx})\,r\,p + I_{xz}\,(r^2 - p^2) + M \qquad (1e)$$

$$I_{zz}\,\dot{r} = (I_{xx} - I_{yy})\,p\,q + I_{xz}\,(\dot{p} - q\,r) + N \qquad (1f)$$

These equations are referred to a body axes set fixed at the centre of gravity of the helicopter so that, referring to Figure 1:

u, v, w	are the vehicle translational velocities referred to the body fixed axes set (x_b, y_b, z_b) and in the directions of the unit vectors $\mathbf{i_b}$, $\mathbf{j_b}$, $\mathbf{k_b}$ respectively,
p, q, r	are the vehicles angular velocities about the body fixed axes set, positive directions being determined by the right hand rule,
m	is the total mass of the helicopter,
I_{xx}, I_{yy}, I_{zz}	are the moments of inertia of the helicopter about the (x_b, y_b, z_b) axes,
I_{xy}	is the product of inertia of the helicopter,
θ, ϕ	are the fuselage pitch and roll attitudes,
X, Y, Z	are the external forces on the helicopter acting at its centre of gravity in the $\mathbf{i_b}$, $\mathbf{j_b}$, $\mathbf{k_b}$ directions respectively,
L, M, N	are the external moments on the helicopter about the body axes (x_b, y_b, z_b).

The rate of change of the attitude angles are related to the body axes angular velocities by the kinematic expressions

$$\dot{\phi} = p + q\sin\phi\tan\theta + r\cos\phi\tan\theta \qquad (2a)$$

$$\dot{\theta} = q\cos\phi - r\sin\phi \qquad (2b)$$

$$\dot{\psi} = q\sin\phi\sec\theta + r\cos\phi\sec\theta \qquad (2c)$$

where ψ is the fuselage heading or azimuth angle. The fuselage attitude is measured relative to an axes set fixed on the ground, earth axes (x_e, y_e, z_e). By transforming the body axes component velocities (u, v, w) into earth axes, via the Euler or attitude angles (ϕ, θ, ψ), Figure 2, the velocities of the helicopter relative the the earth fixed axes set are found to be

$$\begin{bmatrix} \dot{x}_e \\ \dot{y}_e \\ \dot{z}_e \end{bmatrix} = \begin{bmatrix} l_1 & m_1 & n_1 \\ l_2 & m_2 & n_2 \\ l_3 & m_3 & n_3 \end{bmatrix} \begin{bmatrix} u \\ v \\ w \end{bmatrix} \qquad (3)$$

where

$$l_1 = \cos\theta\cos\psi$$

$$l_2 = \cos\theta\sin\psi$$

$$l_3 = -\sin\theta$$

$$m_1 = \sin\phi\sin\theta\cos\psi - \cos\phi\sin\psi$$

$$m_2 = \sin\phi\sin\theta\sin\psi + \cos\phi\cos\psi$$

$$m_3 = \sin\phi \cos\theta$$
$$n_1 = \cos\phi \sin\theta \cos\psi + \cos\phi \sin\psi$$
$$n_2 = \cos\phi \sin\theta \sin\psi - \cos\phi \cos\psi$$
$$n_3 = \cos\phi \cos\theta$$

The position of the helicopter relative to the origin of the earth fixed axes set is obtained by solution of equations (3).

Equations (1 - 3) are of course not unique to the helicopter, they are widely used in many rigid body simulations, and it is in the calculation of the external forces and moments X, Y, Z, L, M, N that the modelling effort is required. The most convenient way of calculating these loads is to split the helicopter into components and derive expressions for their contributions to the overall external force or moment. These expressions will be functions of the fuselage velocities and accelerations, as well as the control positions of the rotors. The relevant components are main rotor (subscript R), tail rotor (TR), fuselage (Fus), tailplane (TP) and fin (Fin), so that the external forces and moments can be expressed in the form :

$$X = X_R + X_{TR} + X_{Fus} + X_{TP} + X_{Fin} \quad (4a)$$
$$Y = Y_R + Y_{TR} + Y_{Fus} + Y_{TP} + Y_{Fin} \quad (4b)$$
$$Z = Z_R + Z_{TR} + Z_{Fus} + Z_{TP} + Z_{Fin} \quad (4c)$$
$$L = L_R + L_{TR} + L_{Fus} + L_{TP} + L_{Fin} \quad (4d)$$
$$M = M_R + M_{TR} + M_{Fus} + M_{TP} + M_{Fin} \quad (4e)$$
$$N = N_R + N_{TR} + N_{Fus} + N_{TP} + N_{Fin} \quad (4f)$$

The methods used to model each component and hence find its contribution to the total external forces and moments are presented in the following sections.

3. The Rotor Model

Due to the complex nature of the flow around the fuselage and empenage of a helicopter, all but the most sophisticated simulations use either simple functions of incidence angles, or look-up tables to find the aerodynamic loads on the fuselage and empenage, (see section 5). Given this fact it becomes clear that the most important factor in creating a helicopter mathematical model is the derivation of the rotor model. Many different type of rotor model have been used in the past but they all adopt the same basic principle to calculate the loads on a rotor blade; both aerodynamic and inertial loads are calculated by integrating the load on an incremental element of the blade, over its whole span. This blade element method is an

extention of simple aerofoil theory to a rotating blade. The velocity of the blade element is expressed as a function of its radial position from the rotor hub, and azimuthal position around the disc. The effective incidence of an element in any position on the disc can then be found, and its aerodynamic loads calculated. Similarly, the acceleration of the blade element can be found, and the inertial load calculated. As the incidence of the blade element is a function of the pitch applied to the blade, and this is varied cyclically around its azimuthal travel, the elemental loads, and hence the total blade load, varies cyclically as it rotates.

The most desirable approach to calculating the rotor loads is to numerically integrate the elemental loads over the span of each blade. This would require an individual blade model where the dynamics and loads of each blade are modelled seperately. Such models are widely used and indeed there are computer systems avaliable which are capable of running them in real time. The Helinv package is implemented on a MicroVax computer and it has been shown by Houston [10] that individual blade rotor models require CPU runtimes of the order of a few hours for basic trim calculations. This implies that for an inverse simulation, such as Helinv, which consists of a series of modified trim calculations, then even for a manoeuvre of short duration, the runtime may extend to days. To ensure managable runtimes it was decided to use a multiblade model as opposed to an individual blade model. Future versions of Helinv will almost certainlly incorporate individual blade models and will be implemented on more powerful computers.

The derivation of a multiblade model requires that the rotor aerodynamic loads should be expressed in closed loop form, and it is then difficult to include any complicated nonlinear aerodynamic effects. This of course is the main advantage of individual blade models where phenomena such as tip Mach effects and retreating blade stall, and configurational aspects such as variable blade geometry or aerofoil sections may be included. Several fundamental assumptions about the blade aerodynamics and geometry therefore have to be made and are now listed. The assumptions about the blade configuration and geometry are summarised as:

i) the blades are assumed to be rigid and of constant chord and aerofoil section,
ii) the blades are centrally hinged with stiffness in flap,
iii) a root cut-out is assumed to extend from the centre of rotation to a distance eR along the span R,
iv) a linear twist variation is incorporated with its slope being θ_{tw}.

The assumptions about the blade aerodynamics are summarised as:

i) Mach number and unsteady aerodynamic effects are not included hence the flow is assumed to be steady and incompressible,
ii) blade stall effects (retreating blade and dynamic) are not modelled,

iii) a constant lift curve slope, a_0, is assumed for the whole blade span so that, considering the above assumptions, 2-d aerodynamic theory can be applied,

iv) the induced velocity is composed of a uniform component over the whole disc with lateral and longitudinal variations over the span and azimuth superimposed, see Appendix 1.

From the above assumptions it is clear that the blade lag dynamics and aeroelastic effects will not be modelled. Again this is a consequence primarily of the choice of a multiblade model; the inclusion of any meaningful aeroelastic effects is only possible with an individual blade model. The inclusion of lag dynamics to the multiblade HGS model is a possible future refinement. The result of making the above assumptions is that the HGS model is in essence similar to the original Helinv model, Helistab, [3]. This proved to be a advantage in verifying the model.

The steps involved in deriving the rotor model are now detailed begining with the calculation of the rotor blade element velocity and acceleration.

3.1 Kinematics of a Blade Element

The equations of motion of the helicopter (1a - 1f) are in terms of the body fixed axes set given by the unit vectors $\mathbf{i_b}$, $\mathbf{j_b}$, $\mathbf{k_b}$. For a general flight state, the velocity and the acceleration of the helicopter's centre of gravity in the body fixed axes set will be given by

$$\mathbf{V_C} = u\,\mathbf{i_b} + v\,\mathbf{j_b} + w\,\mathbf{k_b} \quad \text{and} \quad \mathbf{a_C} = \dot{u}\,\mathbf{i_b} + \dot{v}\,\mathbf{j_b} + \dot{w}\,\mathbf{k_b}$$

and the rotational velocity and acceleration of the body axes set can be expressed as

$$\boldsymbol{\omega_b} = p\,\mathbf{i_b} + q\,\mathbf{j_b} + r\,\mathbf{k_b} \quad \text{and} \quad \boldsymbol{\alpha_b} = \frac{\partial \boldsymbol{\omega_b}}{\partial t} = \dot{p}\,\mathbf{i_b} + \dot{q}\,\mathbf{j_b} + \dot{r}\,\mathbf{k_b}$$

3.1.1 Velocity and Acceleration of the Rotor Hub

The first step in finding the velocity of a the blade element is to determine the velocity of the rotor hub. This is obtained by considering the relative position of the rotor hub (H) with respect to the centre of gravity (C). If it is assumed that the rotor hub lies on the centreline of the helicopter a distance x_{cg} behind the centre of gravity, and a height h_R above it, Figure 3, then its position (with respect to the body axes set) is given by

$$\mathbf{r_{H/C}} = -x_{cg}\,\mathbf{i_b} - h_R\,\mathbf{k_b}$$

(Note that the position directly below the rotor hub on the centre line of the helicopter and at tyhe same height as the centre of gravity wil be taken as the reference point for the positions of other configurational elements. This implies that the model will only be appropriate for c.g. changes fore and aft.) The absolute velocity of the hub, in body axes is then given by

$$\mathbf{V}_{H_b} = \mathbf{V}_C + (\boldsymbol{\omega}_b \times \mathbf{r}_{H/C}) + \frac{d\mathbf{r}_{H/C}}{dt} \tag{5}$$

and evaluating this gives

$$\mathbf{V}_{H_b} = (u - qh_R)\,\mathbf{i}_b + (v + ph_R - rx_{cg})\,\mathbf{j}_b + (w + qx_{cg})\,\mathbf{k}_b \tag{6}$$

The absolute acceleration of the hub in body axes will be given by

$$\mathbf{a}_{H_b} = \mathbf{a}_C + (\boldsymbol{\alpha}_b \times \mathbf{r}_{H/C}) + \boldsymbol{\omega}_b \times (\boldsymbol{\omega}_b \times \mathbf{r}_{H/C}) + 2\,\boldsymbol{\omega}_b \times \frac{d\mathbf{r}_{H/C}}{dt} + \frac{d^2\mathbf{r}_{H/C}}{dt^2} \tag{7}$$

which gives

$$\mathbf{a}_{H_b} = [\dot{u} - (\dot{q} + pr) + (q^2 + r^2)]\,\mathbf{i}_b + [\dot{v} + (\dot{p} - qr) - (\dot{r} + pq)]\,\mathbf{j}_b + [\dot{w} + (p^2 + q^2) + (\dot{q} - pr)]\,\mathbf{k}_b \tag{8}$$

It is probable that the main rotor shaft would be tilted through some angle, the shaft angle, γ_s (taken as positive for a forward tilt), and an axes set (hub axes, subscript h) is placed at the hub with its z-axis pointing down the centre of the shaft. The transformation from body to hub axes, referring to Figure 3, is given by

$$\begin{bmatrix} \mathbf{i}_h \\ \mathbf{j}_h \\ \mathbf{k}_h \end{bmatrix} = \begin{bmatrix} \cos\gamma_s & 0 & \sin\gamma_s \\ 0 & 1 & 0 \\ -\sin\gamma_s & 0 & \cos\gamma_s \end{bmatrix} \begin{bmatrix} \mathbf{i}_b \\ \mathbf{j}_b \\ \mathbf{k}_b \end{bmatrix} \tag{9}$$

and hence the velocity of the hub, in hub axes, is given from (6) and (9) as

$$\mathbf{V}_{H_h} = [(u - qh_R)\cos\gamma_s + (w + qx_{cg})\sin\gamma_s]\,\mathbf{i}_h + (v + ph_R - rx_{cg})\,\mathbf{j}_h + [(w + qx_{cg})\cos\gamma_s - (u - qh_R)\sin\gamma_s]\,\mathbf{k}_h$$

which is rewritten in a simpler form as

$$\mathbf{V}_{H_h} = u_H\,\mathbf{i}_h + v_H\,\mathbf{j}_h + w_H\,\mathbf{k}_h \tag{10}$$

Similarly, from (8) and (9) the acceleration of the hub in hub axes is given by

$$\mathbf{a}_{H_h} = \{[\dot{u} - (\dot{q} + pr) + (q^2 + r^2)]\cos\gamma_s + [\dot{w} + (p^2 + q^2) + (\dot{q} - pr)]\sin\gamma_s\}\,\mathbf{i}_h +$$
$$\{[\dot{v} + (\dot{p} - qr) - (\dot{r} + pq)]\}\,\mathbf{j}_h +$$
$$\{[\dot{w} + (p^2 + q^2) + (\dot{q} - pr)]\cos\gamma_s - [\dot{u} - (\dot{q} + pr) + (q^2 + r^2)]\sin\gamma_s\}\,\mathbf{k}_h$$

which is written in the form

$$\mathbf{a}_{H_h} = a_{H_x}\,\mathbf{i}_h + a_{H_y}\,\mathbf{j}_h + a_{H_z}\,\mathbf{k}_h \qquad (11)$$

Using the transformation (9), the angular velocity and acceleration of the hub axes set are found to be

$$\omega_h = (p\cos\gamma_s + r\sin\gamma_s)\,\mathbf{i}_h + q\,\mathbf{j}_h + (r\cos\gamma_s - p\sin\gamma_s)\,\mathbf{k}_h$$

which, for simplicity can be written in the form

$$\omega_h = p_H\,\mathbf{i}_h + q_H\,\mathbf{j}_h + r_H\,\mathbf{k}_h \qquad (12)$$

and hence

$$\alpha_h = \frac{\partial \omega_h}{\partial t} = (\dot{p}\cos\gamma_s + \dot{r}\sin\gamma_s)\,\mathbf{i}_h + \dot{q}\,\mathbf{j}_h + (\dot{r}\cos\gamma_s - \dot{p}\sin\gamma_s)\,\mathbf{k}_h$$

which is also simplified, and gives

$$\alpha_h = \dot{p}_H\,\mathbf{i}_h + \dot{q}_H\,\mathbf{j}_h + \dot{r}_H\,\mathbf{k}_h \qquad (13)$$

Equations (10) - (13) give the translational velocity and acceleration of the rotor hub (referred to the hub fixed axes set) and the angular velocity and acceleration of the hub axes set. This axes set is fixed in the helicopter and rotates with it. In order to determine the velocity and acceleration of a blade element, which is rotating with respect to the helicopter, and hence with respect to the hub axes set, another axes set is introduced. This is the shaft axes set (denoted by the subscript s) which is fixed in, and rotates with the shaft. Its z-axis points down the shaft and its x-axis along the span of the unflapped blade, as shown in Figure 3. The blade azimuth position is given by the angle ψ measured from aft, as shown in Figure 4. Assuming that the blade is rotating in an anti-clockwise direction when view from above, the transformation from hub to shaft axes will given by

$$\begin{bmatrix} \mathbf{i}_s \\ \mathbf{j}_s \\ \mathbf{k}_s \end{bmatrix} = \begin{bmatrix} -\cos\psi & \sin\psi & 0 \\ -\sin\psi & -\cos\psi & 0 \\ 0 & 0 & 1 \end{bmatrix} \begin{bmatrix} \mathbf{i}_h \\ \mathbf{j}_h \\ \mathbf{k}_h \end{bmatrix} \qquad (14)$$

From (10) and (14) the velocity of the hub in shaft axes is given by

$$\mathbf{V}_{H_s} = (-u_H \cos\psi + v_H \sin\psi)\,\mathbf{i}_s - (u_H \sin\psi + v_H \cos\psi)\,\mathbf{j}_s + w_H\,\mathbf{k}_s \qquad (15)$$

and from (11) and (14) the acceleration of the hub in shaft axes will be

$$\mathbf{a}_{H_s} = (-a_{H_x} \cos\psi + a_{H_y} \sin\psi)\,\mathbf{i}_s - (a_{H_x} \sin\psi + a_{H_y} \cos\psi)\,\mathbf{j}_s + a_{H_z}\,\mathbf{k}_s \qquad (16)$$

The angular velocity of the of the shaft axes set is obtained by first transforming the rotation of the hub axes set to shaft axes, then adding the rotational velocity of the shaft, $-\Omega\mathbf{k}_s$, giving

$$\boldsymbol{\omega}_s = (-p_H \cos\psi + q_H \sin\psi)\,\mathbf{i}_s - (p_H \sin\psi + q_H \cos\psi)\,\mathbf{j}_s + (r_H - \Omega)\,\mathbf{k}_s \qquad (17)$$

3.1.2 Velocity and Acceleration of a Blade Element

In order to calculate the aerodynamic and inertial loads on a blade element it is necessary to express the velocity and acceleration of the element in a local axes set. The blade axes set (denoted by the subscript bl) has its origin at the aerodynamic centre of the element's aerofoil section with its $\mathbf{i}_{bl}$ direction pointing to the blade tip, its $\mathbf{j}_{bl}$ direction from leading edge to trailing edge of the section, and its $\mathbf{k}_{bl}$ direction making up the right handed set, Figure 3. The blade element is positioned a distance r_b along the blade span. The shaft axes set will be aligned with the blade axes set when transformed through the flapping angle β. This transformation is given by

$$\begin{bmatrix} \mathbf{i}_{bl} \\ \mathbf{j}_{bl} \\ \mathbf{k}_{bl} \end{bmatrix} = \begin{bmatrix} \cos\beta & 0 & -\sin\beta \\ 0 & 1 & 0 \\ \sin\beta & 0 & \cos\beta \end{bmatrix} \begin{bmatrix} \mathbf{i}_s \\ \mathbf{j}_s \\ \mathbf{k}_s \end{bmatrix}$$

Assuming the flapping angle to be small gives

$$\begin{bmatrix} \mathbf{i}_{bl} \\ \mathbf{j}_{bl} \\ \mathbf{k}_{bl} \end{bmatrix} = \begin{bmatrix} 1 & 0 & -\beta \\ 0 & 1 & 0 \\ \beta & 0 & 1 \end{bmatrix} \begin{bmatrix} \mathbf{i}_s \\ \mathbf{j}_s \\ \mathbf{k}_s \end{bmatrix} \qquad (18)$$

The velocity of the hub in blade axes is obtained from (15) and (18) :

$$\mathbf{V}_{H_{bl}} = [-u_H \cos\psi + v_H \sin\psi - \beta w_H]\,\mathbf{i}_{bl} + [-u_H \sin\psi - v_H \cos\psi]\,\mathbf{j}_{bl} + [\beta\,(-u_H \cos\psi + v_H \sin\psi) + w_H]\,\mathbf{k}_{bl} \qquad (19)$$

and the acceleration of the hub in blade axes from (16) and (18) :

$$\mathbf{a_{H_{bl}}} = [-a_{H_x}\cos\psi + a_{H_y}\sin\psi - \beta\, a_{H_z}]\,\mathbf{i_{bl}} + [-a_{H_x}\sin\psi - a_{H_y}\cos\psi]\,\mathbf{j_{bl}} + [\beta\,(-a_{H_x}\cos\psi + a_{H_y}\sin\psi) + a_{H_z}]\,\mathbf{k_{bl}} \tag{20}$$

The angular velocity of the blade axes set is found by transforming its shaft axes counterpart to blade axes, then adding the flapping rate $\dot{\beta}\,\mathbf{j_{bl}}$. Hence, from (17) and (18), the angular velocity of the blade axes set is given by

$$\boldsymbol{\omega_{bl}} = [-p_H\cos\psi + q_H\sin\psi - \beta\,(r_H - \Omega)]\,\mathbf{i_{bl}} + [\dot{\beta} - p_H\sin\psi - q_H\cos\psi]\,\mathbf{j_{bl}} + [\beta\,(-p_H\cos\psi + q_H\sin\psi) + (r_H - \Omega)]\,\mathbf{k_{bl}}$$

which, for convenience, can be expressed as

$$\boldsymbol{\omega_{bl}} = \omega_x\,\mathbf{i_{bl}} + \omega_y\,\mathbf{j_{bl}} + \omega_z\,\mathbf{k_{bl}} \tag{21}$$

and by differentiating this with respect to time,

$$\boldsymbol{\alpha_{bl}} = \dot{\omega}_x\,\mathbf{i_{bl}} + \dot{\omega}_y\,\mathbf{j_{bl}} + \dot{\omega}_z\,\mathbf{k_{bl}} \tag{22}$$

where, noting that $\Omega = \dfrac{\partial\psi}{\partial t}$,

$$\dot{\omega}_x = -\dot{p}_H\cos\psi + \dot{q}_H\sin\psi - \dot{\beta}\,(r_H - \Omega) + \Omega\,(p_H\sin\psi + q_H\cos\psi) - \beta\,(\dot{r}_H - \dot{\Omega})$$

$$\dot{\omega}_y = \ddot{\beta} - \dot{p}_H\sin\psi - \dot{q}_H\cos\psi - \Omega\,(p_H\cos\psi - q_H\sin\psi)$$

$$\dot{\omega}_z = \dot{\beta}\,(-p_H\cos\psi + q_H\sin\psi) + (\dot{r}_H - \dot{\Omega}) + \beta\,[\Omega\,(p_H\sin\psi + q_H\cos\psi) - \dot{p}_H\cos\psi + \dot{q}_H\sin\psi]$$

The absolute velocity of a point P a distance r_b from the hub along the span of the blade is given in the local blade axes set by

$$\mathbf{V_{P_{bl}}} = \mathbf{V_{H_{bl}}} + (\boldsymbol{\omega_{bl}} \times \mathbf{r_{P/H}}) + \frac{d\mathbf{r_{P/H}}}{dt}$$

where $\mathbf{r_{P/H}} = r_b\,\mathbf{i_{bl}}$. Hence, using (19) and (21),

$$\mathbf{V_{P_{bl}}} = [-u_H\cos\psi + v_H\sin\psi - \beta w_H]\,\mathbf{i_{bl}} + [-u_H\sin\psi - v_H\cos\psi + r_b\{\beta\,(-p_H\cos\psi + q_H\sin\psi) + (r_H - \Omega)\}]\,\mathbf{j_{bl}} + [\beta\,(-u_H\cos\psi + v_H\sin\psi) + w_H - r_b\{\dot{\beta} - p_H\sin\psi - q_H\cos\psi\}]\,\mathbf{k_{bl}}$$

which can be written more conveniently as

$$\mathbf{V_{P_{bl}}} = V_{x_{bl}}\,\mathbf{i_{bl}} + V_{y_{bl}}\,\mathbf{j_{bl}} + V_{z_{bl}}\,\mathbf{k_{bl}} \qquad (23)$$

The absolute acceleration of the blade element at point P in local blade axes will be given by :

$$\mathbf{a_{P_{bl}}} = \mathbf{a_{H_{bl}}} + (\boldsymbol{\alpha}_{bl} \times \mathbf{r_{P/H}}) + \boldsymbol{\omega}_{bl} \times (\boldsymbol{\omega}_{bl} \times \mathbf{r_{P/H}}) + 2\,\boldsymbol{\omega}_{bl} \times \frac{d\mathbf{r_{P/H}}}{dt} + \frac{d^2\mathbf{r_{P/H}}}{dt^2}$$

Hence, from (20 - 22), :

$$\begin{aligned}\mathbf{a_{P_{bl}}} = {} & [-a_{H_x}\cos\psi + a_{H_y}\sin\psi - \beta\, a_{H_z} - r_b(\omega_y^2 + \omega_z^2)]\,\mathbf{i_{bl}} + \\ & [-a_{H_x}\sin\psi - a_{H_y}\cos\psi + r_b(\dot{\omega}_z + \omega_y\omega_x)]\,\mathbf{j_{bl}} + \\ & [\beta(-a_{H_x}\cos\psi + a_{H_y}\sin\psi) + a_{H_z} + r_b(\omega_x\omega_z - \dot{\omega}_y)]\,\mathbf{k_{bl}}\end{aligned}$$

which is written in the more convenient form

$$\mathbf{a_{P_{bl}}} = a_{x_{bl}}\,\mathbf{i_{bl}} + a_{y_{bl}}\,\mathbf{j_{bl}} + a_{z_{bl}}\,\mathbf{k_{bl}} \qquad (24)$$

The velocity and acceleration of a blade element are now known from equations (23) and (24) respectively, and it is therefore possible to determine the blade loads.

3.2 Calculation of Rotor Forces and Moments

There are two force components acting on the blade element; an aerodynamic force and an inertial force, as indicated in Figure 5. The force per unit span on the blade element at point P on the span can be expressed as

$$\mathbf{F_{P_{bl}}} = -m_0\,a_{x_{bl}}\,\mathbf{i_{bl}} + (f_{y_{bl}} - m_0\,a_{y_{bl}})\,\mathbf{j_{bl}} + (f_{z_{bl}} - m_0\,a_{z_{bl}})\,\mathbf{k_{bl}} \qquad (25)$$

where is the m_0 mass per unit span of the blade, $f_{y_{bl}}$ and $f_{z_{bl}}$ are the aerodynamic force components on the blade element in the $\mathbf{j_{bl}}$ and $\mathbf{k_{bl}}$ directions. In order to find the total force contributions of a single blade this elemental force will be integrated over the whole span. This is most conveniently obtained by looking at the aerodynamic and inertial components individually.

3.2.1 The Rotor Aerodynamic Forces

The aerodynamic components on the blade element are obtained by considering the airflow over the element. The normal and tangential components of the airflow, U_P and U_T are as

indicated in Figure 6, and if the lift and drag forces on the element are denoted by l and d respectively, then the aerodynamic forces on the element are given by

$$f_{z_{bl}} = - l \cos\phi - d \sin\phi \quad (26)$$

$$f_{y_{bl}} = d \cos\phi - l \sin\phi \quad (27)$$

where ϕ is the angle of attack of the element airfoil section and is given by

$$\sin\phi = \frac{U_P}{\sqrt{U_P^2 + U_T^2}}$$

Several assumptions are made here in order to derive a multiblade rotor disc model. Firstly the tangential velocity is assumed to be much greater than the normal velocity ($U_T >> U_P$), and then it is assumed that the angle of attack ϕ is small, so that $l \cos\phi >> d \sin\phi$, and, invoking the usual small angle assumptions, equations (26) and (27) can be simplified to give

$$f_{z_{bl}} = - l \quad (28)$$

$$f_{y_{bl}} = d - l\phi \quad (29)$$

where the angle of attack is now $\phi = U_P/U_T$

The lift force per unit span is calculated using 2-d aerofoil theory, and is given by

$$l = \frac{1}{2} \rho (U_P^2 + U_T^2) c a_0 \alpha_{bl} \quad (30)$$

where ρ is the local air density, c is the blade chord and a_0 is the lift cure slope of the airfoil section (both assumed constant along the span) and α_{bl} is the angle of incidence of the element. The angle of incidence of the blade is the sum of the airflow angle of attack, ϕ and the applied pitch angle, θ.

$$\alpha_{bl} = \theta + U_P/U_T$$

Substituting this into (30) and recalling that $U_T >> U_P$ gives

$$l = \frac{1}{2} \rho c a_0 (U_T^2 \theta + U_P U_T) \quad (31)$$

The drag force per unit span of the blade element is obtained by assuming a profile drag coefficient δ, giving

$$d = \frac{1}{2} \rho c \delta U_T^2 \quad (32)$$

The aerodynamic force in the z blade direction for an element of length dr_b is obtained by substituting (31) into (28) :

$$f_{z_{bl}} = -\frac{1}{2}\rho\, c\, a_0 \,(U_T^2\,\theta + U_P U_T)\, dr_b$$

The aerodynamic force in the y blade direction for an element of length dr_b is obtained by substituting (31) and (32) into (29) :

$$f_{y_{bl}} = \frac{1}{2}\rho\, c\, a_0 \left(\frac{\delta}{a_0} U_T^2 - U_P U_T \theta - U_P^2\right) dr_b$$

To determine the total force from the blade these elemental forces will be integrated over the whole span. This will include a root cut out section of length eR where R is the total span of the blade and e is a fraction ($0 < e < 1$), Figure 7. Hence the total aerodynamic forces from a single blade are given by

$$F_{z_{bl}} = -\frac{1}{2}\rho\, c\, a_0 \int_{eR}^{R} U_T^2\theta + U_T U_P \; dr_b \qquad (33)$$

$$F_{y_{bl}} = \frac{1}{2}\rho\, c\, a_0 \int_{eR}^{R} \frac{\delta}{a_0} U_T^2 - U_T U_P \theta - U_P^2 \; dr_b \qquad (34)$$

These integrals are more conveniently evaluated if normalised by the term $\rho(\Omega R)^2\pi R^2$ to give rotor force coefficients. The rotor force coefficients for a single blade are then given by

$$C_{z_{bl}} = -\frac{1}{2} s\, a_0 \frac{1}{b} \int_0^{1-e} \bar{U}_T^2\theta + \bar{U}_T \bar{U}_P \; d\bar{r}_b \qquad (35)$$

$$C_{y_{bl}} = \frac{1}{2} s\, a_0 \frac{1}{b} \int_0^{1-e} \frac{\delta}{a_0} \bar{U}_T^2 - \bar{U}_T \bar{U}_P \theta - \bar{U}_P^2 \; d\bar{r}_b \qquad (36)$$

where if b is the number of blades then, $s = \dfrac{bc}{\pi R}$ = the rotor solidity.

The other dimensionless parameters are given by :

$$\bar{U}_T = \frac{U_T}{\Omega R}, \quad \bar{U}_P = \frac{U_P}{\Omega R}, \quad \bar{r}_b = \frac{r_b - eR}{R}$$

Before these integrals can be evaluated the normal and tangential components of velocity must be established. Referring to Figure 9,

$$U_T = - V_{y_{bl}} \qquad \text{and} \qquad U_P = V_{z_{bl}} - v_i$$

where v_i is the induced velocity of the flow through the rotor, and $V_{y_{bl}}$ and $V_{z_{bl}}$ are given by equation (23). Hence

$$U_T = u_H \sin\psi + v_H \cos\psi + r_b \{\beta (p_H \cos\psi - q_H \sin\psi) + (\Omega - r_H)\}$$

$$U_P = \beta (-u_H \cos\psi + v_H \sin\psi) + w_H - r_b \{\dot{\beta} - p_H \sin\psi - q_H \cos\psi\} - v_i \qquad (37)$$

The expression for tangential velocity is simplified by noting that main rotor angular velocity Ω is very much greater than the body rotational rates (Ω will be in the region of 30 rad/s whilst the maximum values of body rates may only be in the region of 1 rad/s) so that :

$$\Omega >> \beta (p_H \cos\psi - q_H \sin\psi) - r_H$$

The tangential velocity may then be written

$$U_T = u_H \sin\psi + v_H \cos\psi + r_b \Omega \qquad (38)$$

The induced velocity is given, from Appendix 1, in the form

$$v_i = v_0 + \frac{r_b}{R} (v_{1_s} \sin\psi + v_{1_c} \cos\psi)$$

so that the normal velocity, from (37) becomes

$$U_P = \beta(-u_H \cos\psi + v_H \sin\psi) + w_H - r_b\{\dot{\beta} - p_H \sin\psi - q_H \cos\psi\} - v_0 - \frac{r_b}{R} (v_{1_s} \sin\psi + v_{1_c} \cos\psi) \qquad (39)$$

The blade flapping angle β is written in the form

$$\beta = \beta_0 + \beta_{1_s} \sin\psi + \beta_{1_c} \cos\psi \qquad (40)$$

which, when differentiated with respect to time, gives

$$\dot{\beta} = \dot{\beta}_0 + (\dot{\beta}_{1_s} - \Omega\beta_{1_c}) \sin\psi + (\dot{\beta}_{1_c} + \Omega\beta_{1_s}) \cos\psi \qquad (41)$$

where β_0 = the coning angle
β_{1_c} = the blade longitudinal flapping angle
β_{1_s} = the blade lateral flapping angle

The flap rate can be expressed as a function of blade azimuth position :

$$\beta' = \frac{d\beta}{d\psi} = \frac{dt}{d\psi}\frac{d\beta}{dt} = \frac{\dot{\beta}}{\Omega}$$

so that, from (41),

$$\beta' = \beta'_0 + (\beta'_{1_s} - \beta_{1_c})\sin\psi + (\beta'_{1_c} + \beta_{1_s})\cos\psi \qquad (42)$$

where $$\beta'_0 = \frac{\dot{\beta}_0}{\Omega}, \quad \beta'_{1_s} = \frac{\dot{\beta}_{1_s}}{\Omega}, \quad \beta'_{1_c} = \frac{\dot{\beta}_{1_c}}{\Omega}$$

The normalised blade velocities are therefore given, from (38) and (39), by

$$\bar{U}_T = \mu_x \sin\psi + \mu_y \cos\psi + \bar{r}_b + e \qquad (43)$$

$$\bar{U}_P = (e\alpha_{1_c} - \beta\mu_x)\cos\psi + (e\alpha_{1_s} + \beta\mu_y)\sin\psi + \mu_z - \lambda_0 - e\beta_0' + \bar{r}_b(-\beta_0' + \alpha_{1_c}\cos\psi + \alpha_{1_s}\sin\psi) \qquad (44)$$

where

$$\mu_x = \frac{u_H}{\Omega R}, \quad \mu_y = \frac{v_H}{\Omega R}, \quad \mu_z = \frac{w_H}{\Omega R}$$

$$\alpha_{1c} = \bar{q}_H - \lambda_{1_c} - \beta'_{1_c} - \beta_{1_s} \qquad \alpha_{1s} = \bar{p}_H - \lambda_{1_s} - \beta'_{1_s} + \beta_{1_c}$$

$$\bar{q}_H = \frac{q_H}{\Omega}, \quad \bar{p}_H = \frac{p_H}{\Omega}$$

$$\lambda_0 = \frac{v_0}{\Omega R}, \quad \lambda_{1_c} = \frac{v_{1_c}}{\Omega R}, \quad \lambda_{1_s} = \frac{v_{1_s}}{\Omega R}$$

The blade pitch angle is given by the expression

$$\theta = \theta_0 + \theta_{1_s}\sin\psi + \theta_{1_c}\cos\psi + \frac{r_b}{R}\theta_{tw} \qquad (45)$$

The control inputs are a collective pitch angle, θ_0 which is applied to all of the blades together, longitudinal and lateral cyclic pitch, θ_{1_s} and θ_{1_c}, which vary the pitch of the blade cyclicly as it rotates. Added to this is a linear blade twist variation, the gradient of which is θ_{tw}.

After the blade flapping angle, β, given by (40) is substituted into (44) it is possible to evaluate expressions for the blade aerodynamic coefficients $C_{z_{bl}}$ and $C_{y_{bl}}$ from equations (35) and (36). The integration with respect to $\bar{r}_b$ of the resulting expressions are straight forward as they are simply polynomial functions of $\bar{r}_b$. The difficulty lies in the manipuation of lengthy terms in $\cos\psi$ and $\sin\psi$ and their powers which result from the substitution of the expressions for β, (40) into the blade element velocity expression (44) and pitch angle θ, (45), into (35) and (36). As the aim of this work was to retain as many of the unsteady terms as possible, rather that attempt to simplify the blade velocity terms (43) and (44) any further, it was decided to use the symbolic algebra computer package Mathematica, [11], to do the algebraic manipulation. Mathematica was also used to express the power terms of $\cos\psi$ and $\sin\psi$ as multiple angles. The result of this is that expressions were found which give the total aerodynamic force coefficients (referred to the blade axes set) of a single blade as a function of its azimuth position, ψ, around its 360 degrees of travel.

$$C_{Z_A} = -\frac{1}{2} sa_0 \frac{1}{b} (C_{Z_{A_0}} + C_{Z_{A_{1c}}} \cos\psi + C_{Z_{A_{1s}}} \sin\psi + C_{Z_{A_{2c}}} \cos 2\psi + ...)$$

$$C_{Y_A} = \frac{1}{2} sa_0 \frac{1}{b} (C_{Y_{A_0}} + C_{Y_{A_{1c}}} \cos\psi + C_{Y_{A_{1s}}} \sin\psi + C_{Y_{A_{2c}}} \cos 2\psi + ...)$$

Up to fourth harmonic terms were actually calculated, however, as the blade flap and cyclic pitch variations are only expressed to first harmonic form, it was decided that for consistency the force coefficients should be expressed to the same degree of accuracy.

The force coefficient harmonic components were found to be

$$C_{Z_{A_0}} = -\frac{1}{3}\beta_0'(1 - e^3) + \frac{1}{2}(1 - e^2)(\mu_z - \lambda_0) + \frac{1}{4}(1 - e^2)[\mu_x(\alpha_{1s} - \beta_{1_c}) + \mu_y(\alpha_{1c} + \beta_{1_s})] + \frac{1}{2}(1 - e^2)(\theta_{1_c}\mu_y + \theta_{1_s}\mu_x) + [\frac{1}{3}(1 - e^3) + \frac{1}{2}(1 - e)\mu^2]\theta_0 + [\frac{1}{4}\{1 + \mu^2(1 - e)^2\} - \frac{1}{3}e]\theta_{tw}$$

$$C_{Z_{A_{1c}}} = \frac{1}{3}\alpha_{1c}(1 - e^3) + \mu_y(1 - e)(\mu_z - \lambda_0) - \frac{1}{2}(1 - e^2)(\beta_0'\mu_y + \beta_0\mu_x) - \frac{1}{4}(1 - e)\beta_{1_s}(\mu_x^2 - \mu_y^2) + \frac{1}{2}(1 - e)(\theta_{1_s} - \beta_{1_c})\mu_x\mu_y + [\frac{1}{3}(1 - e^3) + (1 - e)(\frac{1}{4}\mu^2 + \frac{1}{2}\mu_y^2)]\theta_{1_c} + \mu_y(1 - e^2)\theta_0 + \mu_y(\frac{2}{3} - e + \frac{1}{3}e^3)\theta_{tw}$$

$$C_{Z_{A_{1s}}} = \frac{1}{3}\alpha_{1s}(1-e^3) + \mu_x(1-e)(\mu_z-\lambda_0) - \frac{1}{2}(1-e^2)(\beta_0'\mu_x - \beta_0\mu_y) - \frac{1}{4}(1-e)\beta_{1c}(\mu_x^2-\mu_y^2) +$$
$$\frac{1}{2}(1-e)(\theta_{1c}+\beta_{1s})\mu_x\mu_y + [\frac{1}{3}(1-e^3) + (1-e)(\frac{1}{4}\mu^2 + \frac{1}{2}\mu_x^2)]\theta_{1s} + \mu_x(1-e^2)\theta_0 +$$
$$\mu_x(\frac{2}{3} - e + \frac{1}{3}e^3)\theta_{tw}$$

$$C_{Y_{A_{1c}}} = \theta_{1c}\{\frac{1}{3}\beta_0'(1-e^3) - \frac{1}{2}(1-e^2)(\mu_z-\lambda_0) - \frac{1}{8}(1-e^2)[(\alpha_{1s}-3\beta_{1c})\mu_x + (3\alpha_{1c}+\beta_{1s})\mu_y] +$$
$$\frac{1}{2}(1-e)\beta_0\mu_x\mu_y\} +$$
$$\theta_{1s}\{-\frac{1}{8}(1-e^2)[(\alpha_{1c}-\beta_{1s})\mu_x + (\alpha_{1s}+\beta_{1c})\mu_y] + \frac{1}{4}(1-e)\beta_0(\mu_x^2-\mu_y^2)\} +$$
$$\theta_0\{-\frac{1}{3}(1-e^3)\alpha_{1c} + \frac{1}{2}(1-e^2)(\beta_0'\mu_y + \beta_0\mu_x) - \mu_y(1-e)(\mu_z-\lambda_0) +$$
$$\frac{1}{4}(1-e)\beta_{1s}(\mu_x^2-\mu_y^2) + \frac{1}{2}(1-e)\beta_{1c}\mu_x\mu_y\} +$$
$$\theta_{tw}\{-\alpha_{1c}(\frac{1}{4} - \frac{1}{3}e) + \frac{1}{3}(1-\frac{3}{2}e+\frac{1}{2}e^3)(\beta_0'\mu_y + \beta_0\mu_x) - \frac{1}{2}\mu_y(\mu_z-\lambda_0)(1-e)^2 +$$
$$\frac{1}{8}\beta_{1s}(\mu_x^2 - \mu_y^2)(1-e)^2 + \frac{1}{4}\beta_{1c}\mu_x\mu_y(1-e)^2\} +$$
$$\alpha_{1c}[\frac{2}{3}(1-e^3)\beta_0' - (\mu_z-\lambda_0)(1-e^2) + \frac{3}{4}\beta_{1c}\mu_x(1-e^2) - \frac{1}{4}\beta_{1s}\mu_y(1-e^2)] +$$
$$\frac{1}{4}\alpha_{1s}(1-e^2)(\beta_{1s}\mu_x - \beta_{1c}\mu_y) + \beta_0\mu_x[-\beta_0'(1-e^2) + 2(1-e)(\mu_z-\lambda_0) - \frac{3}{2}\beta_{1c}\mu_x(1-e) +$$
$$\beta_{1s}\mu_y(1-e)] - \frac{1}{2}\beta_0\beta_{1c}\mu_y^2(1-e) + \frac{\delta}{a_0}(1-e^2)\mu_y$$

$$C_{Y_{A_{1s}}} = \theta_{1c}\{-\frac{1}{8}(1-e^2)[(\alpha_{1c}-\beta_{1s})\mu_x + (\alpha_{1s}+\beta_{1c})\mu_y] + \frac{1}{4}(1-e)\beta_0(\mu_x^2-\mu_y^2)\} +$$
$$\theta_{1s}\{\frac{1}{3}\beta_0'(1-e^3) - \frac{1}{2}(1-e^2)(\mu_z-\lambda_0) - \frac{1}{8}(1-e^2)[(3\alpha_{1s}-\beta_{1c})\mu_x + (\alpha_{1c}+3\beta_{1s})\mu_y] -$$
$$\frac{1}{2}(1-e)\beta_0\mu_x\mu_y\} +$$
$$\theta_0\{-\frac{1}{3}(1-e^3)\alpha_{1s} + \frac{1}{2}(1-e^2)(\beta_0'\mu_x - \beta_0\mu_y) - \mu_x(1-e)(\mu_z-\lambda_0) + \frac{1}{4}(1-e)\beta_{1c}(\mu_x^2 -$$
$$\mu_y^2) - \frac{1}{2}(1-e)\beta_{1s}\mu_x\mu_y\} +$$
$$\theta_{tw}\{-\alpha_{1s}(\frac{1}{4} - \frac{1}{3}e) + \frac{1}{3}(1-\frac{3}{2}e+\frac{1}{2}e^3)(\beta_0'\mu_x - \beta_0\mu_y) - \frac{1}{2}\mu_x(\mu_z-\lambda_0)(1+2e-e^2) +$$
$$\frac{1}{8}\beta_{1c}(\mu_x^2 - \mu_y^2)(1-e)^2 - \frac{1}{4}\beta_{1s}\mu_x\mu_y(1-e)^2\} +$$
$$\alpha_{1s}[\frac{2}{3}(1-e^3)\beta_0' - (\mu_z-\lambda_0)(1-e^2) - \frac{3}{4}\beta_{1s}\mu_y(1-e^2) + \frac{1}{4}\beta_{1c}\mu_x(1-e^2)] +$$
$$\frac{1}{4}\alpha_{1c}(1-e^2)(\beta_{1s}\mu_x - \beta_{1c}\mu_y) + \beta_0\mu_y[\beta_0'(1-e^2) - 2(1-e)(\mu_z-\lambda_0) - \frac{3}{2}\beta_{1s}\mu_y(1-e) +$$
$$\beta_{1c}\mu_x(1-e)] - \frac{1}{2}\beta_0\beta_{1x}\mu_x^2(1-e) + \frac{\delta}{a_0}(1-e^2)\mu_x$$

It will be shown later that the coefficient $C_{Y_{A_0}}$ is not required.

3.2.2 The Rotor Inertial Forces

From equation (25), the inertial forces of a blade element of length dr_b are given by

$$dX_{I_{bl}} = -m_0\, a_{x_{bl}}\, dr_b \qquad dY_{I_{bl}} = -m_0\, a_{y_{bl}}\, dr_b \qquad dZ_{I_{bl}} = -m_0\, a_{z_{bl}}\, dr_b$$

and to determine the total inertial forces associated with a single blade, these elemental forces are integrated over the whole span for $r_b = eR$ to R. Substituting the blade accelerations given by equation (24) gives

$$X_{I_{bl}} = -\int_{eR}^{R} m_o \left[-a_{H_x}\cos\psi + a_{H_y}\sin\psi - \beta a_{H_z} - r_b\left(\omega_z^2 + \omega_y^2\right)\right] dr_b$$

$$Y_{I_{bl}} = -\int_{eR}^{R} m_o \left[-a_{H_x}\sin\psi - a_{H_y}\cos\psi + r_b\left(\dot{\omega}_z + \omega_x\omega_y\right)\right] dr_b$$

$$Z_{I_{bl}} = -\int_{eR}^{R} m_o \left[\beta\left(-a_{H_x}\cos\psi + a_{H_y}\sin\psi\right) + a_{H_z} + r_b\left(\omega_x\omega_z - \dot{\omega}_y\right)\right] dr_b$$

which can be rewritten as

$$X_{I_{bl}} = \left(a_{H_x}\cos\psi - a_{H_y}\sin\psi + \beta\, a_{H_z}\right) m_b + \left(\omega_y{}^2 + \omega_z{}^2\right) M_\beta$$

$$Y_{I_{bl}} = \left(a_{H_x}\sin\psi + a_{H_y}\cos\psi\right) m_b - \left(\dot{\omega}_z + \omega_y\omega_z\right) M_\beta$$

$$Z_{I_{bl}} = \left[\beta\left(a_{H_x}\cos\psi - a_{H_y}\sin\psi\right) - a_{H_z}\right] m_b - \left(\omega_x\omega_z - \dot{\omega}_y\right) M_\beta$$

where m_b = the blade mass $= \int_{eR}^{R} m_o\, dr_b$

M_β = the blade moment of mass $= \int_{eR}^{R} m_o\, r_b\, dr_b$

These forces are normalised, as with the aerodynamic forces, by division by $\rho(\Omega R)^2\pi R^2$ to give

$$C_{X_I} = \left(\eta_x\cos\psi - \eta_y\sin\psi + \beta\,\eta_z\right)\bar{m}_b + \bar{M}_\beta\left(\omega_y{}^2 + \omega_z{}^2\right)/\Omega^2 \qquad (46a)$$

$$C_{Y_I} = \left(\eta_x\sin\psi + \eta_y\cos\psi\right)\bar{m}_b - \bar{M}_\beta\left(\dot{\omega}_z + \omega_y\omega_x\right)/\Omega^2 \qquad (46b)$$

$$C_{Z_I} = \left[\beta\left(\eta_x\cos\psi - \eta_y\sin\psi\right) - \eta_z\right]\bar{m}_b - \bar{M}_\beta\left(\omega_x\omega_z - \dot{\omega}_y\right)/\Omega^2 \qquad (46c)$$

where $\eta_x = \dfrac{a_{H_x}}{\Omega^2 R}$, $\eta_y = \dfrac{a_{H_y}}{\Omega^2 R}$, $\eta_z = \dfrac{a_{H_z}}{\Omega^2 R}$

and $$\bar{m}_b = \frac{m_b}{\rho\pi R^3}, \qquad \bar{M}_\beta = \frac{M_\beta}{\rho\pi R^4}$$

Assuming that the angular velocity of the rotor is much greater than any of the rotational velocities of the hub frame, the blade axes component angular velocities are given from (21) by

$$\omega_x = -p_H \cos\psi + q_H \sin\psi + \beta\Omega \tag{47a}$$

$$\omega_y = \dot{\beta} - p_H \sin\psi - q_H \cos\psi \tag{47b}$$

$$\omega_z = -\Omega \tag{47c}$$

so that

$$\dot{\omega}_y = \ddot{\beta} - (\dot{p}_H - \Omega q_H) \sin\psi - (\dot{q}_H + \Omega p_H) \cos\psi \tag{48a}$$

$$\dot{\omega}_z = -\dot{\Omega} \tag{48b}$$

Differentiation of equation (41) with respect to time gives

$$\ddot{\beta} = \ddot{\beta}_0 + (\ddot{\beta}_{1_c} + \dot{\Omega}\beta_{1_s} + 2\Omega\dot{\beta}_{1_s} - \Omega^2\beta_{1_c}) \cos\psi + (\ddot{\beta}_{1_s} - \dot{\Omega}\beta_{1_c} - 2\Omega\dot{\beta}_{1_c} - \Omega^2\beta_{1_s}) \sin\psi$$

This is substituted into equation (48a), whilst equation (40) for β is substituted into (47a), and that for its time derivative, (41), is substituted into (47b). Equations (47) and (48) are then substituted into equations (46). The resulting expressions contain terms with products and powers of $\sin\psi$ and $\cos\psi$ which are converted to multiple angles, as with the aerodynamic coefficients. Listing first harmonic terms only (for consistency), the blade inertial force coefficients are found to be

$$C_{X_I} = C_{X_{I_0}} + C_{X_{I_{1c}}} \cos\psi + C_{X_{I_{1s}}} \sin\psi \tag{49a}$$

$$C_{Y_I} = C_{Y_{I_0}} + C_{Y_{I_{1c}}} \cos\psi + C_{Y_{I_{1s}}} \sin\psi \tag{49b}$$

$$C_{Z_I} = C_{Z_{I_0}} + C_{Z_{I_{1c}}} \cos\psi + C_{Z_{I_{1s}}} \sin\psi \tag{49c}$$

where

$$C_{X_{I_0}} = \eta_z \beta_0 \bar{m}_b + \bar{M}_\beta \left[1 + \beta_0'^2 + \tfrac{1}{2}(\varepsilon_{1_s}^2 + \varepsilon_{1_c}^2)\right]$$

$$C_{X_{I_{1c}}} = (\eta_x + \eta_z \beta_{1_c}) \bar{m}_b + 2\beta_0' \varepsilon_{1_c} \bar{M}_\beta$$

$$C_{X_{I_{1s}}} = -(\eta_y - \eta_z \beta_{1_s}) \bar{m}_b + 2\beta_0' \varepsilon_{1_s} \bar{M}_\beta$$

$$C_{Y_{I_0}} = -\bar{M}_\beta \left[\beta_0 \beta_0' - \frac{\dot{\Omega}}{\Omega^2} + \tfrac{1}{2}\varepsilon_{1_c}(\beta_{1_c} - \bar{p}_H) + \tfrac{1}{2}\varepsilon_{1_s}(\beta_{1_s} + \bar{q}_H)\right]$$

$$C_{Y_{I_{1c}}} = \eta_y \bar{m}_b - \bar{M}_\beta \left[\beta_0 \varepsilon_{1_c} + \beta_0' (\beta_{1_c} - \bar{p}_H)\right]$$

$$C_{Y_{I_{1s}}} = \eta_x \bar{m}_b - \bar{M}_\beta \left[\beta_0 \varepsilon_{1_s} + \beta_0' (\beta_{1_s} + \bar{q}_H)\right]$$

$$C_{Z_{I_0}} = -[\eta_z + \tfrac{1}{2}(\eta_y \beta_{1_s} - \eta_x \beta_{1_c})]\,\bar{m}_b + \bar{M}_\beta\,(\beta_0 + \beta_0'')$$

$$C_{Z_{I_{1c}}} = \eta_x\,\beta_0\,\bar{m}_b + \bar{M}_\beta\,(\gamma_{1_c} + \beta_{1_c} - \bar{p}_H)$$

$$C_{Z_{I_{1s}}} = -\eta_y\,\beta_0\,\bar{m}_b + \bar{M}_\beta\,(\gamma_{1_s} + \beta_{1_s} + \bar{q}_H)$$

and $$\varepsilon_{1c} = \beta'_{1c} + \beta_{1_s} - \bar{q}_H, \qquad \varepsilon_{1s} = \beta'_{1\,s} - \beta_{1_c} - \bar{p}_H$$

$$\gamma_{1c} = \beta''_{1c} + \frac{\dot{\Omega}}{\Omega^2}\beta_{1_s} + 2\beta'_{1_s} - \beta_{1_c} - \frac{\dot{q}_H}{\Omega^2} - \bar{p}_H, \qquad \gamma_{1s} = \beta''_{1s} - \frac{\dot{\Omega}}{\Omega^2}\beta_{1_c} - 2\beta'_{1c} - \beta_{1_s} - \frac{\dot{p}_H}{\Omega^2} + \bar{q}_H$$

with $$\beta_0'' = \frac{\ddot{\beta}_0}{\Omega^2}, \quad \beta''_{1_s} = \frac{\ddot{\beta}_{1_s}}{\Omega^2}, \quad \beta''_{1c} = \frac{\ddot{\beta}_{1c}}{\Omega^2}$$

3.2.3 Total Rotor Forces

The coefficient of the total rotor force, aerodynamic plus inertial, can be expressed in blade axes as

$$\mathbf{C_{F_{bl}}} = C_{X_{bl}}\,\mathbf{i_{bl}} + C_{Y_{bl}}\,\mathbf{j_{bl}} + C_{Z_{bl}}\,\mathbf{k_{bl}} \qquad (50)$$

where $C_{Z_{bl}} = C_{Z_I} + C_{Z_A}$ etc, giving component coefficients of the form :

$$C_{X_{bl}} = C_{X_0} + C_{X_{1c}}\cos\psi + C_{X_{1s}}\sin\psi$$

$$C_{Y_{bl}} = C_{Y_0} + C_{Y_{1c}}\cos\psi + C_{Y_{1s}}\sin\psi$$

$$C_{Z_{bl}} = C_{Z_0} + C_{Z_{1c}}\cos\psi + C_{Z_{1s}}\sin\psi$$

which are made up of aerodynamic and inertial contributions :

$$C_{X_0} = C_{X_{I_0}}, \qquad C_{X_{1c}} = C_{X_{I_{1c}}}, \qquad C_{X_{1s}} = C_{X_{I_{1s}}}$$

$$C_{Y_0} = \frac{sa_0}{2b}C_{Y_{A_0}} + C_{Y_{I_0}}, \quad C_{Y_{1c}} = \frac{sa_0}{2b}C_{Y_{A_{1c}}} + C_{Y_{I_{1c}}}, \quad C_{Y_{1s}} = \frac{sa_0}{2b}C_{Y_{A_{1s}}} + C_{Y_{I_{1s}}}$$

$$C_{Z_0} = -\frac{sa_0}{2b}C_{Z_{A_0}} + C_{Z_{I_0}}, \quad C_{Z_{1c}} = -\frac{sa_0}{2b}C_{Z_{A_{1c}}} + C_{Z_{I_{1c}}}, \quad C_{Z_{1s}} = -\frac{sa_0}{2b}C_{Z_{A_{1s}}} + C_{Z_{I_{1s}}}$$

As the vehicle equations of motion are expressed in body axes the rotor force is required to be referred to this axes set. This is achieved by first transforming equation (50) to hub axes by use of the transpose of equations (14) and (18), which give

$$\begin{bmatrix} \mathbf{i}_h \\ \mathbf{j}_h \\ \mathbf{k}_h \end{bmatrix} = \begin{bmatrix} -\cos\psi & -\sin\psi & -\beta\cos\psi \\ \sin\psi & -\cos\psi & \beta\sin\psi \\ -\beta & 0 & 1 \end{bmatrix} \begin{bmatrix} \mathbf{i}_{b1} \\ \mathbf{j}_{b1} \\ \mathbf{k}_{b1} \end{bmatrix} \tag{51}$$

Substituting equation (40) for β, and using (51) to transform (50) to hub axes, the force coefficients are found to be harmonic, with steady components, for a rotor with b blades, given by

$$C_{X_h} = -\frac{b}{2}[C_{X_{1c}} + C_{Y_{1s}} + \beta_0 C_{Z_{1c}} + \beta_{1_c} C_{Z_o}] \tag{52a}$$

$$C_{Y_h} = \frac{b}{2}[C_{X_{1s}} - C_{Y_{1c}} + \beta_0 C_{Z_{1s}} + \beta_{1_s} C_{Z_o}] \tag{52b}$$

$$C_{Z_h} = \frac{b}{2}[2C_{Z_o} - 2\beta_0 C_{Z_o} - \beta_{1_c} C_{X_{1c}} - \beta_{1_s} C_{X_{1s}}] \tag{52c}$$

In reality the rotor forces are periodic and could be more fully described by retaining terms in higher harmonics of ψ. For many applications, such as in vibration and the study of unsteady aerodynamic and blade structural loadings these harmonic terms would have to be retained to ensure high frequency effects were being modelled. Indeed this form of multiblade model may not even be appropriate for this type of problem; an individual blade model would be required. As this model has been created primarily for use with inverse simulation where the low frequency modes of the helicopter dynamics are of importance it will be sufficient only to consider the steady form of the rotor forces given by equations (52). This value corresponds to the average force around the azimuth travel of the blade.

The final stage is to transform these force coefficients into body axes for inclusion in the vehicle eqautions of motion. The transformation from hub to body axes follows from equation (9) and is

$$\begin{bmatrix} \mathbf{i}_b \\ \mathbf{j}_b \\ \mathbf{k}_b \end{bmatrix} = \begin{bmatrix} \cos\gamma_s & 0 & -\sin\gamma_s \\ 0 & 1 & 0 \\ \sin\gamma_s & 0 & \cos\gamma_s \end{bmatrix} \begin{bmatrix} \mathbf{i}_h \\ \mathbf{j}_h \\ \mathbf{k}_h \end{bmatrix} \tag{53}$$

The contribution to the external forces of the helicopter due to the main rotor are therefore given by :

$$X_R = \rho(\Omega R)^2 \pi R^2 [C_{X_h} \cos\gamma_s - C_{Z_h} \sin\gamma_s] \tag{54a}$$

$$Y_R = \rho(\Omega R)^2 \pi R^2 C_{Y_h} \tag{54b}$$

$$Z_R = \rho(\Omega R)^2 \pi R^2 [C_{X_h} \sin\gamma_s + C_{Z_h} \cos\gamma_s] \tag{54c}$$

3.2.4 The Rotor Moments

The hub moment per unit span due to the forces on an element at position P on a blade span can be expressed, referred to the blade axes set, as

$$\mathbf{M}_{P_{bl}} = \mathbf{r}_{P/H_{bl}} \times \mathbf{F}_{P_{bl}}$$

where $\mathbf{F}_{P_{bl}}$ is given by equation (25) and $\mathbf{r}_{P/H_{bl}} = r_b\, \mathbf{i}_{bl}$, giving

$$\mathbf{M}_{P_{bl}} = - r_b (f_{z_{bl}} - m_0 a_{z_{bl}})\, \mathbf{j}_{bl} + r_b (f_{y_{bl}} - m_0 a_{y_{bl}})\, \mathbf{k}_{bl} \qquad (55)$$

The component of this moment about the z_{bl} axis is effectively the torque contribution of the blade element, whilst the component about the y_{bl} axis gives the elemental contribution to the blade flapping moment. The total moments can be obtained by integration of the elemental moments over the span, however the flapping moment is more readily obtained by noting that flapping motion is resisted by the stiffness of the rotor hub, denoted by K_β. If the blade has flapped through an angle β, then the moment at the hub due to this flapping motion, M_{flap}, can be expresed (in blade axes) as

$$M_{flap_{bl}} = K_\beta\, \beta\, \mathbf{j}_{bl}$$

Integrating the elemental flapping moments over the span, and equating this to the hub flapping moment gives the blade flapping equation

$$\int_{eR}^{R} (f_{z_{bl}} - m_0 a_{z_{bl}})\, r_b\, dr_b + \beta\, K_\beta = 0 \qquad (56)$$

When expanded, as shown in the following section, equation (56) describes the flapping motion of the rotor blades. The rotor torque, Q, is obtained by integrating the elemental torques over the blade span

$$\int_{eR}^{R} (f_{y_{bl}} - m_0 a_{y_{bl}})\, r_b\, dr_b = Q \qquad (57)$$

As with the rotor forces this is more conveniently dealt with by deriving the aerodynamic and inertial contributions seperately. If the torque is normalised (by division by $\rho(\Omega R)^2 \pi R^3$) then, with reference to equation (36), the aerodynamic contribution, C_{Q_A}, to the coefficient of torque, C_Q, for 1 blade is given by

$$C_{Q_A} = \frac{1}{2}\, s\, a_0\, \frac{1}{b} \int_0^{1-e} \left[\frac{\delta}{a_0} \bar{U}_T^2 - \bar{U}_T \bar{U}_P \theta - \bar{U}_P^2 \right] (\bar{r}_b + e)\, d\bar{r}_b \qquad (58)$$

The blade element velocities $\bar{U}_T$ and $\bar{U}_P$, and the blade pitch angle, θ, are given by equations (43), (44) and (45) respectively. As with the blade forces, equation (58) was evaluated by using Mathematica, and the resulting expression gives the aerodynamic contribution to the main rotor torque, referred to the blade axes set, of a single blade. For consistency, including only the first harmonic terms, the aerodynamic torque coefficient is given by

$$C_{Q_A} = C_{Q_{A_0}} + C_{Q_{A_{1c}}} \cos\psi + C_{Q_{A_{1s}}} \sin\psi$$

where

$$C_{Q_{A_0}} = \theta_{1_c}\left\{-\tfrac{1}{8}(1-e^4)\alpha_{1c} + \tfrac{1}{6}(1-e^3)(\beta_0'\mu_y + \beta_0\mu_x) + \tfrac{1}{16}(1-e^2)\beta_{1s}(\mu_x^2 - \mu_y^2) - \tfrac{1}{4}\mu_y(1-e^2)(\mu_z - \lambda_0) + \tfrac{1}{8}(1-e^2)\beta_{1c}\mu_x\mu_y\right\} +$$
$$\theta_{1_s}\left\{-\tfrac{1}{8}(1-e^4)\alpha_{1s} + \tfrac{1}{6}(1-e^3)(\beta_0'\mu_x - \beta_0\mu_y) + \tfrac{1}{16}(1-e^2)\beta_{1c}(\mu_x^2 - \mu_y^2) - \tfrac{1}{4}\mu_x(1-e^2)(\mu_z - \lambda_0) - \tfrac{1}{8}(1-e^2)\beta_{1_s}\mu_x\mu_y\right\} +$$
$$\theta_0\left\{\tfrac{1}{4}(1-e^4)\beta_0' - \tfrac{1}{3}(1-e^3)(\mu_z - \lambda_0) - \tfrac{1}{6}(1-e^3)[(\alpha_{1s} - \beta_{1_c})\mu_x + (\alpha_{1c} + \beta_{1_s})\mu_y]\right\} +$$
$$\theta_{tw}\left\{\left(\tfrac{1}{5} - \tfrac{1}{4}e + \tfrac{1}{20}e^5\right)\beta_0' - \left(\tfrac{1}{4} - \tfrac{1}{3}e + \tfrac{1}{12}e^4\right)\left[(\mu_z - \lambda_0) - \tfrac{1}{2}[(\alpha_{1s} - \beta_{1_c})\mu_x + (\alpha_{1c} + \beta_{1_s})\mu_y]\right]\right\} -$$
$$\tfrac{1}{8}(1-e^4)[\alpha_{1c}^2 + \alpha_{1s}^2 + 2\beta_0'^2] + (\mu_z - \lambda_0)\left[\tfrac{2}{3}\beta_0'(1-e^3) - \tfrac{1}{2}(1-e^2)\{(\mu_z - \lambda_0) - (\beta_{1c}\mu_x - \beta_{1s}\mu_y)\}\right] + \tfrac{1}{3}(1-e^3)[\beta_0(\alpha_{1c}\mu_x - \alpha_{1s}\mu_y) + \beta_0'(\beta_{1s}\mu_y - \beta_{1c}\mu_x)] + (1-e^2)\left[-\tfrac{1}{4}\beta_0^2\mu^2 + \tfrac{1}{4}\beta_{1s}\beta_{1c}\mu_x\mu_y - \tfrac{1}{16}\mu^2(\beta_{1s}^2 + \beta_{1c}^2) - \tfrac{1}{8}(\beta_{1c}^2\mu_x^2 + \beta_{1s}^2\mu_y^2)\right] + \tfrac{1}{4}(1-e^2)(1+e^2+\mu^2)\frac{\delta}{a_0}$$

$$C_{Q_{A_{1c}}} = \theta_{1_c}\left\{\tfrac{1}{4}\beta_0'(1-e^4) + (1-e^3)\left[-\tfrac{1}{3}(\mu_z - \lambda_0) - \tfrac{1}{12}(\alpha_{1s}\mu_x + \beta_{1_s}\mu_y) + \tfrac{1}{4}(\beta_{1c}\mu_x - \alpha_{1c}\mu_y)\right] + \tfrac{1}{4}(1-e^2)\beta_0\mu_x\mu_y\right\} +$$
$$\theta_{1_s}\left\{\tfrac{1}{8}(1-e^2)\beta_0(\mu_x^2 - \mu_y^2) + \tfrac{1}{12}(1-e^3)[(\beta_{1_s} - \alpha_{1c})\mu_x - (\alpha_{1s} + \beta_{1_c})\mu_y]\right\} +$$
$$\theta_0\left\{-\tfrac{1}{4}(1-e^4)\alpha_{1c} + \tfrac{1}{3}(1-e^3)(\beta_0'\mu_y + \beta_0\mu_x) + \tfrac{1}{2}(1-e^2)\left[\tfrac{1}{4}\beta_{1s}(\mu_x^2 - \mu_y^2) - \mu_y(\mu_z - \lambda_0) + \tfrac{1}{2}\beta_{1c}\mu_x\mu_y\right]\right\} +$$
$$\theta_{tw}\left\{-\alpha_{1c}\left(\tfrac{1}{5} - \tfrac{1}{4}e + \tfrac{1}{20}e^5\right) + \left(\tfrac{1}{4} - \tfrac{1}{3}e + \tfrac{1}{12}e^4\right)(\beta_0'\mu_y + \beta_0\mu_x) + \tfrac{1}{2}(1-e^3)\left[\tfrac{1}{2}\beta_{1s}(\mu_x^2 - \mu_y^2) + \beta_{1c}\mu_x\mu_y - 2\mu_y(\mu_z - \lambda_0)\right]\right\} +$$
$$\tfrac{1}{2}(1-e^4)\alpha_{1c}\beta_0' + (1-e^2)\left[\beta_0\mu_x(\mu_z - \lambda_0) - \tfrac{1}{2}\beta_0\beta_{1c}(\mu_x^2 - \tfrac{1}{2}\mu^2) + \tfrac{1}{2}\beta_0\beta_{1_s}\mu_x\mu_y\right] -$$

$$\frac{2}{3}(1 - e^3)[\alpha_{1c}(\mu_z - \lambda_0) + \beta_0\beta'_0\mu_x - \frac{\delta}{a_0}\mu_y + \frac{1}{4}\beta_{1s}(\alpha_{1c}\mu_y - \alpha_{1s}\mu_x) + \frac{1}{4}\beta_{1c}(\alpha_{1s}\mu_y - 3\alpha_{1c}\mu_x)]$$

$$C_{QA_{1s}} = \theta_{1c}\{\frac{1}{8}(1 - e^2)\beta_0(\mu_x^2 - \mu_y^2) + \frac{1}{12}(1 - e^3)[(\beta_{1s} - \alpha_{1c})\mu_x - (\alpha_{1s} + \beta_{1c})\mu_y]\} +$$
$$\theta_{1s}\{\frac{1}{4}\beta'_0(1 - e^4) + (1 - e^3)[-\frac{1}{3}(\mu_z - \lambda_0) - \frac{1}{4}(\alpha_{1s}\mu_x + \beta_{1s}\mu_y) + \frac{1}{12}(\beta_{1c}\mu_x - \alpha_{1c}\mu_y)]$$
$$-\frac{1}{4}(1 - e^2)\beta_0\mu_x\mu_y\} +$$
$$\theta_0\{-\frac{1}{4}(1 - e^4)\alpha_{1s} + \frac{1}{3}(1 - e^3)(\beta'_0\mu_x - \beta_0\mu_y) + \frac{1}{2}(1 - e^2)[\frac{1}{4}\beta_{1c}(\mu_x^2 - \mu_y^2) - \mu_x(\mu_z - \lambda_0)$$
$$-\frac{1}{2}\beta_{1s}\mu_x\mu_y]\} +$$
$$\theta_{tw}\{-\alpha_{1s}(\frac{1}{5} - \frac{1}{4}e + \frac{1}{20}e^5) + (\frac{1}{4} - \frac{1}{3}e + \frac{1}{12}e^4)(\beta'_0\mu_x - \beta_0\mu_y) + \frac{1}{2}(1 - e^3)[\frac{1}{2}\beta_{1c}(\mu_x^2 -$$
$$\mu_y^2) - \beta_{1s}\mu_x\mu_y - 2\mu_x(\mu_z - \lambda_0)]\} +$$
$$\frac{1}{2}(1 - e^4)\alpha_{1s}\beta'_0 + (1 - e^2)[-\beta_0\mu_y(\mu_z - \lambda_0) - \frac{1}{2}\beta_0\beta_{1s}(\mu_y^2 + \frac{1}{2}\mu^2) + \frac{1}{2}\beta_0\beta_{1c}\mu_x\mu_y] -$$
$$\frac{2}{3}(1 - e^3)[\alpha_{1s}(\mu_z - \lambda_0) - \beta_0\beta'_0\mu_y - \frac{\delta}{a_0}\mu_x + \frac{1}{4}\beta_{1s}(\alpha_{1c}\mu_x - 3\alpha_{1s}\mu_y) + \frac{1}{4}\beta_{1c}(\alpha_{1s}\mu_x - \alpha_{1c}\mu_y)]$$

The inertial contribution to the rotor torque is obtained from the integral

$$Q_{I_{bl}} = -\int_{eR}^{R} m_0\, a_{y_{bl}}\, r_b\, dr_b$$

which, on substitution of $a_{y_{bl}}$ from equation (24), gives

$$Q_{I_{bl}} = (a_{H_x}\sin\psi + a_{H_y}\cos\psi)\, M_\beta - (\dot{\omega}_z + \omega_y\omega_z)\, I_\beta$$

where M_β is the mass moment of the blade, as before, and I_β is the moment of inertia of the blade which is defined as

$$I_\beta = \int_{eR}^{R} m_0\, r_b^2\, dr_b$$

Substitution for $\dot{\omega}_z$, ω_y, and ω_z, from equations (48b) and (47b and c), then normalising (by division by $\rho(\Omega R)^2\pi R^3$) gives the inertial torque contribution of 1 blade in the form

$$C_{Q_I} = C_{Q_{I_0}} + C_{Q_{I_{1c}}}\cos\psi + C_{Q_{I_{1s}}}\sin\psi$$

where

$$C_{Q_{I_0}} = -\bar{I}_\beta \left[\beta_0 \beta_0' - \frac{\dot{\Omega}}{\Omega^2} + \frac{1}{2}\varepsilon_{1c}(\beta_{1c} - \bar{p}_H) + \frac{1}{2}\varepsilon_{1s}(\beta_{1s} + \bar{q}_H)\right]$$

$$C_{Q_{I_{1c}}} = \eta_y \bar{M}_\beta - \bar{I}_\beta \left[\beta_0 \varepsilon_{1c} + \beta_0'(\beta_{1c} - \bar{p}_H)\right]$$

$$C_{Q_{I_{1s}}} = \eta_x \bar{M}_\beta - \bar{I}_\beta \left[\beta_0 \varepsilon_{1s} + \beta_0'(\beta_{1s} + \bar{q}_H)\right]$$

and $$\bar{I}_\beta = \frac{I_\beta}{\rho \pi R^5}$$

Thus, for a single blade, the total torque coefficient is written in the form

$$C_Q = C_{Q_0} + C_{Q_{1c}} \cos\psi + C_{Q_{1s}} \sin\psi$$

where

$$C_{Q_0} = \frac{sa_0}{2b} C_{Q_{A_0}} + C_{Q_{I_0}}, \quad C_{Q_{1c}} = \frac{sa_0}{2b} C_{Q_{A_{1c}}} + C_{Q_{I_{1c}}}, \quad C_{Q_{1s}} = \frac{sa_0}{2b} C_{Q_{A_{1s}}} + C_{Q_{I_{1s}}}$$

Referring to equation (55), the hub moment due to a single blade may be written in the form

$$\mathbf{M_{hub_{bl}}} = K_\beta \beta \, \mathbf{j_{bl}} + Q \, \mathbf{k_{bl}} \tag{59}$$

where Q is written in the form

$$Q = Q_0 + Q_{1_c} \cos\psi + Q_{1_s} \sin\psi$$

and $Q_0 = \rho(\Omega R)^2 \pi R^3 C_{Q_0}$ etc.

Expressing β in its harmonic form (40), and using the transformation given by equation (51), the hub moment given by equation (59) can then be refered to the hub axes set. Hence, for a rotor with b blades, the roll, pitch and yaw hub moments are given by

$$L_h = -\frac{b}{2}\left[K_\beta \beta_{1_s} + Q_0 \beta_{1_c} + Q_{1_c} \beta_0\right] \tag{60a}$$

$$M_h = \frac{b}{2}\left[\beta_{1_s} Q_0 + \beta_0 Q_{1_s} - K_\beta \beta_{1_c}\right] \tag{60b}$$

$$N_h = b \, Q_0 \tag{60c}$$

If the helicopter's transmission is assumed to have an inertia, I_{tr}, then the yawing moment at the hub can be rewritten, from equation (60c)

$$N_h = b\, Q_0 + I_{tr}\, \dot{\Omega} \tag{61}$$

The total moments acting at the helicopter centre of gravity are obtained by transforming the moments given by (60a), (60b) and (61) to the body axes frame by using equation (53), then adding the moments due to the rotor hub forces given by equations (54),being offset from the centre of gravity. The contribution to the external moments of the helicopter due to the main rotor are therefore given by

$$L_R = L_h \cos\gamma_s - N_h \sin\gamma_s + h_R\, Y_R \tag{62a}$$

$$M_R = M_h - h_R\, X_R + x_{cg}\, Z_R \tag{62b}$$

$$N_R = L_h \sin\gamma_s + N_h \cos\gamma_s - x_{cg}\, Y_R \tag{62c}$$

3.3 Blade Flapping Dynamics

3.3.1 The Blade Flapping Equation

The flapping angles, β_0, β_{1_c}, β_{1_s}, are determined by solution of the blade flapping equation, which for a blade, i, from (56) is given by

$$\int_{eR}^{R} (f_{z_H} - m_0 a_{z_H})\, r_b\, dr_b + \beta_i\, K_\beta = 0 \tag{63}$$

where, from (24), (47), and (48)

$$a_{z_{bl}} = \beta_i\, (-a_{H_x} \cos\psi_i + a_{H_y} \sin\psi_i) + a_{H_z} +$$
$$r_b\, [-\ddot{\beta}_i - \Omega^2 \beta_i + (\dot{q}_H + 2\Omega p_H) \cos\psi_i + (\dot{p}_H - 2\Omega q_H) \sin\psi_i]$$

so that referring (33), equation (63) can be rewritten

$$-\frac{1}{2} \rho c a_0 \int_{eR}^{R} (U_T^2\, \theta + U_T\, U_P)\, r_b\, dr_b - [\beta_i\, (-a_{H_x} \cos\psi_i + a_{H_y} \sin\psi_i) + a_{H_z}] \int_{eR}^{R} m_0\, r_b\, dr_b$$

$$- [-\ddot{\beta}_i - \Omega^2 \beta_i + (\dot{q}_H + 2\Omega p_H)\cos\psi_i + (\dot{p}_H - 2\Omega q_H)\sin\psi_i] \int_{eR}^{R} m_0\, r_b^2\, dr_b + \beta_i\, K_\beta = 0$$

Substituting for the blade moments of mass and inertia, M_β and I_β, and rearranging, gives

$$\ddot{\beta}_i + \left[\Omega^2 + \frac{K_\beta}{I_\beta} + \frac{M_\beta}{I_\beta}(a_{H_x}\cos\psi_i - a_{H_y}\sin\psi_i)\right]\beta_i = \frac{1}{2}\frac{\rho c a_0}{I_\beta}\int_{eR}^{R}\left(U_T^2\,\theta + U_T\,U_P\right) r_b\,dr_b$$

$$+ \frac{M_\beta}{I_\beta}a_{H_Z} + (\dot{q}_H + 2\Omega p_H)\cos\psi_i + (\dot{p}_H - 2\Omega q_H)\sin\psi_i$$

This is normalised by dividing throughout by Ω^2, giving

$$\beta_i'' + \left[\lambda_\beta^2 + \frac{M_\beta R}{I_\beta}(\eta_x\cos\psi_i - \eta_y\sin\psi_i)\right]\beta_i = 4n_\beta\int_0^{1-e}\left[\bar{U}_T^2\,\theta + \bar{U}_T\,\bar{U}_P\right](\bar{r}_b + e)\,d\bar{r}_b$$

$$+ \frac{M_\beta R}{I_\beta}\eta_z + 2\left[\left(\frac{q'_H}{2} + \bar{p}_H\right)\cos\psi_i + \left(\frac{p'_H}{2} - \bar{q}_H\right)\sin\psi_i\right] \qquad (64)$$

where

$$\beta_i'' = \frac{d^2\beta_i}{d\psi^2}\,, \quad \lambda_\beta^2 = 1 + \frac{K_\beta}{I_\beta\,\Omega^2}\,, \quad n_\beta = \frac{\rho c a_0 R^4}{8I_\beta}\,, \quad q'_H = \frac{\dot{q}_H}{\Omega^2}\,, \quad p'_H = \frac{\dot{p}_H}{\Omega^2}$$

The integral part of the forcing term of equation (64) is evaluated by substitution of θ from equation (45), $\bar{U}_T$ from equation (43),

$$\bar{U}_T = \mu_x\sin\psi_i + \mu_y\cos\psi_i + \bar{r}_b + e$$

and $\bar{U}_P$ from (39),

$$\bar{U}_P = \beta_i(-\mu_x\cos\psi_i + \mu_y\sin\psi_i) + \mu_z - \lambda_0 - (\bar{r}_b + e)[\beta_i' + (\lambda_{1_s} - \bar{p}_H)\sin\psi_i + (\lambda_{1_c} - \bar{q}_H)\cos\psi_i]$$

This was evaluated using Mathematica, and the flapping equation (64), then becomes

$$\beta_i'' + n_\beta\left[1 - e^4 + \frac{4}{3}(1 - e^3)(\mu_y\cos\psi_i + \mu_x\sin\psi_i)\right]\beta_i' + \left[\lambda_\beta^2 - \frac{M_\beta R}{I_\beta}(-\eta_x\cos\psi_i + \eta_y\sin\psi_i) + \right.$$
$$\left. n_\beta\left\{\frac{4}{3}(1 - e^3)(\mu_x\cos\psi_i - \mu_y\sin\psi_i) + 2(1 - e^2)(\mu_x\mu_y\cos 2\psi_i + \frac{1}{2}(\mu_x^2 - \mu_y^2)\sin 2\psi_i)\right\}\right]\beta_i =$$

$$\frac{M_\beta R}{I_\beta}\eta_z + 2\left[(\bar{p}_H + \frac{q'_H}{2})\cos\psi_i - (\bar{q}_H - \frac{p'_H}{2})\sin\psi_i\right] +$$
$$4n_\beta\left\{\frac{1}{6}(1 - e^3)[2(\mu_z - \lambda_0) + [(2\theta_{1_c} - \lambda_{1_s} + \bar{p}_H)\mu_y + (2\theta_{1_s} - \lambda_{1_c} + \bar{q}_H)\mu_x]] + \right.$$
$$\frac{1}{4}(1 - e^2)(1 + e^2 + \mu^2)\theta_0 + [\frac{1}{5} - \frac{1}{4}e + \frac{1}{20}e^5 + (\frac{1}{6} - \frac{1}{4}e + \frac{1}{12}e^3)\mu^2]\theta_{tw} +$$
$$\left.[\frac{1}{4}(1 - e^2)[(1 + e^2 + \frac{1}{2}\mu^2 + \mu_y^2)\theta_{1_c} + \mu_x\mu_y\theta_{1_s}] + \frac{2}{3}(1 - e^3)\mu_y\theta_0 + (\frac{1}{2} - \frac{2}{3}e + \frac{1}{6}e^4)\mu_y\theta_{tw} + \right.$$

$$\tfrac{1}{2}(1 - e^2)(\mu_z - \lambda_0)\mu_y - \tfrac{1}{4}(1 - e^4)(\lambda_{1_c} - \bar{q}_H)\Big]\cos\psi_i +$$
$$\Big[\tfrac{1}{4}(1 - e^2)\Big[(1 + e^2 + \tfrac{1}{2}\mu^2 + \mu_x^2)\theta_{1_s} + \mu_x\mu_y\theta_{1_c}\Big] + \tfrac{2}{3}(1 - e^3)\mu_x\theta_0 + (\tfrac{1}{2} - \tfrac{2}{3}e + \tfrac{1}{6}e^4)\mu_x\theta_{tw} +$$
$$\tfrac{1}{2}(1 - e^2)(\mu_z - \lambda_0)\mu_x - \tfrac{1}{4}(1 - e^4)(\lambda_{1_s} - \bar{p}_H)\Big]\sin\psi_i\Big\} \qquad (65)$$

(Note that terms in $2\psi_i$ and above on the right hand side are not presented here as they do not influence the final result.)

3.3.2 The Multiblade Transformation

In order to solve equation (65) the multiblade transformation [3] is applied. Effectively this converts the individual blade flapping angles, β_i, into rotor disc multiblade angles, coning, β_0, longitudinal and lateral flapping, β_{1_c}, and β_{1_s}, and the differential flap angle, β_d. For a rotor with four individual blades, their flapping angles can be expressed as

$$\beta_I = [\beta_1, \beta_2, \beta_3, \beta_4]^T \qquad (66)$$

where the azimuth position of successive blades will be given by

$$\psi_i = \psi - (i - 1)\frac{\pi}{2} \qquad (67)$$

and equation (65) can be expressed in the form

$$\beta_I'' + C_I\,\beta_I' + D_I\,\beta_I = h_I \qquad (68)$$

The matrices C_I, D_I, and h_I, are obtained by substituting for successive values of ψ_i for each blade from equation (67). The matrices and C_I are D_I therefore diagonal with, for example,

$$C_I = \begin{bmatrix} c_{I_{11}} & 0 & 0 & 0 \\ 0 & c_{I_{22}} & 0 & 0 \\ 0 & 0 & c_{I_{33}} & 0 \\ 0 & 0 & 0 & c_{I_{44}} \end{bmatrix}$$

where

$$c_{I_{11}} = n_\beta\left[1 - e^4 + \tfrac{4}{3}(1 - e^3)(\mu_y\cos\psi_i + \mu_x\sin\psi_i)\right]$$
$$c_{I_{22}} = n_\beta\left[1 - e^4 + \tfrac{4}{3}(1 - e^3)(\mu_y\sin\psi_i - \mu_x\cos\psi_i)\right]$$
$$c_{I_{33}} = n_\beta\left[1 - e^4 - \tfrac{4}{3}(1 - e^3)(\mu_y\cos\psi_i + \mu_x\sin\psi_i)\right]$$

$$c_{I_{44}} = n_\beta \left[1 - e^4 - \frac{4}{3}(1 - e^3)(\mu_y \sin\psi_i - \mu_x \cos\psi_i)\right]$$

The transformation from individual blade angle to a multiblade angles is given in Reference (3) as

$$\beta_0 = \frac{1}{b}\sum_{i=1}^{b} \beta_i \qquad \beta_d = \frac{1}{b}\sum_{i=1}^{b} \beta_i (-1)^i \qquad \beta_{j_c} = \frac{2}{b}\sum_{i=1}^{b} \beta_i \cos j\psi_i \qquad \beta_{j_s} = \frac{2}{b}\sum_{i=1}^{b} \beta_i \sin j\psi_i$$

which, expressing the multiblade angles in the form

$$\beta_M = [\beta_0, \beta_d, \beta_{1_c}, \beta_{1_s}]^T$$

for a 4 bladed rotor, can be expressed in matrix notation as

$$\beta_I = L_\beta \beta_M \tag{69}$$

where, applying (67) for 4 blades

$$L_\beta = \begin{bmatrix} 1 & -1 & \cos\psi & \sin\psi \\ 1 & 1 & \sin\psi & -\cos\psi \\ 1 & -1 & -\cos\psi & -\sin\psi \\ 1 & 1 & -\sin\psi & \cos\psi \end{bmatrix}$$

Differentiation of (69) with respect to ψ, then substituting into equation (68) gives the flapping equation referred to the multiblade angles

$$\beta''_M + C_M \beta'_M + D_M \beta_M = h_M \tag{70}$$

where $C_M = L_\beta^{-1}(2L'_\beta + C_I L_\beta)$

$D_M = L_\beta^{-1}(L''_\beta + C_I L'_\beta + D_I L_\beta)$

$h_M = L_\beta^{-1} h_I$

and

$$L'_\beta = \begin{bmatrix} 0 & 0 & -\sin\psi & \cos\psi \\ 0 & 0 & \cos\psi & \sin\psi \\ 0 & 0 & \sin\psi & -\cos\psi \\ 0 & 0 & -\cos\psi & -\sin\psi \end{bmatrix} \qquad L''_\beta = \begin{bmatrix} 0 & 0 & -\cos\psi & -\sin\psi \\ 0 & 0 & -\sin\psi & \cos\psi \\ 0 & 0 & \cos\psi & \sin\psi \\ 0 & 0 & \sin\psi & -\cos\psi \end{bmatrix}$$

$$L_\beta^{-1} = \frac{1}{4}\begin{bmatrix} 1 & 1 & 1 & 1 \\ -1 & 1 & -1 & 1 \\ 2\cos\psi & 2\sin\psi & -2\cos\psi & -2\sin\psi \\ 2\sin\psi & -2\cos\psi & -2\sin\psi & 2\cos\psi \end{bmatrix}$$

These expressions will give the matrices C_M, D_M, and h_M, in harmonic form. As with the blade force calculations the periodic terms are neglected to give the nonperiodic flapping equation

$$\beta''_M + C_{M_0}\beta'_M + D_{M_0}\beta_M = h_{M_0} \tag{71}$$

where

$$C_{M_0} = \begin{bmatrix} (1-e^4)n_\beta & 0 & \frac{2}{3}\mu_y(1-e^3)n_\beta & \frac{2}{3}\mu_x(1-e^3)n_\beta \\ 0 & (1-e^4)n_\beta & 0 & 0 \\ \frac{4}{3}\mu_y(1-e^3)n_\beta & 0 & (1-e^4)n_\beta & 2 \\ \frac{4}{3}\mu_x(1-e^3)n_\beta & 0 & -2 & (1-e^4)n_\beta \end{bmatrix}$$

$$D_{M_0} = \begin{bmatrix} \lambda_\beta^2 & 0 & \frac{M_\beta R}{2I_\beta}\eta_x & -\frac{M_\beta R}{2I_\beta}\eta_y \\ 0 & \lambda_\beta^2 & 0 & 0 \\ \frac{M_\beta R}{I_\beta}\eta_x + \frac{4}{3}\mu_x(1-e^3)n_\beta & 0 & \lambda_\beta^2 - 1 + \mu_x\mu_y(1-e^2)n_\beta & \left[1-e^4+\frac{1}{2}(1-e^2)(\mu_x^2-\mu_y^2)\right]n_\beta \\ -\frac{M_\beta R}{I_\beta}\eta_y + \frac{4}{3}\mu_y(1-e^3)n_\beta & 0 & -\left[1-e^4+\frac{1}{2}(1-e^2)(\mu_x^2-\mu_y^2)\right]n_\beta & \lambda_\beta^2 - 1 - \mu_x\mu_y(1-e^2)n_\beta \end{bmatrix}$$

$$h_{M_0} = \begin{bmatrix} h_0 \\ 0 \\ h_{1_c} \\ h_{1_s} \end{bmatrix}$$

and

$$h_0 = \frac{M_\beta R}{I_\beta}\eta_z + n_\beta\left\{\frac{2}{3}(1-e^3)\left[2(\mu_z-\lambda_0)+[(2\theta_{1_c}-\lambda_{1_s}+\bar{p}_H)\mu_y+(2\theta_{1_s}-\lambda_{1_c}+\bar{q}_H)\mu_x]\right]+\right.$$
$$\left.(1-e^2)(1+e^2+\mu^2)\theta_0+\left[\frac{4}{5}-e+\frac{1}{5}e^5+(\frac{2}{3}-e+\frac{1}{3}e^3)\mu^2\right]\theta_{tw}\right\}$$

$$h_{1_c} = 2(\bar{p}_H+\frac{\dot{q}_H}{2})+n_\beta\left\{(1-e^2)[(1+e^2+\frac{1}{2}\mu^2+\mu_y^2)\theta_{1_c}+\mu_x\mu_y\theta_{1_s}]+\frac{8}{3}(1-e^3)\mu_y\theta_0+\right.$$
$$\left.(2-\frac{8}{3}e+\frac{2}{3}e^4)\mu_y\theta_{tw}+2(1-e^2)(\mu_z-\lambda_0)\mu_y-(1-e^4)(\lambda_{1_c}-\bar{q}_H)\right\}$$

$$h_{1_s} = -2(\bar{q}_H-\frac{\dot{p}_H}{2})+n_\beta\left\{(1-e^2)[(1+e^2+\frac{1}{2}\mu^2+\mu_x^2)\theta_{1_s}+\mu_x\mu_y\theta_{1_c}]+\frac{8}{3}(1-e^3)\mu_x\theta_0+\right.$$
$$\left.(2-\frac{8}{3}e+\frac{2}{3}e^4)\mu_x\theta_{tw}+2(1-e^2)(\mu_z-\lambda_0)\mu_x-(1-e^4)(\lambda_{1_s}-\bar{p}_H)\right\}$$

Equation (71) can then be solved for the multiblade flapping angles for a given set of control angles and hub velocities. The solution of (71) is often simplified by assuming that the blade flapping dynamics are decoupled from the body dynamics and therefore have little effect on the forces and moments applied by the rotor to the vehicle body. This assumption is made on the grounds that the blade flap modes are very much faster than those of the body. The quasi-steady blade flap equation becomes

$$\beta_M = D_{M_0}^{-1} h_{M_0} \tag{72}$$

which, due to its algebraic nature, can be solved simply to give the blade flap angles at a discrete point in time.

4. The Tail Rotor Model

The modelling of the tail rotor is essentially the same as the for the main rotor, the major exception being that the tail rotor hub is assumed to be rigid so that no blade flapping occurs. As with the main rotor, it is assumed that the blades are of constant chord and lift curve slope, a linear blade twist is incorporated, and a root cut out section is also included. The same form of inflow model is also used, however the inertial forces of the blades are assumed to be small, and are therefore ignored. Due to the similarity with the main rotor, only brief details of the formulation of the tail rotor forces and moments are given here.

4.1 Tail Rotor Kinematics

The tail rotor hub (TRH) is positioned a distance l_{TR} behind the fuselage reference point (directly below the rotor hub), and a height h_{TR} above it. The position vector, in body axes, of the tail rotor hub with respect to the centre of gravity is therefore given by

$$\mathbf{r}_{TRH/C} = -(l_{TR} + x_{cg})\,\mathbf{i_b} - h_{TR}\,\mathbf{k_b}$$

The velocity of the tail rotor hub, in body axes, is given by

$$\mathbf{V}_{TRH_b} = \mathbf{V}_C + (\boldsymbol{\omega}_b \times \mathbf{r}_{TRH/C}) + \frac{d\mathbf{r}_{TRH/C}}{dt}$$

which is found to be

$$\mathbf{V}_{TRH_b} = (u - qh_{TR})\,\mathbf{i_b} + [v - r(l_{TR} + x_{cg}) + ph_{TR}]\,\mathbf{j_b} - [w + q(l_{TR} + x_{cg})]\,\mathbf{k_b} \qquad (73)$$

An axes set fixed at the tail rotor hub is now introduced (subscript trh), Figure 9, with its x direction coinciding with that of the body fixed set, its y-axis down, and its z-axis in the direction of the flow through the tail rotor. This implies a "pusher" tail rotor. The transformation from body axes to tail rotor hub axes is then given by

$$\begin{bmatrix} \mathbf{i}_{trh} \\ \mathbf{j}_{trh} \\ \mathbf{k}_{trh} \end{bmatrix} = \begin{bmatrix} 1 & 0 & 0 \\ 0 & 0 & 0 \\ 0 & -1 & 0 \end{bmatrix} \begin{bmatrix} \mathbf{i_b} \\ \mathbf{j_b} \\ \mathbf{k_b} \end{bmatrix} \qquad (74)$$

The tail rotor hub velocity, in tail rotor hub axes, is then obtained by (73) and (74) as

$$\mathbf{V}_{TRH_{trh}} = (u - qh_{TR})\,\mathbf{i}_{trh} + [w + q(l_{TR} + x_{cg})]\,\mathbf{j}_{trh} - [v - r(l_{TR} + x_{cg}) + ph_{TR}]\,\mathbf{k}_{trh}$$

which is more conveniently expressed as

$$\mathbf{V}_{TRH_{trh}} = u_{H_{TR}}\,\mathbf{i}_{trh} + v_{H_{TR}}\,\mathbf{j}_{trh} + w_{H_{TR}}\,\mathbf{k}_{trh} \qquad (75)$$

Using (74), the angular velocity of the hub axes set will be given by

$$\boldsymbol{\omega}_{trh} = p\,\mathbf{i}_{trh} + r\,\mathbf{j}_{trh} - q\,\mathbf{k}_{trh}$$

which, again, is written in the form

$$\omega_{trh} = p_{H_{TR}}\,\mathbf{i}_{trh} + q_{H_{TR}}\,\mathbf{j}_{trh} + r_{H_{TR}}\,\mathbf{k}_{trh} \tag{76}$$

An axes set, tail rotor blade axes (trbl) is now fixed at a position P on a tail rotor blade a distance $r_{b_{tr}}$ from the hub. Referring to Figure 9, the transformation from tail rotor hub to tail rotor blade axes is given by

$$\begin{bmatrix} \mathbf{i}_{trbl} \\ \mathbf{j}_{trbl} \\ \mathbf{k}_{trbl} \end{bmatrix} = \begin{bmatrix} -\cos\psi_{TR} & \sin\psi_{TR} & 0 \\ -\sin\psi_{TR} & -\cos\psi_{TR} & 0 \\ 0 & 0 & 1 \end{bmatrix} \begin{bmatrix} \mathbf{i}_{trh} \\ \mathbf{j}_{trh} \\ \mathbf{k}_{trh} \end{bmatrix} \tag{77}$$

From (75) and (77) the tail rotor hub velocity in tail rotor blade axes is then

$$\mathbf{V}_{TRH_{trbl}} = (-u_{H_{TR}}\cos\psi_{TR} + v_{H_{TR}}\sin\psi_{TR})\,\mathbf{i}_{trbl} - (u_{H_{TR}}\sin\psi_{TR} + v_{H_{TR}}\cos\psi_{TR})\,\mathbf{j}_{trbl} + w_{H_{TR}}\,\mathbf{k}_{trbl} \tag{78}$$

and from (76) and (75) the angular velocity of the tail rotor hub axes set is

$$\omega_{trbl} = (-p_{H_{TR}}\cos\psi_{TR} + q_{H_{TR}}\sin\psi_{TR})\,\mathbf{i}_{trbl} - (p_{H_{TR}}\sin\psi_{TR} + q_{H_{TR}}\cos\psi_{TR})\,\mathbf{j}_{trbl} + (r_{H_{TR}} - \Omega_{TR})\,\mathbf{k}_{trbl} \tag{79}$$

The position of the blade element with respect to the tail rotor hub is given by

$$\mathbf{r}_{P/TRH} = r_{b_{TR}}\,\mathbf{i}_{trbl}$$

and the velocity of the blade element is obtained from

$$\mathbf{V}_{P_{trbl}} = \mathbf{V}_{TRH_{trbl}} + (\omega_{trbl} \times \mathbf{r}_{P/TRH}) + \frac{d\mathbf{r}_{P/TRH}}{dt}$$

which gives

$$\begin{aligned} \mathbf{V}_{P_{trbl}} = {} & [-u_{H_{TR}}\cos\psi_{TR} + v_{H_{TR}}\sin\psi_{TR}]\,\mathbf{i}_{trbl} + \\ & [-u_{H_{TR}}\sin\psi_{TR} - v_{H_{TR}}\cos\psi_{TR} + r_{b_{TR}}(r_{H_{TR}} - \Omega_{TR})]\,\mathbf{j}_{trbl} + \\ & [w_{H_{TR}} + r_{b_{TR}}(p_{H_{TR}}\sin\psi_{TR} + q_{H_{TR}}\cos\psi_{TR})]\,\mathbf{k}_{trbl} \end{aligned} \tag{80}$$

4.2 Tail Rotor Forces and Moments

The forces and moments from the tail rotor are obtained in a similar manner to those of the mian rotor. Neglecting the inertial components of the elemental forces, the forces and torque of a single blade will be given by

$$Z_{TR_{rbl}} = -\frac{1}{2}\rho c_{TR} a_{0_{TR}} \int_{e_{TR}R_{TR}}^{R_{TR}} U_{T_{TR}}^2 \theta_{TR} + U_{T_{TR}} U_{P_{TR}}\, dr_{b_{TR}}$$

$$Y_{TR_{rbl}} = \frac{1}{2}\rho c_{TR} a_{0_{TR}} \int_{e_{TR}R_{TR}}^{R_{TR}} \frac{\delta_{TR}}{a_{0_{TR}}} U_{T_{TR}}^2 - U_{T_{TR}} U_{P_{TR}} \theta_{TR} - U_{P_{TR}}^2\, dr_{b_{TR}}$$

$$Q_{TR_{rbl}} = \frac{1}{2}\rho c_{TR} a_{0_{TR}} \int_{e_{TR}R_{TR}}^{R_{TR}} \left[\frac{\delta_{TR}}{a_{0_{TR}}} U_{T_{TR}}^2 - U_{T_{TR}} U_{P_{TR}} \theta_{TR} - U_{P_{TR}}^2\right] r_{b_{TR}}\, dr_{b_{TR}}$$

where c_{TR}, e_{TR} and R_{TR} describe the planform of the blade, see Figure 7, $a_{0_{TR}}$ is the constant lift curve slope and δ_{TR} is the constant profile drag coefficient of the tail rotor blades. The blade element tangential and normal velocities, $U_{T_{TR}}$ and $U_{P_{TR}}$, are obtained from equation (80), and by assuming an inflow distribution of the form

$$v_{i_{TR}} = v_{0_{TR}} + \frac{r_{b_{TR}}}{R_{TR}}\left(v_{1_{s_{TR}}} \sin\psi_{TR} + v_{1_{c_{TR}}} \cos\psi_{TR}\right)$$

Assuming a linear variation of twist $\theta_{tw_{TR}}$ and a collective input $\theta_{0_{TR}}$, the pitch of the blade is given by

$$\theta_{TR} = \theta_{0_{TR}} + \frac{r_{b_{TR}}}{R_{TR}} \theta_{tw_{TR}}$$

Normalising by division by $\rho(\Omega_{TR}R_{TR})^2\pi R_{TR}^2$ for the forces, and $\rho(\Omega_{TR}R_{TR})^2\pi R_{TR}^3$ for torque, the force and torque coefficients for the whole rotor will be given by

$$C_{Z_{TR_{rbl}}} = -\frac{1}{2} s_{TR} a_{0_{TR}} \int_0^{1-e_{TR}} \bar{U}_{T_{TR}}^2 \theta_{TR} + \bar{U}_{T_{TR}} \bar{U}_{P_{TR}}\, d\bar{r}_{b_{TR}}$$

$$C_{Y_{TR_{rbl}}} = \frac{1}{2} s_{TR} a_{0_{TR}} \int_0^{1-e_{TR}} \frac{\delta_{TR}}{a_{0_{TR}}} \bar{U}_{T_{TR}}^2 - \bar{U}_{T_{TR}} \bar{U}_{P_{TR}} \theta_{TR} - \bar{U}_{P_{TR}}^2\, d\bar{r}_{b_{TR}}$$

$$C_{Q_{TR_{rbl}}} = \frac{1}{2} s_{TR} a_{0_{TR}} \int_0^{1-e_{TR}} \left[\frac{\delta_{TR}}{a_{0_{TR}}} \bar{U}_{T_{TR}}^2 - \bar{U}_{T_{TR}} \bar{U}_{P_{TR}} \theta_{TR} - \bar{U}_{P_{TR}}^2\right] \bar{r}_{b_{TR}}\, dr_{b_{TR}}$$

where s_{TR} is the solidity of the tail rotor. Using Mathematica to evaluate these expressions, neglecting terms in $2\psi_{TR}$ and higher, gives

$$C_{Z_{TR_{trbl}}} = -\frac{1}{2} s_{TR}\, a_{0_{TR}} (C_{Z_{0_{TR}}} + C_{Z_{1c_{TR}}} \cos\psi_{TR} + C_{Z_{1s_{TR}}} \sin\psi_{TR}) \qquad (81)$$

where, listing only the coefficients actually required after transformation to hub axes (see below),

$$C_{Z_{0_{TR}}} = \theta_{0_{TR}}\left[\tfrac{1}{3}(1 - e_{TR}^3) + \tfrac{1}{2}(1 - e_{TR})\,\mu_{TR}^2\right] + \theta_{tw_{TR}}\left[\tfrac{1}{4} - \tfrac{1}{3} e_{TR} + \tfrac{1}{4}(1 - e_{TR})^2 \mu_{TR}^2\right] +$$
$$\tfrac{1}{4}(1 - e_{TR}^2)[(\bar{p}_{TR} - \lambda_{1s_{TR}})\mu_{x_{TR}} + (\bar{q}_{TR} - \lambda_{1c_{TR}})\mu_{y_{TR}} + 2(\mu_{z_{TR}} - \lambda_{0_{TR}})]$$

and

$$\mu_{x_{TR}} = \frac{u_{H_{TR}}}{\Omega_{TR} R_{TR}}, \quad \text{etc;} \qquad \bar{q}_{TR} = \frac{q_{H_{TR}}}{\Omega_{TR}}, \quad \text{etc;} \qquad \lambda_{0_{TR}} = \frac{v_{0_{TR}}}{\Omega_{TR} R_{TR}} \quad \text{etc.}$$

Similarly,

$$C_{Y_{TR_{trbl}}} = -\frac{1}{2} s_{TR}\, a_{0_{TR}} (C_{Y_{0_{TR}}} + C_{Y_{1c_{TR}}} \cos\psi_{TR} + C_{Y_{1s_{TR}}} \sin\psi_{TR}) \qquad (82)$$

where

$$C_{Y_{1c_{TR}}} = \theta_{0_{TR}}\left[-\tfrac{1}{3}(1 - e_{TR}^3)(\bar{q}_{TR} - \lambda_{1c_{TR}}) - (\mu_{z_{TR}} - \lambda_{0_{TR}})(1 - e_{TR})\mu_{y_{TR}}\right] +$$
$$\theta_{tw_{TR}}\left[-(\tfrac{1}{4} - \tfrac{1}{3} e_{TR} + \tfrac{1}{12} e_{TR}^4)(\bar{q}_{TR} - \lambda_{1c_{TR}}) - \tfrac{1}{2}(1 - e_{TR})^2 (\mu_{z_{TR}} - \lambda_{0_{TR}})\mu_{y_{TR}}\right] +$$
$$\frac{\delta_{TR}}{a_{0_{TR}}}(1 - e_{TR}^2)\mu_{y_{TR}} - (\bar{q}_{TR} - \lambda_{1c_{TR}})(1 - e_{TR}^2)(\mu_{z_{TR}} - \lambda_{0_{TR}})$$

$$C_{Y_{1s_{TR}}} = \theta_{0_{TR}}\left[-\tfrac{1}{3}(\bar{p}_{TR} - \lambda_{1s_{TR}})(1 - e_{TR}^3) - (\mu_{z_{TR}} - \lambda_{0_{TR}})(1 - e_{TR})\mu_{y_{TR}}\right] +$$
$$\theta_{tw_{TR}}\left[-(\tfrac{1}{4} - \tfrac{1}{3} e_{TR} + \tfrac{1}{12} e_{TR}^4)(\bar{p}_{TR} - \lambda_{1s_{TR}}) - \tfrac{1}{2}(1 - e_{TR})^2 (\mu_{z_{TR}} - \lambda_{0_{TR}})\mu_{x_{TR}}\right] +$$
$$\frac{\delta_{TR}}{a_{0_{TR}}}(1 - e_{TR}^2)\mu_{x_{TR}} - (\bar{p}_{TR} - \lambda_{1s_{TR}})(1 - e_{TR}^2)(\mu_{z_{TR}} - \lambda_{0_{TR}})$$

and

$$C_{Q_{TR_{trbl}}} = -\frac{1}{2} s_{TR}\, a_{0_{TR}} (C_{Q_{0_{TR}}} + C_{Q_{1c_{TR}}} \cos\psi_{TR} + C_{Q_{1s_{TR}}} \sin\psi_{TR}) \qquad (83)$$

where

$$C_{Q_{0_{TR}}} = -\left[\tfrac{1}{3}(1 - e_{TR}^3)\theta_{0_{TR}} + (\tfrac{1}{4} - \tfrac{1}{3} e_{TR} + \tfrac{1}{12} e_{TR}^4)\theta_{tw_{TR}}\right]\{(\mu_{z_{TR}} - \lambda_{0_{TR}}) +$$

$$\frac{1}{2}[(\bar{p}_{TR} - \lambda_{1s_{TR}})\mu_{x_{TR}} + (\bar{q}_{TR} - \lambda_{1c_{TR}})\mu_{y_{TR}}]\} + \frac{\delta_{TR}}{a_{0_{TR}}}(1 - e_{TR}^2)(1 + e_{TR}^2 + \mu_{TR}^2) -$$
$$\frac{1}{8}(1 - e_{TR}^4)[(\bar{p}_{TR} - \lambda_{1s_{TR}})^2 + (\bar{q}_{TR} - \lambda_{1c_{TR}})^2] - \frac{1}{2}(1 - e_{TR}^2)(\mu_{z_{TR}} - \lambda_{0_{TR}})^2$$

These coefficients are transformed to tail rotor hub axes by applying the transpose of equation (77) to equations (81), (82), (83)

$$C_{X_{TR_{trh}}} = -\frac{1}{4} s_{TR}\, a_{0_{TR}}\, C_{Y_{1s_{TR}}}$$
$$C_{Y_{TR_{trh}}} = -\frac{1}{4} s_{TR}\, a_{0_{TR}}\, C_{Y_{1c_{TR}}}$$
$$C_{Z_{TR_{trh}}} = -\frac{1}{2} s_{TR}\, a_{0_{TR}}\, C_{Z_{0_{TR}}}$$
$$C_{Q_{TR_{trh}}} = -\frac{1}{2} s_{TR}\, a_{0_{TR}}\, C_{Q_{0_{TR}}}$$

(Note that the tail rotor thrust coefficient, $C_{T_{TR}}$ is given by $C_{T_{TR}} = C_{Z_{TR_{trh}}}$)

Finally, these coefficients are transformed to the body fixed set using the transpose of equation (74), then denormalised. Thus, adding the moment componets due to the offset of the tail rotor hub forces from the centre of gravity, the force and moment contributions of the tail rotor to the total external forces and moments of the vehicle are given by

$$X_{TR} = \rho(\Omega_{TR}R_{TR})^2\pi R_{TR}^2\, C_{X_{TR_{trh}}} \quad (84a)$$
$$Y_{TR} = -\rho(\Omega_{TR}R_{TR})^2\pi R_{TR}^2\, C_{Z_{TR_{trh}}} \quad (84b)$$
$$Z_{TR} = \rho(\Omega_{TR}R_{TR})^2\pi R_{TR}^2\, C_{Y_{TR_{trh}}} \quad (84c)$$
$$L_{TR} = h_{TR}\, Y_{TR} \quad (84d)$$
$$M_{TR} = -\rho(\Omega_{TR}R_{TR})^2\pi R_{TR}^3\, C_{Q_{TR_{trh}}} + (x_{cg} + l_{TR})\, Z_{TR} - h_{TR}\, X_{TR} \quad (84e)$$
$$N_{TR} = -(x_{cg} + l_{TR})\, Y_{TR} \quad (84f)$$

5. The Fuselage and Empenage Model

The aerodynamic forces and moments are calculated using look-up tables of aerodynamic coefficents as functions of angle of attack and sideslip derived from wind-tunnel tests. This calculation has been included in such a way that the look-up table could be replaced by a simpler appropriate polynomial representation.

5.1 Fuselage Aerodynamic Forces and Moments

The fuselage angle of incidence is given by

$$\alpha_{Fus} = \tan^{-1}\left(\frac{w}{u}\right) \tag{85}$$

and the fuselage sideslip angle is given by

$$\beta_{Fus} = \sin^{-1}\left(\frac{v}{V_f}\right) \tag{86}$$

where V_f is the flight velocity (i.e. the resultant velocity of the helicopter's centre of gravity) given by

$$V_f = \sqrt{u^2 + v^2 + w^2} \tag{87}$$

The force coefficients in the x and z directions (effectively the drag and lift of the fuselage), $C_{X_{Fus}}$ and $C_{Z_{Fus}}$ and the moment coefficient about the y body axis (effectively the pitching moment), $C_{M_{Fus}}$, are all functions of the angle of incidence α_{Fus}. The fuselage force coefficent in the y axis direction (the side force), $C_{Y_{Fus}}$, and the moment coefficient about the z body axis (effectively the yawing moment), $C_{N_{Fus}}$, are functions the fuselage sideslip angle, β_{Fus}. The wind tunnel data used in the look-up tables were measured relative to the fuselage reference point, directly below the rotor hub. Thus, the moments due to the offset of the aerodynamic forces from the centre of gravity, a distance x_{cg} ahead of it (see Figure 3) must be included. The contributions of the fuselage to the external forces and moments are therefore given by

$$X_{Fus} = \rho(\Omega R)^2 \pi R^2 C_{X_{Fus}} \tag{88a}$$
$$Y_{Fus} = \rho(\Omega R)^2 \pi R^2 C_{Y_{Fus}} \tag{88b}$$
$$Z_{Fus} = \rho(\Omega R)^2 \pi R^2 C_{Z_{Fus}} \tag{88c}$$
$$L_{Fus} = 0 \tag{88d}$$
$$M_{Fus} = \rho(\Omega R)^2 \pi R^3 C_{M_{Fus}} + x_{cg} Z_{Fus} \tag{88e}$$
$$N_{Fus} = \rho(\Omega R)^2 \pi R^3 C_{N_{Fus}} - x_{cg} Y_{Fus} \tag{88f}$$

5.2 Tailplane Forces and Moment

The tailplane is located a distance l_{TP} behind the fuselage reference point and a height h_{TP} above it. The velocity at the tailplane can be expressed in body axes as

$$\mathbf{V}_{TP_b} = (u - q\,h_{TP})\,\mathbf{i_b} + (v + ph_{TP} - r\,(x_{cg} + l_{TP}))\,\mathbf{j_b} + (w + q\,(x_{cg} + l_{TP}))\,\mathbf{k_b}$$

and thus the local angle of incidence at the tailplane is found to be

$$\alpha_{TP} = \alpha_T + \tan^{-1}\left(\frac{w + q\,(x_{cg} + l_{TP})}{u - q\,h_{TP}}\right) \tag{89}$$

where α_T is the fixed incidence of the tail surface. The z-force coefficient corresponding to the incidence angle α_{TP} is obtained from look-up tables. The drag and pitching moment of the tailplane are ignored. The contributions of the tailplane to the external forces and moments are therefore given by

$$X_{TP} = 0 \tag{90a}$$
$$Y_{TP} = 0 \tag{90b}$$
$$Z_{TP} = \rho(\Omega R)^2 S_{TP} C_{Z_{TP}} \tag{90c}$$
$$L_{TP} = 0 \tag{90d}$$
$$M_{TP} = Z_{TP}\,(x_{cg} + l_{TP}) \tag{90e}$$
$$N_{TP} = 0 \tag{90f}$$

where S_{TP} is the tailplane area.

5.3 Fin Forces and Moments

The fin is located a distance l_{Fin} behind the fuselage reference point and a height h_{Fin} above it. The velocity at the fin can be expressed in body axes as

$$\mathbf{V_{Fin_b}} = (u - q\,h_{Fin})\,\mathbf{i_b} + (v + ph_{Fin} - r\,(x_{cg} + l_{Fin}))\,\mathbf{j_b} + (w + q\,(x_{cg} + l_{Fin}))\,\mathbf{k_b}$$

thus the local angle of sideslip is found to be

$$\beta_{Fin} = \beta_F + \sin^{1}\left(\frac{v + p\,h_{Fin} - r\,(x_{cg} + l_{Fin})}{\sqrt{(u - q\,h_{Fin})^2 + (v + ph_{Fin} - r\,(x_{cg} + l_{Fin}))^2 + (w + q\,(x_{cg} + l_{Fin}))^2}}\right) \tag{91}$$

where β_F is the fixed setting of the fin relative to the fuselage centreline. The coefficient of the force in the y direction due to the fin correpsonding to β_{Fin} is obtained also from a lookup table The contributions of the fin to the external forces and moments are therefore given by

$$X_{Fin} = 0 \tag{92a}$$
$$Y_{Fin} = \rho(\Omega R)^2\, S_{Fin}\, C_{Y_{Fin}} \tag{92b}$$

$$Z_{Fin} = 0 \tag{92c}$$

$$L_{Fin} = Y_{Fin}\, h_{Fin} \tag{92d}$$

$$M_{Fin} = 0 \tag{92e}$$

$$N_{Fin} = Y_{Fin}\,(x_{cg} + l_{Fin}) \tag{92f}$$

where S_{Fin} is the fin surface area.

6. Presentation of Some Results

As indicated in the introduction, by creating the mathematical model in the modular form given in this report, it has been possible to write a series of algorithms capable of performing many of the common flight mechanics studies. Consequently, as well as driving the helicopter inverse simulation Helinv, HGS is also used to calculate trim conditions for steady flight, aerodynamic derivatives, eigenvalues and response time histories to control inputs. The aim of this section is to present some results from conventional simulations as well as from the Helinv inverse simulation and thereby show that the HGS model gives qualitatively correct trends. Ideally it would be desirable to perform a validation exercise at this stage, however only limited appropriate flight data is available. It is hoped that more data will become available in the near future, at which time a comprehensive validation process will be reported. The alogrithms used to calculate the follwing results will also be documented at a later date. All of the results presented were calculated using a set of configurational data representing a Westland Lynx helicopter.

6.1 Results from Conventional Simulations

6.1.1 Trim Results

The equations of motion (1a - 1f) are solved for a steady flight condition by firstly setting the acceleration terms to zero. For the results presented here it was assumed that the vehicle was in straight line flight and therefore the body angular velocities were all zero. Hence, from equations (1) and from the engine equation (A2.2) the trim problem reduces to the solution of the following seven nonlinear algebraic equations

$$X - mg\sin\theta = 0$$

$$Y + mg\cos\theta\sin\phi = 0$$

$$Z + mg\cos\theta\cos\phi = 0$$

$$L = 0$$

$$M = 0$$

$$N = 0$$

$$K_3 (\Omega - \Omega_i) - Q_E = 0$$

The seven unkonown variables are the four controls, main rotor collective, longitudinal and lateral cyclic and tail rotor collective, the fuselage pitch and roll angles, and the rotor speed. Figures 10 - 13 show the trim values of the helicopter states, controls and rotor parameters for a Westland Lynx helicopter at a range of constant velocities.

Figure 10 shows the control angles necessary to trim the vehicle at a range of flight velocities. The main rotor collective plot is of a familiar form, there is an initial decrease in required collective as increased forward velocity allows a reduction in pitch whilst still maintaining the necessary thrust. As speed increases and the disc is titled forward, indicated by increasing longitudinal flapping angle, Figure 11, and decreasing longitudinal cyclic, Figure 10 (note that the negative sign denotes a forward stick input), the thrust vector is tilted forward. Thus, to maintain a component able to balance the vehicle weight, the total thrust is increased by additional collective. The coning angle of the rotor disc, shown in Figure 11, follows the collective pitch : all of the blades flapping by a similar amount in response to a collective pitch input. The effect of the forward tilt of the rotor is that a nose down pitching moment is produced and the fuselage tends to pitch in this direction, Figure 12.

Tail rotor collective produces a thrust, and hence torque about the centre of gravity, proportional to, but in the opposite sense to, the torque produced by the main rotor. Changes in main rotor collective (and hence torque) will be accompanied by changes to tail rotor collective. The trend of main and tail rotors are therefore similar, the main additional influence being the sidesforce of the fin which produces a torque about the centre of gravity. This influence becomes greater at higher velocities.

The power required is shown in Figure 13 and, as the rotor drag is a function of the blade pitch angle, the power curve follows the same trend as collective. Also plotted in Figure 13 are the engine torque, rotor speed and rotor induced velocity.

6.1.2 Response to Control Inputs

The effect on the external forces and moments on the vehicle due to changes in the controls can be calculated using the expressions given in sections 3 and 4. This allows equations (1) to be solved to give the vehicle response to these applied control inputs.

Examples of the Lynx response to two inputs, both are applied from an 80 knots trimmed flight state, are presented here. The full flapping equations (71) are also solved simultaneously with the body equations (1).

a) One Degree Step in Collective

The step is applied at the start of the time history and is positive signifying an increase in the pitch angle of the blades. The state response to this input is shown in Figure 14, the attitude response in Figure 15 and the flapping angles in Figure 16. The immediate effect of the collective input is to cause the rotor disc to tilt back thereby producing a nose-up pitching moment on the fuselage. The nose-up attitude causes the helicopter to decelerate as it begins to climb. As the disc begins to tilt forward again and the nose pitches down, the additional thrust due to the increased collective allows the helicopter to climb at a higher rate. The additional rotor torque due to increased collective has not been balanced by the tailrotor, and therefore the aircraft begins to yaw and roll.

b) Longitudinal Cyclic Doublet

The input for this doublet is shown in Figure 17, with the initial stick motion being forward. The state response to this input is shown in Figure 18, the attitude response in Figure 19 and the flapping angles in Figure 20. The initial response is for the helicopter's nose to pitch down, Figure 19, as the disc tilts forward (increased longitudinal flapping, Figure 20). The aircraft then begins to accelerate and descend. Shortly after the input direction is reversed (at one second) the nose begins to pitch up again reducing the acceleration and descent rate and there is a reversal in the direction of roll. On returning the longitudinal cyclic to its trim value aircraft continues to pitch nose up losing speed and climbing.

6.2 Results from Inverse Simulations

6.2.1 The Pop-up Manoeuvre

The flight path profile of a Pop-up manoeuvre for use in a Helinv inverse simulation is shown in Figure 21, and its mathematical description is given in Reference 12. This manoeuvre would typically be used to avoid an obstacle whilst flying at some forward flight speed. The height of the obstacle and the distance from it at the entry to the manoeuvre are defined as well as a constant flight velocity. In the example given here, the obstacle height is 25m and the manoeuvre is initiated from a distance of 200m at a velocity of 80 knots. The control displacements calculated by Helinv are shown in Figure 22 whilst the body attitudes and velocities are shown in Figures 23 and 24 respectively. The initial control inputs, Figure

22, consist of a rapid increase of collective along with a decrease in longitudinal cyclic indicating a rearward motion of the stick causing the aircraft to pitch up, Figure 23, and climb. As the collective is increased the longitudinal cyclic starts to decrease (stick forward) in order to maintain the demanded constant forward speed. This pull-up phase is over after about two seconds and is followed by a push-over between two and four seconds. During this phase the stick is pushed forward and thrust reduced until the nose pitches down to a minimum of 10 degrees. After four seconds there is a rapid increase in thrust and a forward motion of the stick to ensure a level exit condition.

6.2.2 The Side-step Manoeuvre

The profile for this lateral repositioning manoeuvre is shown in Figure 25 and its mathematical description is given in Reference 12. It is assumed that this manoeuvre is flown at constant height and heading. Figures 26, 27 and 28 show the control inputs, attitude and velocity time histories for a simulated Lynx helicopter flying a sidestep of length 100m and with a maximum lateral velocity of 40 knots. Figure 26 shows that the manoeuvre is initiated by a rapid input of lateral cyclic. This tilts the disc in he appropriate direction and is followed (at about 1 second) by an input of collective to produce the thrust required for the lateral acceleration. The aircraft rolls to about 30 degrees, Figure 27, and accelerates to a sideslip velocity of approximately 20 m/s, Figure 28. This maximum velocity is demanded at the midway point of the manoeuvre, just after 5 seconds, and zero acceleration is also specified at this point. Consequently, as this point is approached, collective is reduced, and opposite lateral cyclic applied. In the second half of the manoeuvre the aircraft is decelerated back to the hover. This is initiated by continued decreasing of thrust and allowing the vehicle to roll in the opposite direction. As the end of the manoeuvre approaches there is a rapid input of lateral cyclic to bring the aircraft back to an upright attitude in the hover.

6.2.3 The Transient Turn Manoeuvre

Figure 29 (a) shows the method used to define a transient turn manoeuvre, and Figure 29 (b) shows the resulting track. The main body of the manoeuvre consists of a circular arc of radius R_c. Flying this part of the manoeuvre the helicopter will have a finite turn rate. Clearly, as the vehicle approaches and leaves the manoeuvre in straight line flight, transient sections covering the region between straight line flight and flight around a circular arc are required. The turn rate function used is shown in Figure 29 (a). The resulting turn can be compared to a circular arc with equivalent radius R_e as shown in Figure 29 (b). Figures 30, 31 and 32 show the control, attitude and velocity time histories of a simulated Lynx helicopter flying a 90 degrees, right hand, transient turn manoeuvre where the equivalent radius is 200m and the constant velocity is 80 knots. The manoeuvre was assumed to be at constant height and the

transient portions accounted for 15% of the total turn each (the figure of 15% was obtained by comparison with flight data, [12]).

The manoeuvre is initiated by a pulse in lateral cyclic, Figure 30, which is accompanied by an increase in thrust (to maintain constant height as the helicopter rolls) and a forward motion of the stick (to maintain constant velocity). The helicopter rolls to about 50 degrees after approximately 2 seconds, Figure 31 after encountering its peak roll rate of 45 degrees/s, Figure 32. This attitude, and the control positions are maintained throughout the circular portion of the manoeuvre until after about 6 seconds the helicpter is rolled in the opposite direction until a level straight line flight state is attained.

7. Conclusions

1. It has been possible to create a rotor multiblade disc model but still maintain many important terms by using a symbolic algebra computer package to perform the necessary algebraic manipulation.

2. A comprehensive validation exercise will be performed on the HGS model in the near future - initial results are encouraging.

3. The inclusion of meaningful nonlinear aerodynamic effects in a multiblade model is still difficult despite the use of computational algebra.

4. Future small scale upgrades and modifications to the HGS multiblade model are likely.

5. Any future major modification the the Helinv inverse simulation model will almost certainly be to replace the multiblade HGS model by an individual blade model.

Appendix 1 : Rotor Induced Flow

In its current form the HGS model has a rudimentery, but possibly the most widely used, induced flow model. This is based on the assumption that the induced flow consists of a uniform component over the whole disc, v_0, and longitudinal and lateral components which vary from the root to the tip of each blade, v_{1_s} and v_{1_c}. The induced velocity can then be written in the form

$$v_i = v_0 + \frac{r_b}{R}(v_{1_s}\sin\psi + v_{1_c}\cos\psi) \qquad \text{(A1.1)}$$

which is normalised (dividing by ΩR) to give

$$\lambda_i = \lambda_0 + (1 - e)\bar{r}_b(\lambda_{1_s}\sin\psi + \lambda_{1_c}\cos\psi) \qquad \text{(A1.2)}$$

where $$\lambda_0 = \frac{v_0}{\Omega R}, \quad \lambda_{1_c} = \frac{v_{1_c}}{\Omega R}, \quad \lambda_{1_s} = \frac{v_{1_s}}{\Omega R}$$

The uniform component is obtained from momentum theory and is given by

$$\lambda_0 = \frac{C_T}{2\sqrt{\mu^2 + (\mu_z - \lambda_0)^2}} \qquad \text{(A1.3)}$$

where μ_z is the normal velocity component of the rotor hub, μ is the rotor hub in-plane normalised velocity given by

$$\mu = \sqrt{\mu_x^2 + \mu_y^2}$$

and C_T is the main rotor thrust coefficient ($C_T = C_{Z_{A_0}}$) derived in section (3.2.1). This equation may be solved iteratively to obtain the uniform inflow component λ_0 for a particular velocity and thrust coefficient.

To obtain the harmonic components of the induced velocity a new axes set, known as hub-wind axes (denoted by the subscript w), is introduced. This is an axes set alligned with the resultant in-plane velocity vector of the rotor hub, Figure A1(a) and is obtained by a rotation about the hub z axis through the rotor sideslip angle ψ_w. The rotor sideslip angle is given by

$$\tan\psi_w = \frac{\mu_y}{\mu_x} \tag{A1.4}$$

and the transformation from hub to hub wind axes is then

$$\begin{bmatrix} \mathbf{i}_w \\ \mathbf{j}_w \\ \mathbf{k}_w \end{bmatrix} = \begin{bmatrix} \cos\psi_w & \sin\psi_w & 0 \\ -\sin\psi_w & \cos\psi_w & 0 \\ 0 & 0 & 1 \end{bmatrix} \begin{bmatrix} \mathbf{i}_h \\ \mathbf{j}_h \\ \mathbf{k}_h \end{bmatrix} \tag{A1.5}$$

The effect of the rotor continuously shedding circular vortex rings is modelled by including a fore and aft distribution of induced velocity. This is given in the form

$$\lambda_{1c_w} = \lambda_0 \tan\frac{\chi_w}{2} \qquad \chi_w < \frac{\pi}{2}$$

$$\lambda_{1c_w} = \lambda_0 \cot\frac{\chi_w}{2} \qquad \chi_w > \frac{\pi}{2} \tag{A1.6}$$

where the rotor wake angle χ_w, defined in Figure A1(b), is given by

$$\tan\chi_w = \frac{\mu}{(\mu_z - \lambda_0)} \tag{A1.7}$$

By making the transformation to hub-wind axes that lateral component of the induced velocity is zero,

$$\lambda_{1s_w} = 0 \tag{A1.8}$$

The harmonic components of the induced velocity in hub axes, λ_{1s} and λ_{1c} are then obtained by transformation using equation (A1.5).

Work has recently been completed in the upgrade of the HGS model to include dynamic inflow [13] and also to model the vortex ring state, a region of the flight envelope in which momentum theory is not valid.

Appendix 2 : Engine Model

The response of the rotor in terms of its angular velocity associated with torque changes is modelled in HGS by the inclusion of an engine and rotorspeed governer model. This model is esentially that given by Padfield [3] and therefore only brief details are given here. Rotorspeed can be equated to engine torque Q_E, by the equation

$$\dot{\Omega} = (Q_E - Q_R - Q_{TR} - Q_{tr})/I_R + \dot{r} \qquad \text{(A2.1)}$$

where the rotor torque, Q_R, and transmission torque, Q_{tr}, are given by equation (61) as

$$Q_R = b\,Q_0 \quad \text{and} \quad Q_{tr} = I_{tr}\,\dot{\Omega}$$

The rotor inertia I_R, is the sum of the inertia of the individual blades i.e. $I_R = b\,I_\beta$. The tailrotor torque is given by (84e) as

$$Q_{TR} = \rho(\Omega_{TR}R_{TR})^2\pi R_{TR}^3\, C_{Q_{TR_{trh}}}$$

The engine governer equation is given by Padfield as

$$\ddot{Q}_E = \frac{1}{\tau_{e_1}\tau_{e_2}}\left[-(\tau_{e_1} + \tau_{e_3})\dot{Q}_E - Q_E + K_3(\Omega - \Omega_i + \tau_{e_2}\dot{\Omega})\right] \qquad \text{(A2.2)}$$

where Ω_i is the angular velocity of the rotor at idle.

This equation was derived by considering the engine and rotorspeed governer as two first order systems with feedback loops. Firstly, in response to a change in the rotorspeed, the governer would demand a change in the fuel flow. The time constant associated with this lag is τ_{e_1}. Secondly, there will be a lag associated with the engine response to the change in fuel flow rate. The time constants associated with this lag are τ_{e_2} and τ_{e_3} whilst the gain is given by K_3. The time constant τ_{e_1} does not vary with engine torque, however it is assumed that τ_{e_2} and τ_{e_3} are linear functions of engine torque and take the form

$$\tau_{e_2} = \tau_{2_0} + \tau_{2_1}(Q_E/Q_{E_{100\%}})$$
$$\tau_{e_3} = \tau_{3_0} + \tau_{3_1}(Q_E/Q_{E_{100\%}})$$

where τ_{2_0}, τ_{2_1}, τ_{3_0}, and τ_{3_1} are constants and is the engine torque at 100% power.

References

1. Thomson, D.G., "Evaluation of Helicopter Agility Through Inverse Solution of the Equations of Motion", Ph.D. Dissertation, Department of Aeronautics and Fluid Mechanics, University of Glasgow, May 1987.

2. Thomson, D.G., "An Analytical Method of Quantifying Helicopter Agility", Paper 45, Proceedings of the 12th European Rotorcraft Forum, Garmisch-Partenkirchen, Federal Republic of Germany, Spetember 1986.

3. Padfield, G.D., "A Theoretical Model of Helicopter Flight Mechanics for Application to Piloted Simulation", Royal Aircraft Establishment, TR 81048, April 1981.

4. Thomson, D.G., Bradley, R., "Development and Verification of an Algorithm for Helicopter Inverse Simulation", Vertica, Vol. 14, No. 2, May 1990.

5. Thomson, D.G., Bradley, R., "Prediction of the Dynamic Characteristics of Helicopters in Constrained Flight", The Aeronautical Journal, Dec. 1990.

6. Thomson, D.G., Bradley, R. "Mathematical Representation of Manoeuvres Commonly Found in Helicopter Nap-of-the-Earth Flight", Department of Aeronautics and Fluid Mechanics, University of Glasgow, Internal Report, Aero. Report 8801, Feb.1988.

7. Thomson, D.G., Bradley, R., "Modelling and Classification of Helicopter Combat Manoeuvres", Proceedings of ICAS Congress, Stockholm, Sweden, September 1990.

8. Thomson, D.G., Bradley, R., "Validation of Helicopter Mathematical Models by Comparison of Data from Nap-of-the-Earth Flight Tests and Inverse Simulations", Paper No. 78, Proceedings of the 14th European Rotorcraft Forum, Milan, Italy, September 1988.

9. Bradley, R., Padfield, G.D., Murray-Smith, D.J., Thomson, D.G., "Validation of Helicopter Mathematical Models", Transactions of the Institute of Measurement and Control, Vol. 12, No. 4, 1990.

10. Houston, S.S., "Rotorcraft Simulation for Design Applications", Proceedings of the 1992 European Simulation Multiconference, June 1992, ISBN 1-56555-013-7

11. Wolfram, S., "Mathematica. A System for Doing Mathematics by Computer", 2nd Edition, Addison-Wesley, ISBN 0-201-51502-4, 1991.

12. Thomson, D.G., Bradley, R., "Mathematical Definition of Helicopter Manoeuvres", University of Glasgow, Department of Aerospace Engineering Internal Report 9225, June 1992.

13. Taylor, C., Thomson, D.G., Bradley, R., "Rotor Inflow Modelling Enhancements to Helicopter Generic Simulation Mathematical Model", University of Glasgow, Department of Aerospace Engineering Internal Report 9215, June 1992.

Acknowledgements

The author wishes to thank The Royal Society for their continued support of this work. The co-operation Dr Gareth Padfield of the Defence Research Agency, RAE Bedford, is also appreciated, with particular reference to the use of look-up tables and helicopter configurational data.

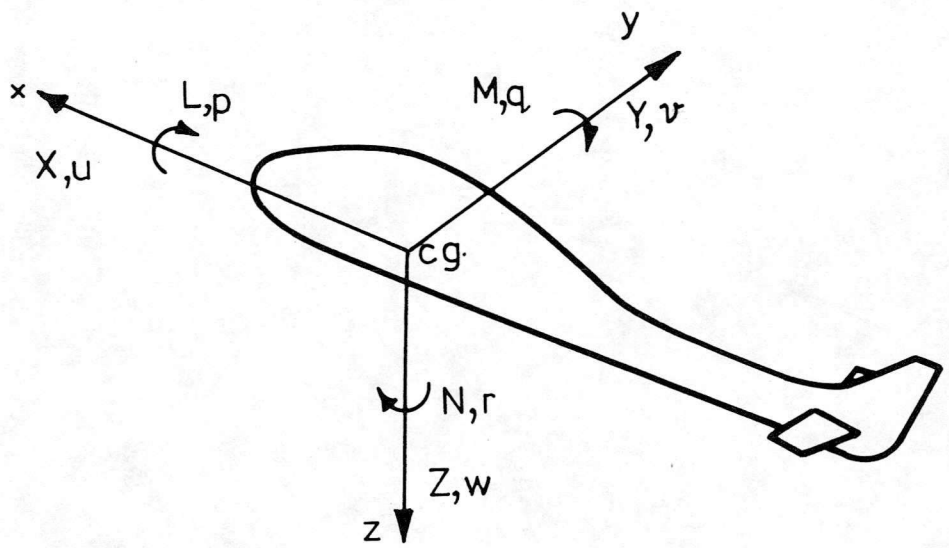

Figure 1 : The Body Fixed Axes Set

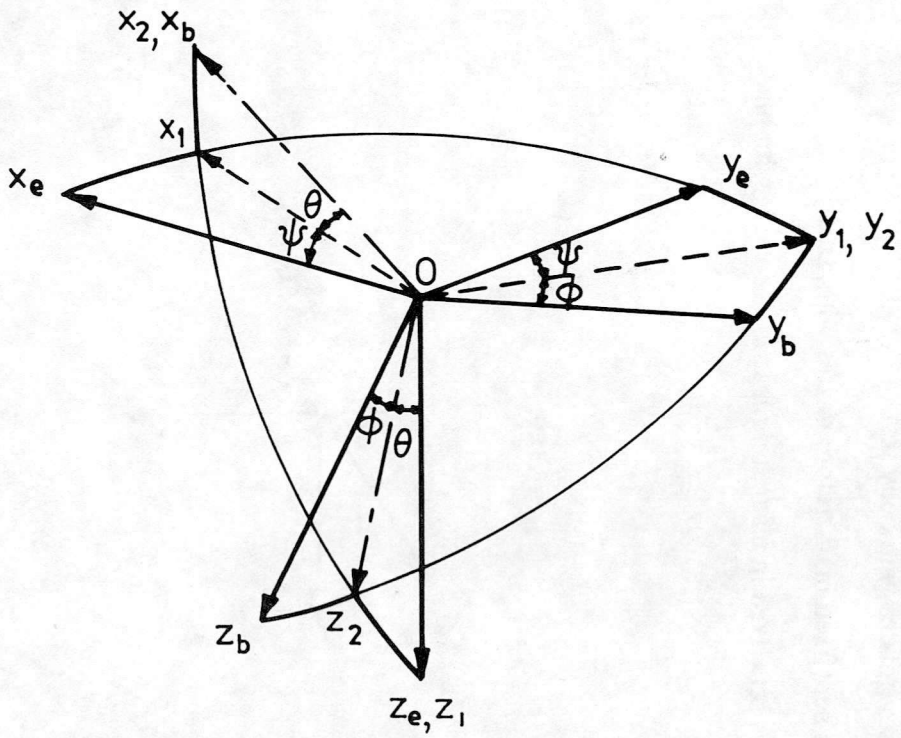

Figure 2 : Euler Angle Transformation

b body axes set

h hub axes set (rotates with body set)

s shaft axes set (fixed in, therefore rotates with, shaft)

bl blade axes set (fixed in blade, origin at root, rotates with blade)

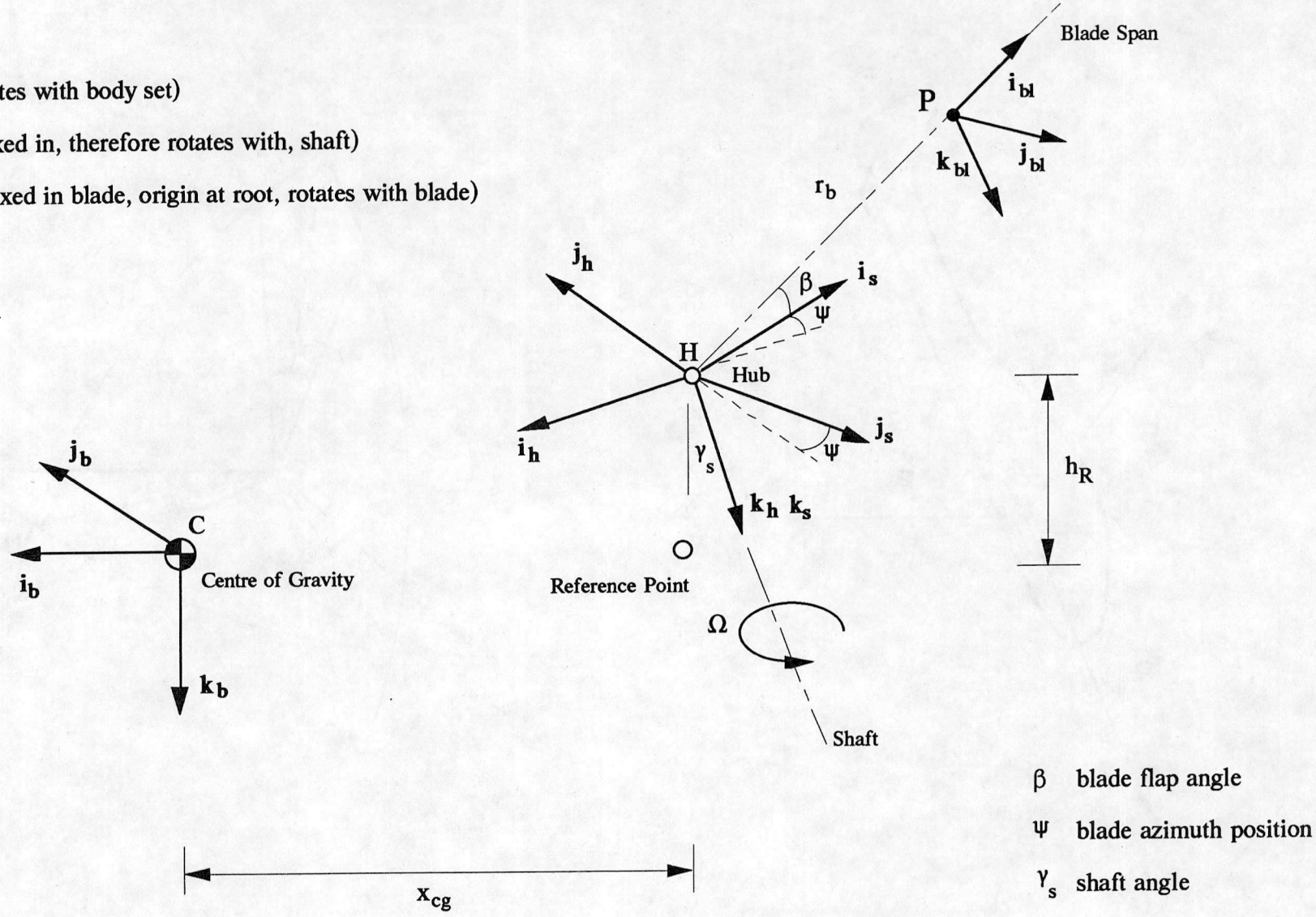

β blade flap angle

ψ blade azimuth position

γ_s shaft angle

Figure 3 : Axes Sets for Blade Kinematics and Calculation of Blade Loads

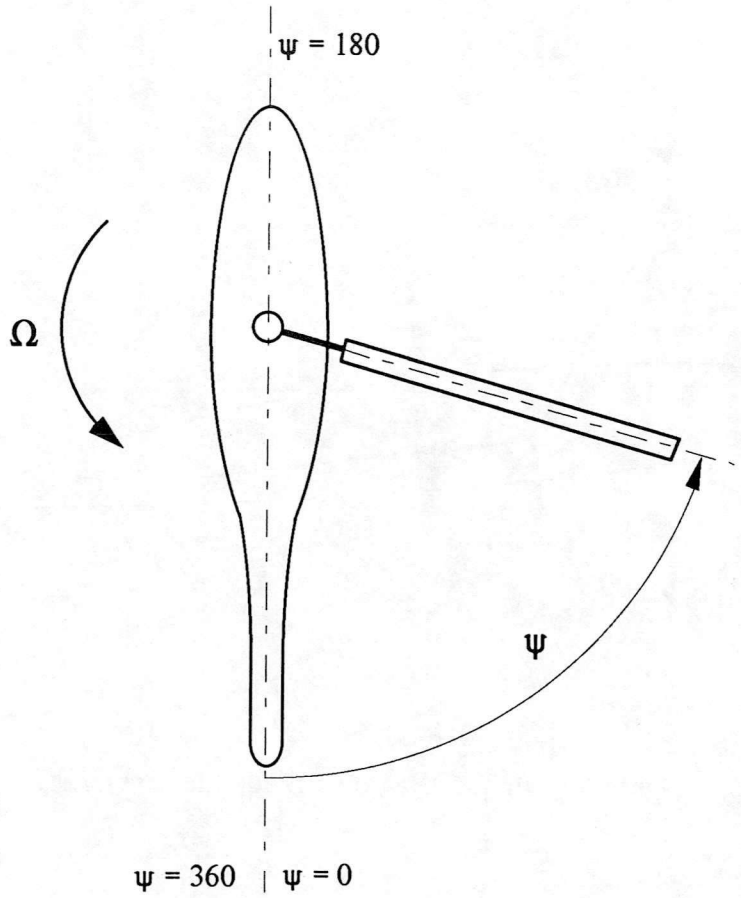

Figure 4 : Measurement of Azimuth Angle

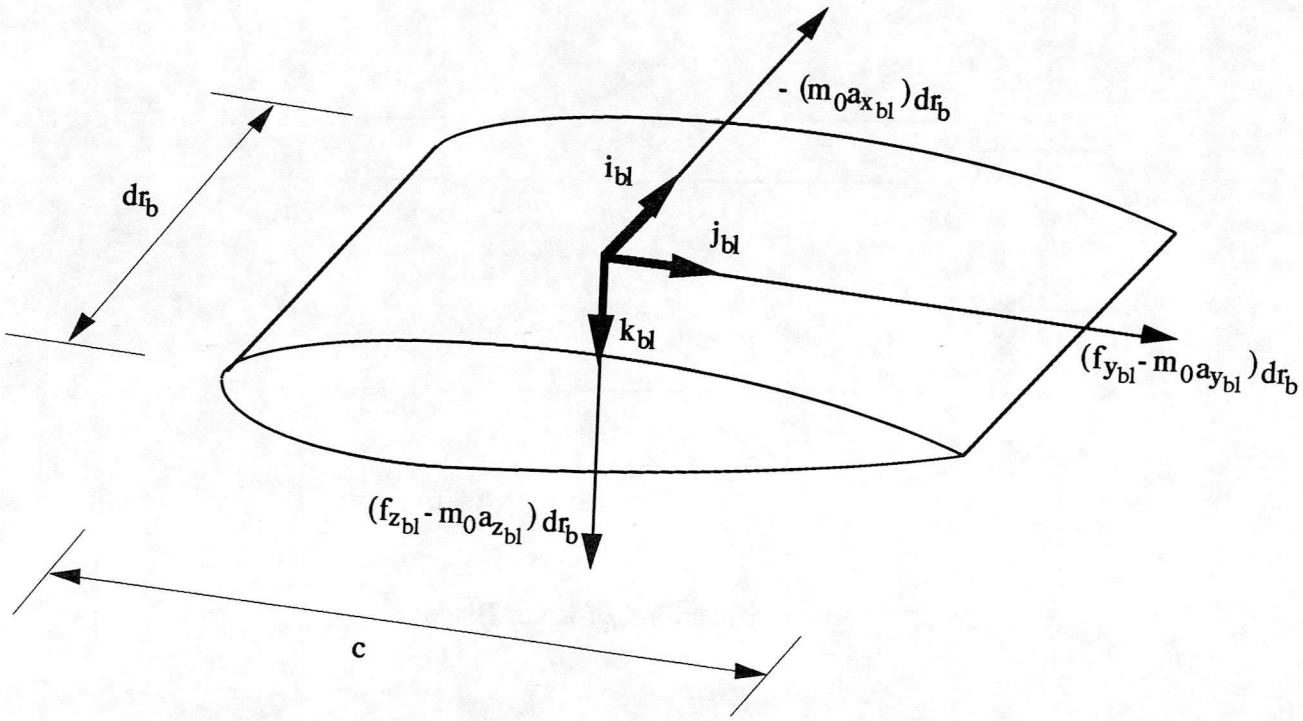

Figure 5 : Forces on a Blade Element

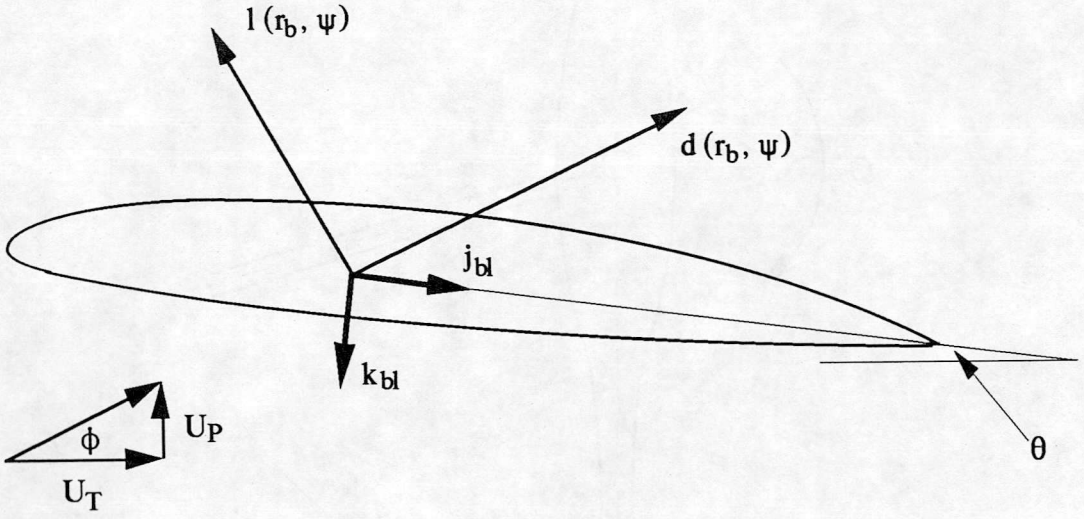

Figure 6 : Lift and Drag on a Blade Element

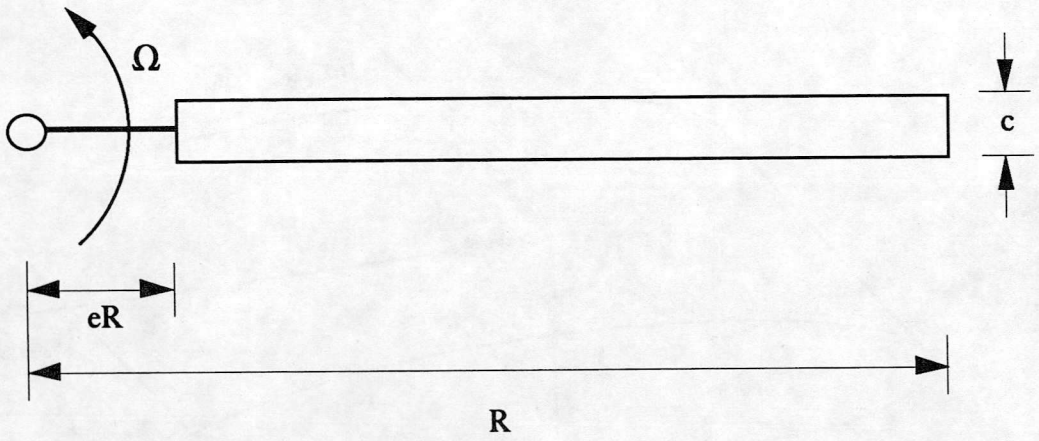

Figure 7 : Planform of Rotor Blade

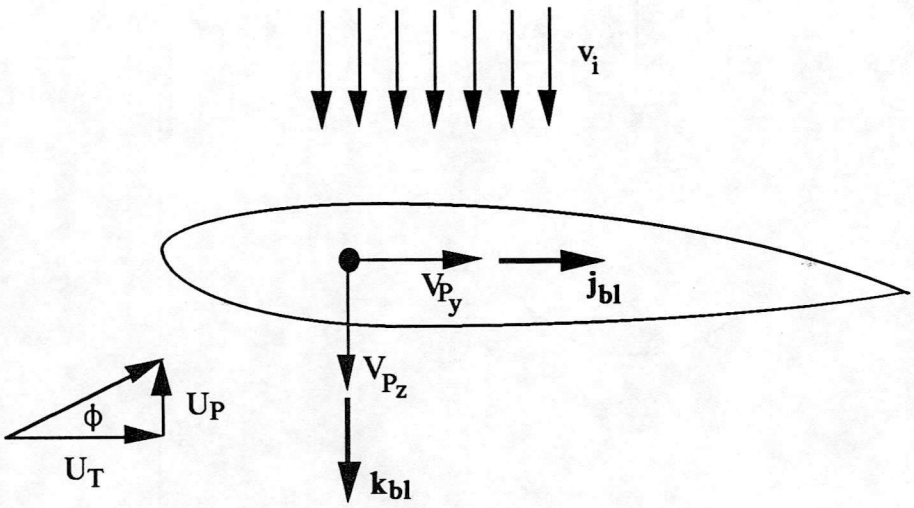

Figure 8 : Blade Element Velocities

b body axes set

htr tail rotor hub axes set (rotates with body set)

bltr tail rotor blade axes set (fixed in blade, origin at root, rotates with blade)

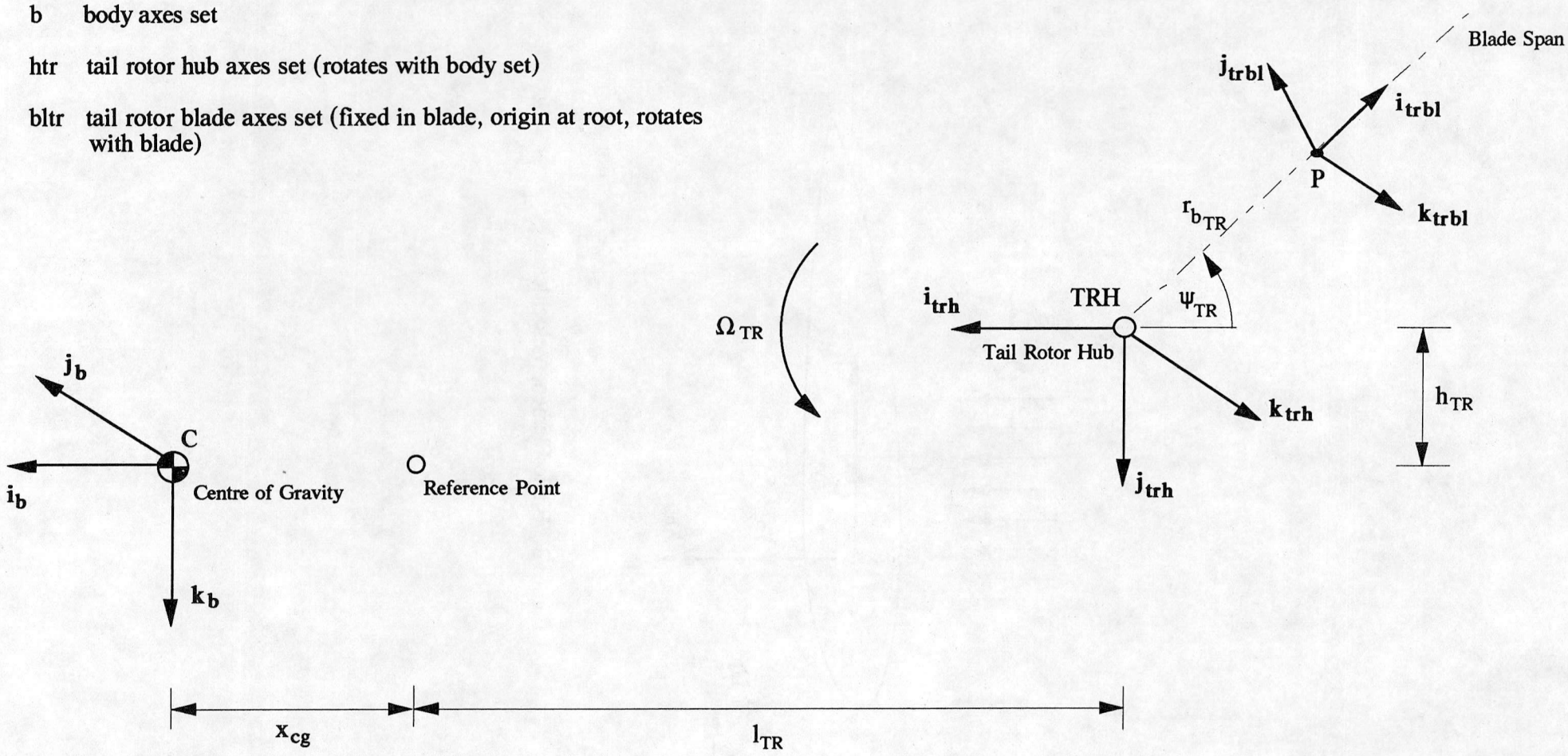

Figure 9 : Axes Sets for Tail Rotor Blade Kinematics and Load Calculation

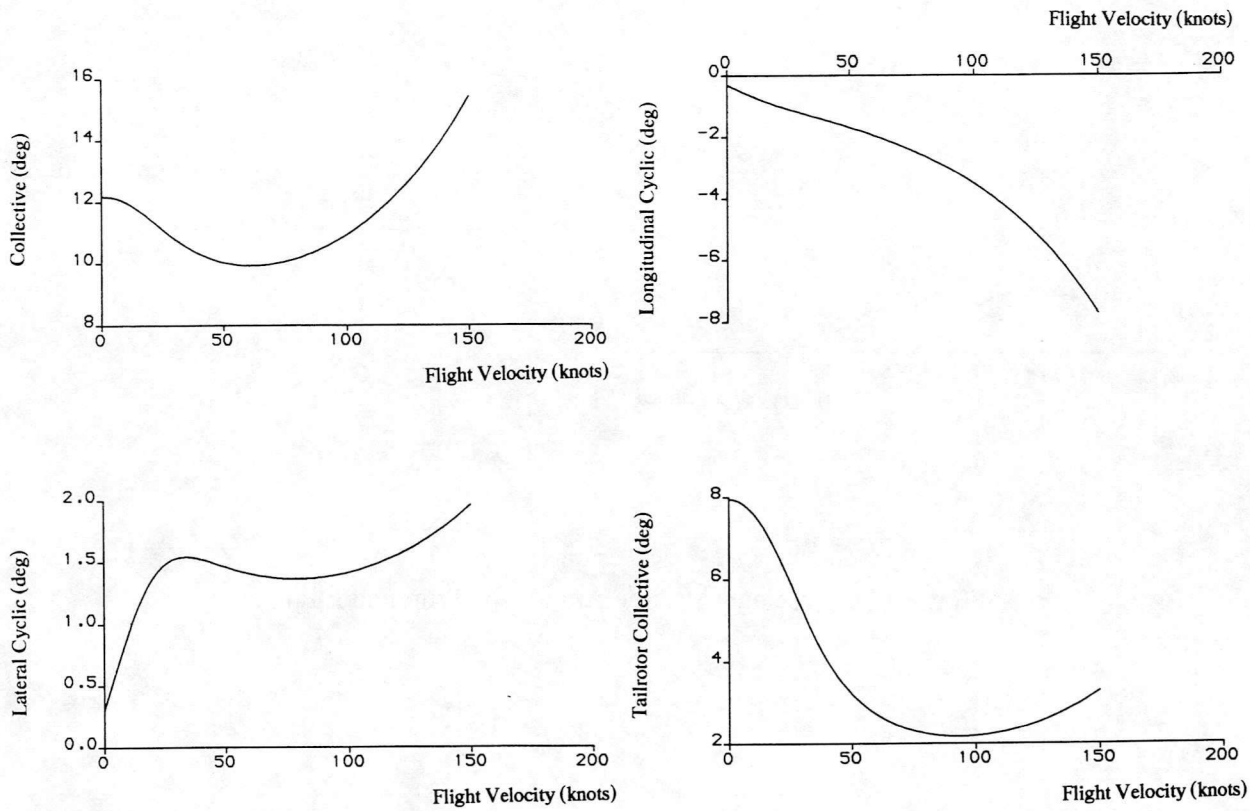

Figure 10 : Control Angles for Westland Lynx to Trim at a Range of Flight Velocities

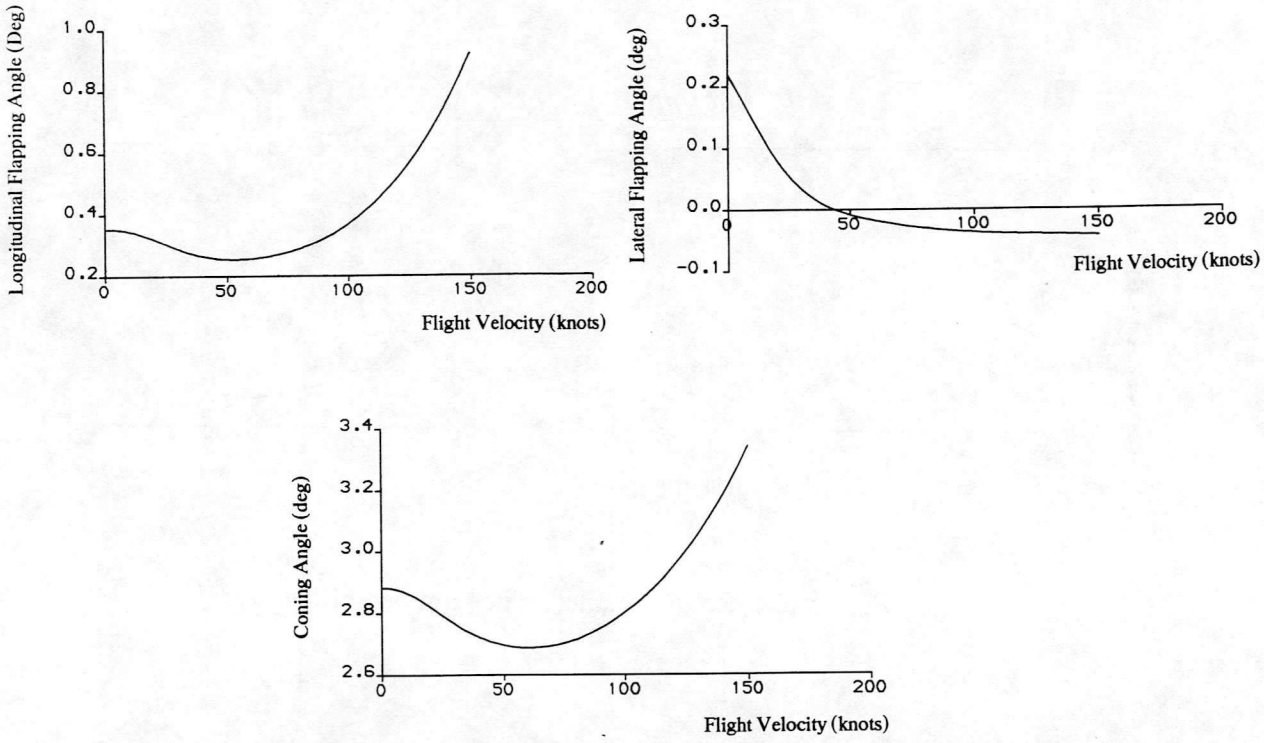

Figure 11 : Main Rotor Flapping Angles for Trimmed Flight

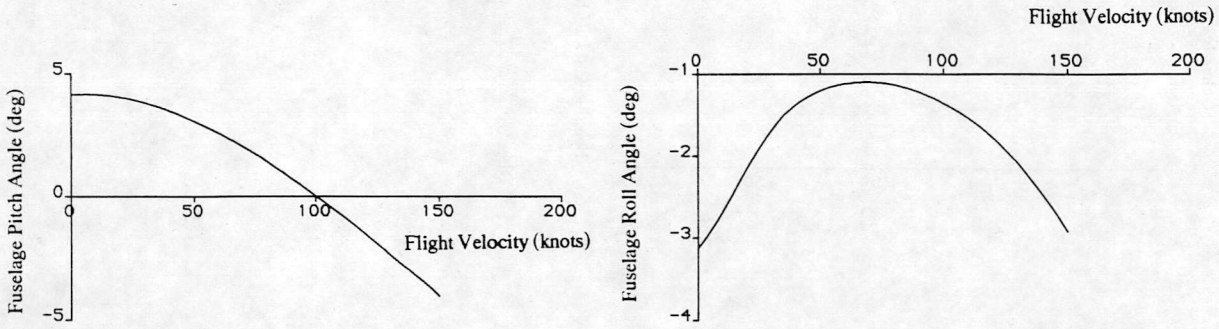

Figure 12 : Fuselage Attitude Angles for Trimmed Flight

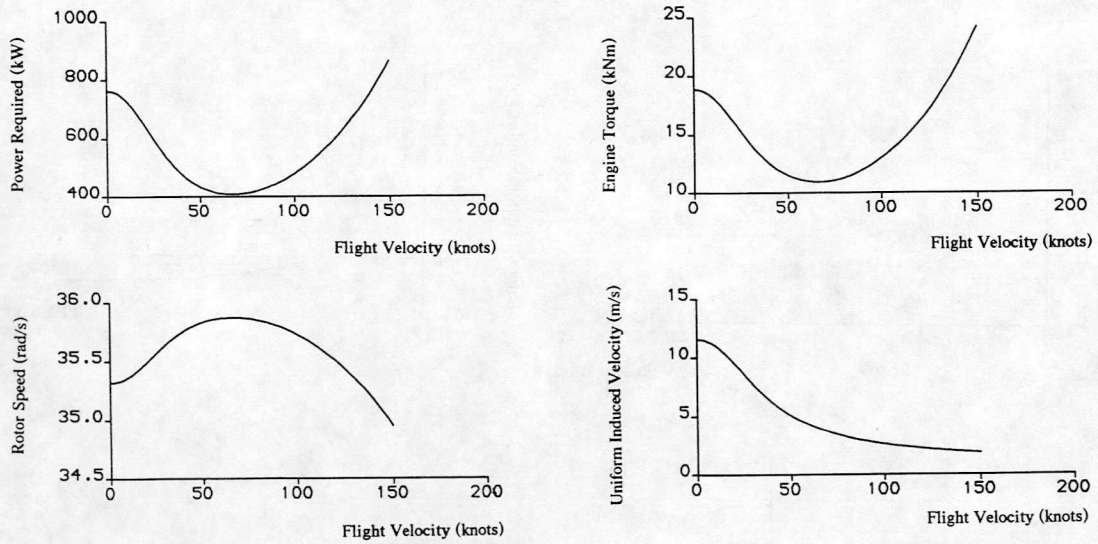

Figure 13 : Rotor Parameters in Trimmed Flight

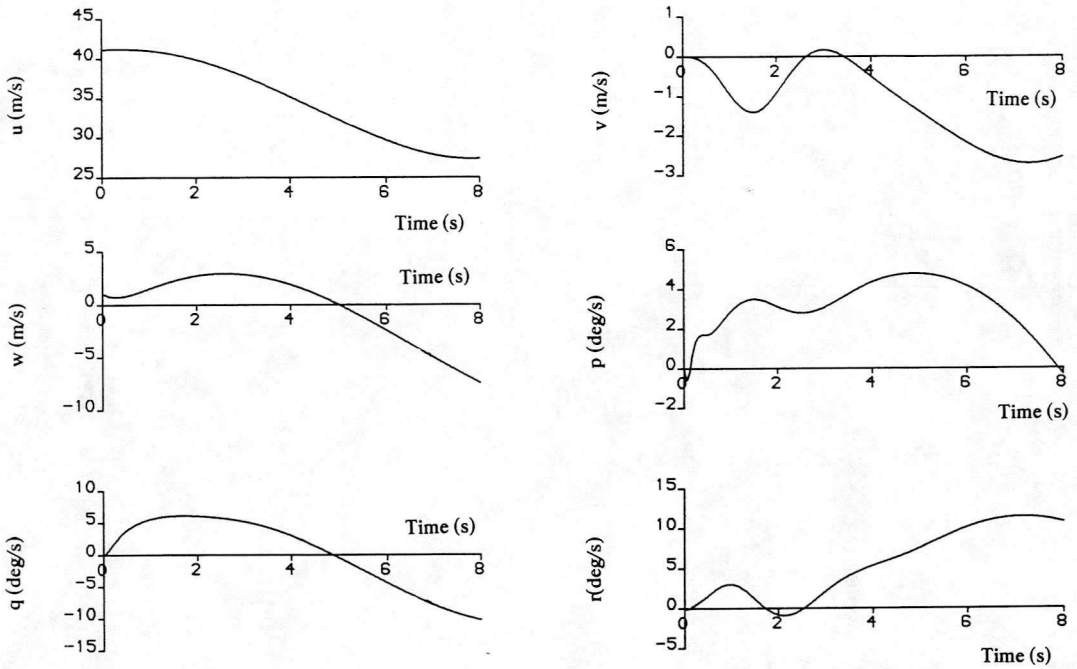

Figure 14 : State Response of Lynx Flying at 80 knots to a 1 Degree Step Input of Collective

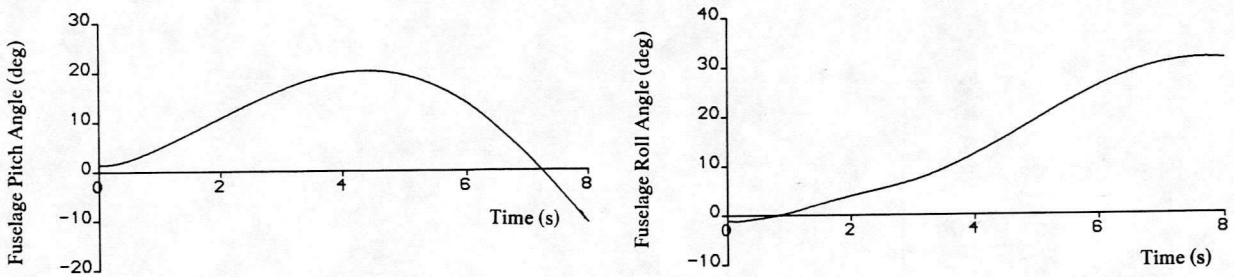

Figure 15 : Attitude Response of Lynx Flying at 80 knots to a 1 Degree Step Input of Collective

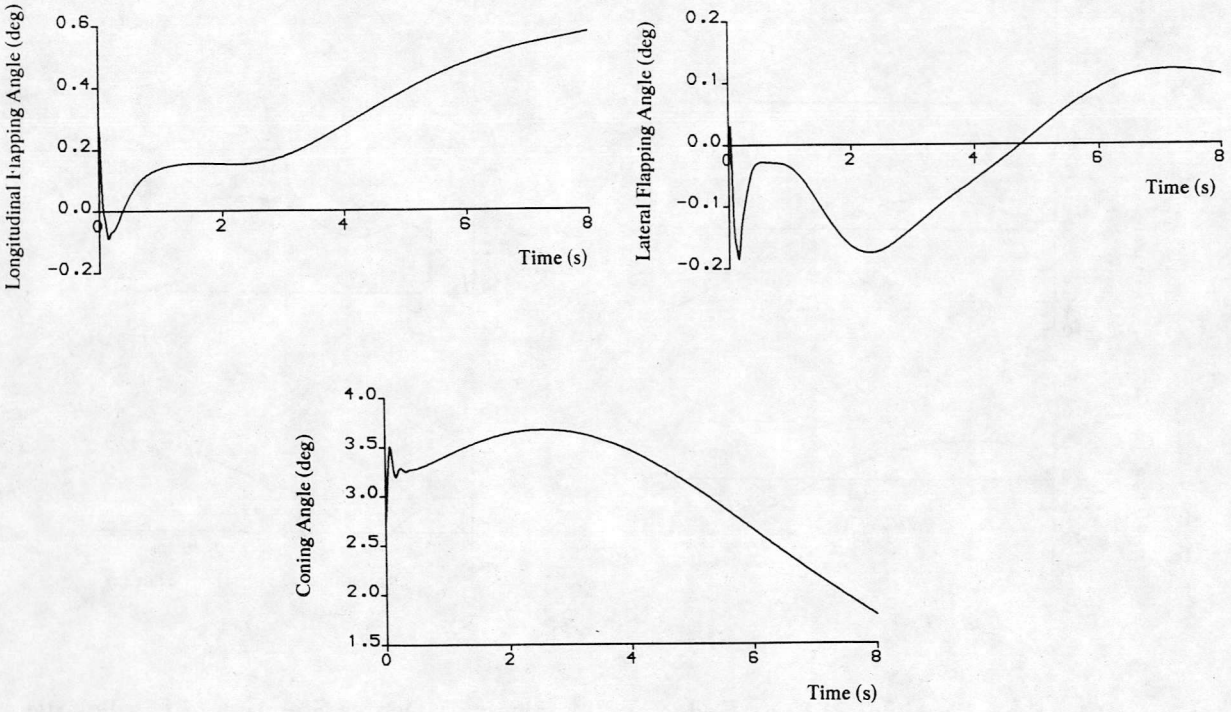

Figure 16 : Blade Flapping Response of Lynx Flying a 80 knots to a 1 Degree Step Input of Collective

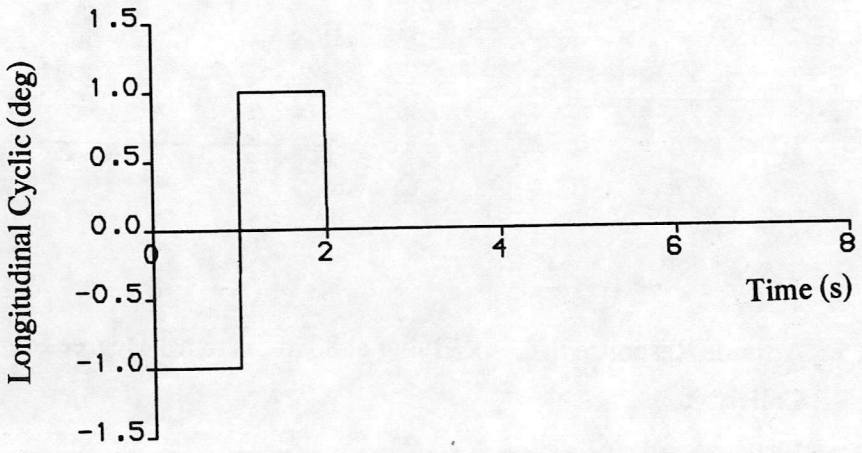

Figure 17 : One Degree Doublet Input in Longitudinal Cyclic

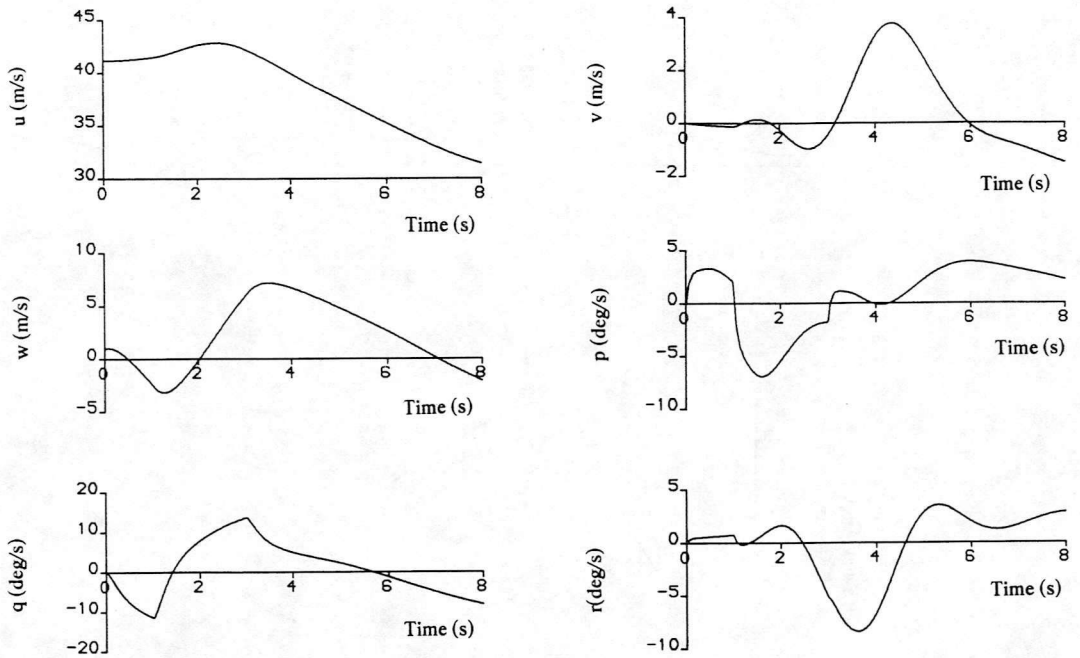

Figure 18 : State Response of Lynx Flying at 80 knots to a 1 Degree Doublet Input of Longitudinal Cyclic

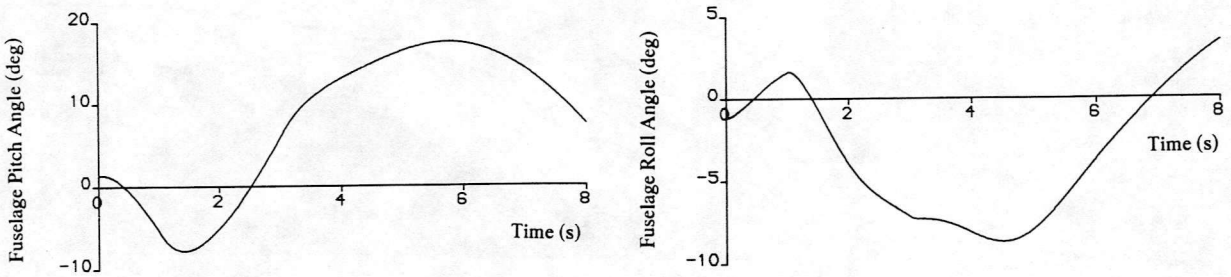

Figure 19 : Attitude Response of Lynx Flying at 80 knots to a 1 Degree Doublet Input of Longitudinal Cyclic

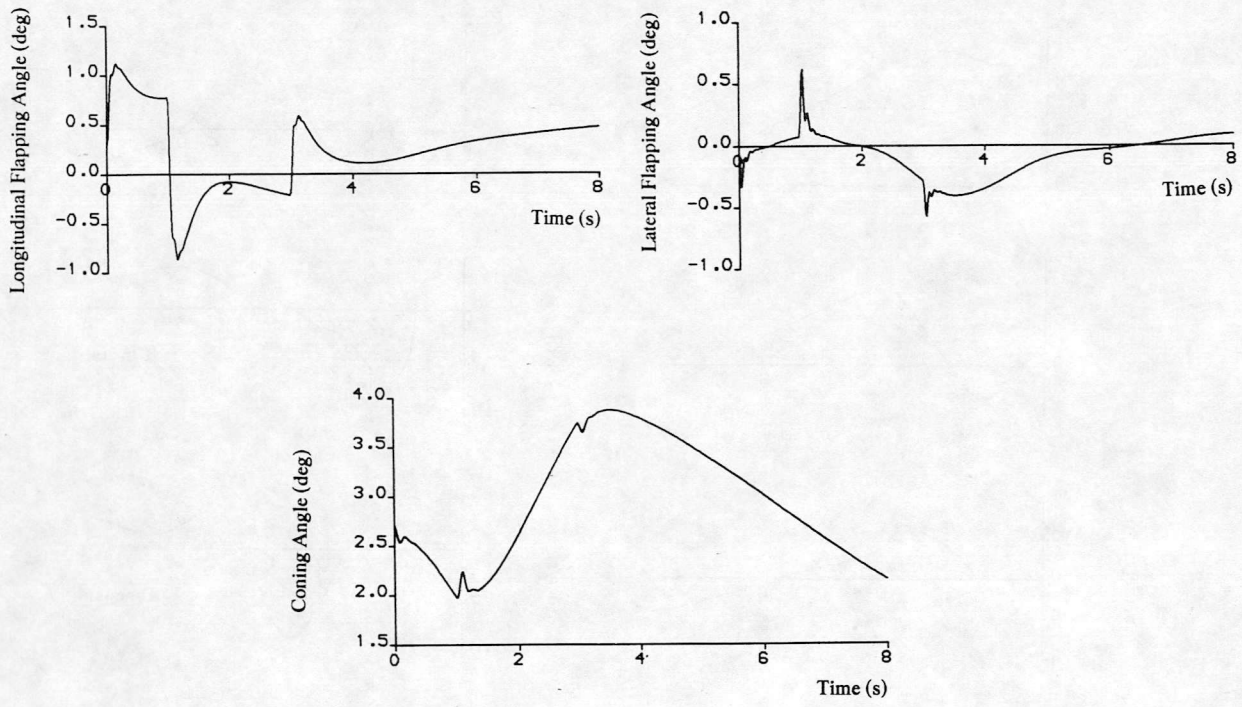

Figure 20 : Blade Flapping Response of Lynx Flying a 80 knots to a 1 Degree Doublet Input of Longitudinal Cyclic

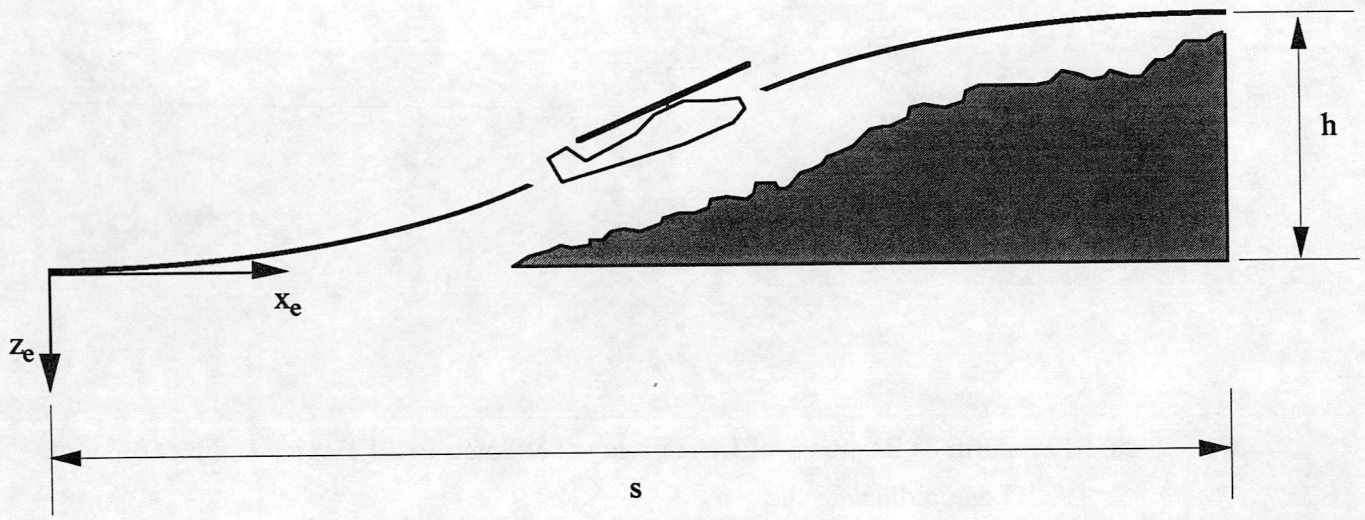

Figure 21 : The Pop-up Manoeuvre

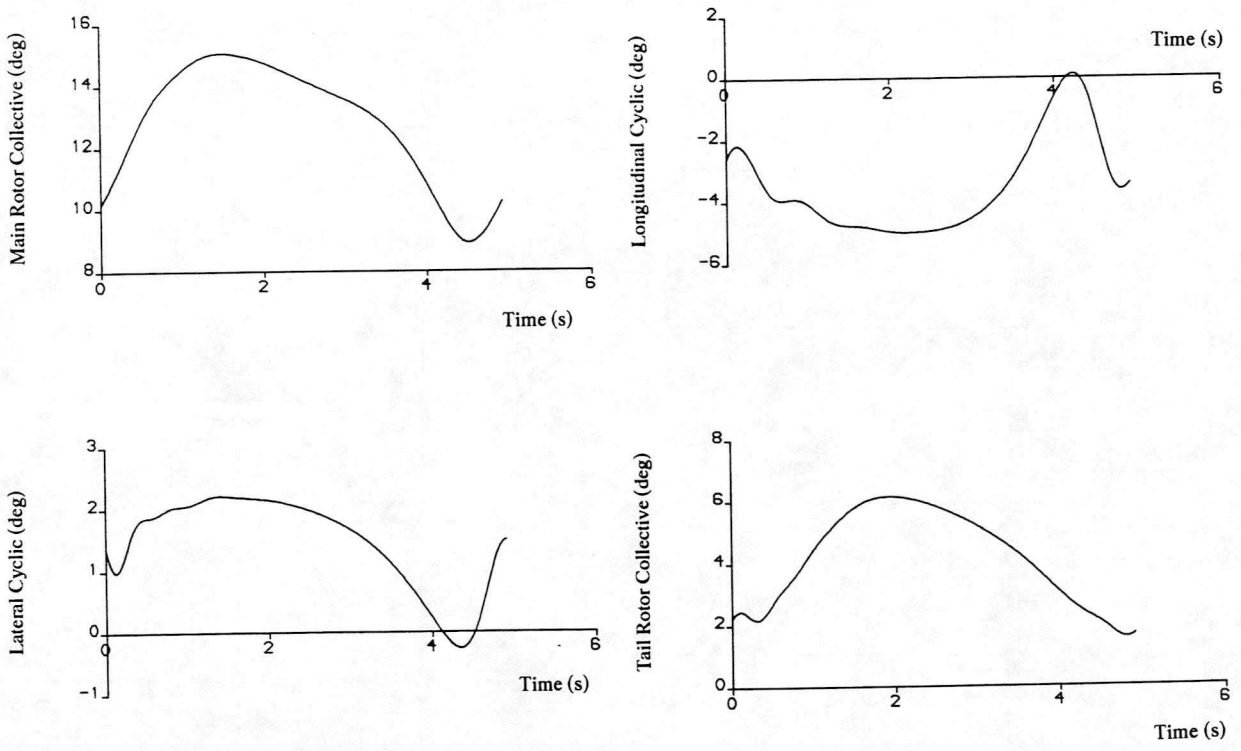

Figure 22 : Control Displacements from Inverse Simulation of Lynx Flying a Pop-up Manoeuvre (s = 200m, h = 25m, V = 80knots)

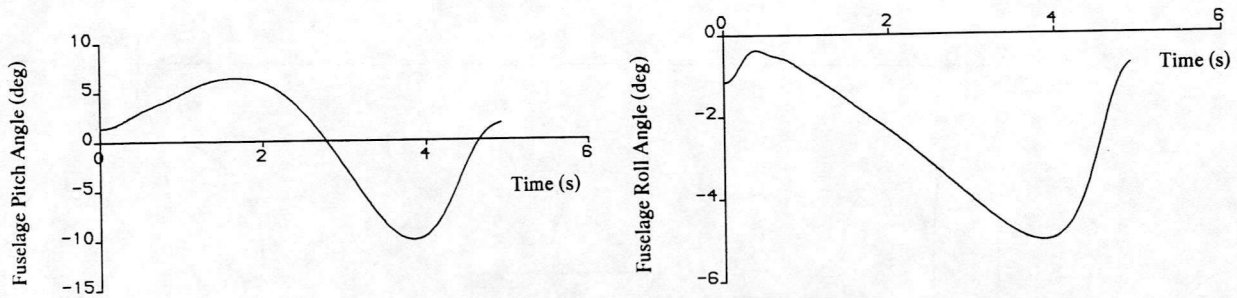

Figure 23 : Fuselage Attitude Angles from Inverse Simulation of Lynx Flying a Pop-up Manoeuvre (s = 200m, h = 25m, V = 80knots)

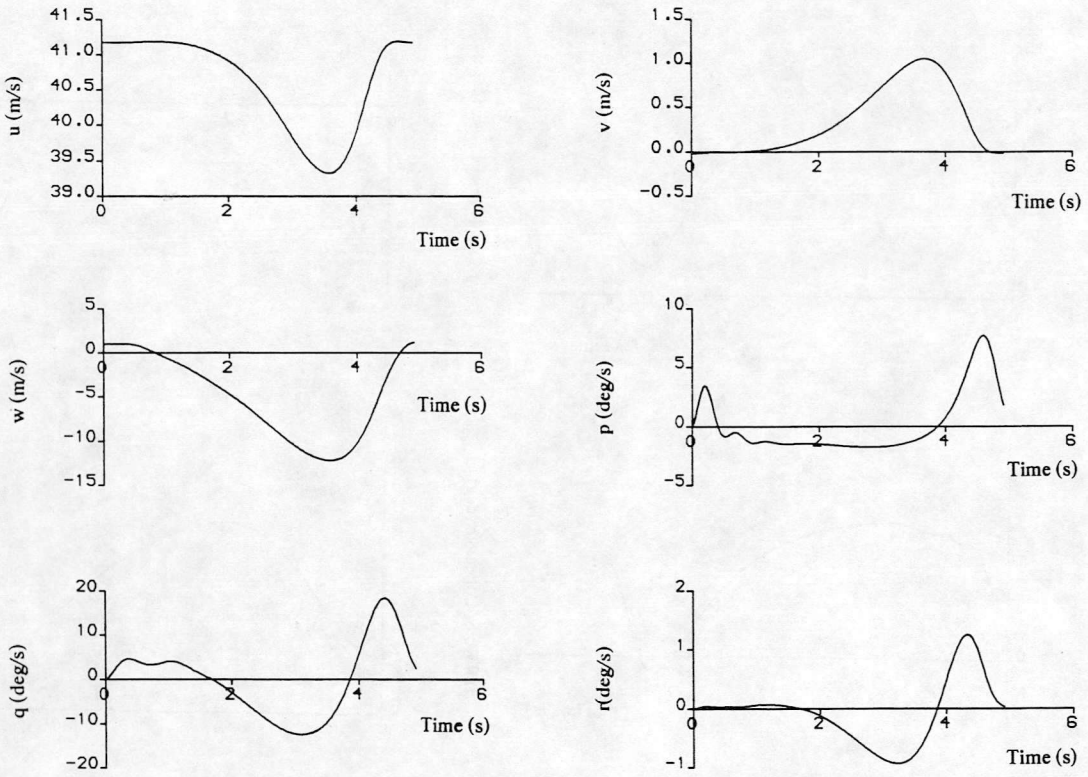

Figure 24 : Body Velocities from Inverse Simulation of Lynx Flying a Pop-up Manoeuvre (s = 200m, h = 25m, V = 80knots)

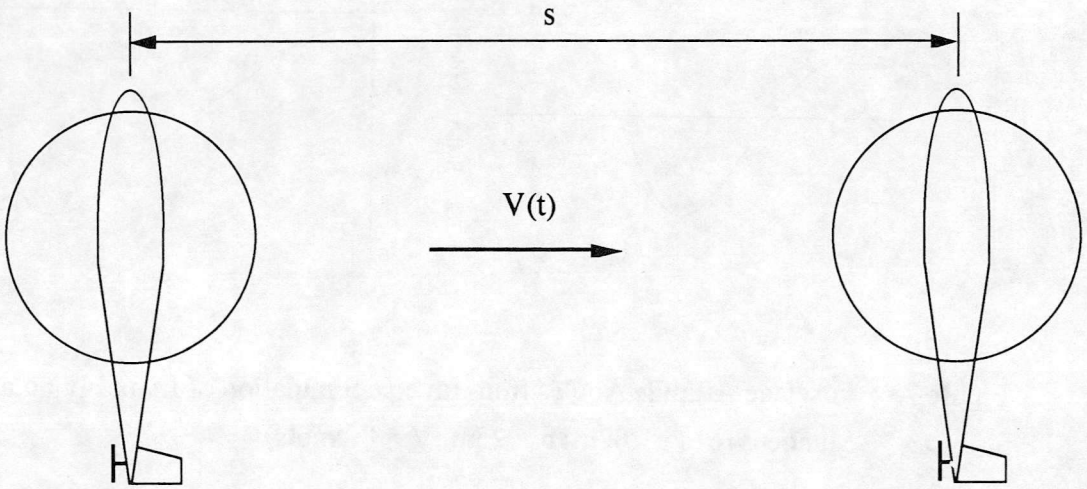

Figure 25 : The Side-step Manoeuvre

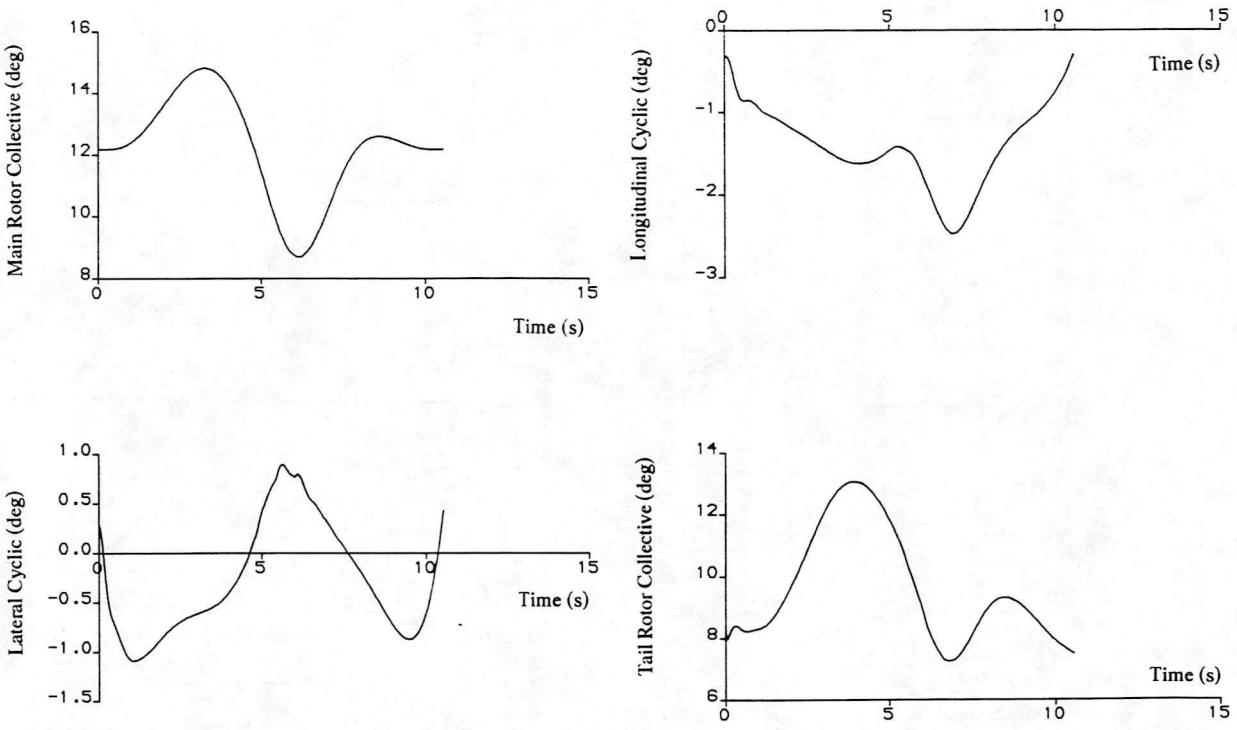

Figure 26 : Control Displacements from Inverse Simulation of Lynx Flying a Side-step Manoeuvre (s = 100m, V_{max} = 40knots)

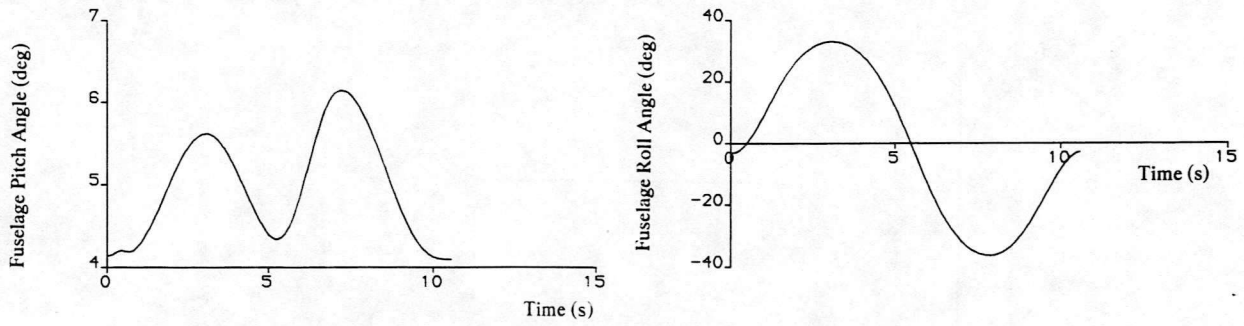

Figure 27 : Fuselage Attitude Angles from Inverse Simulation of Lynx Flying a Side-step Manoeuvre (s = 100m, V_{max} = 40knots)

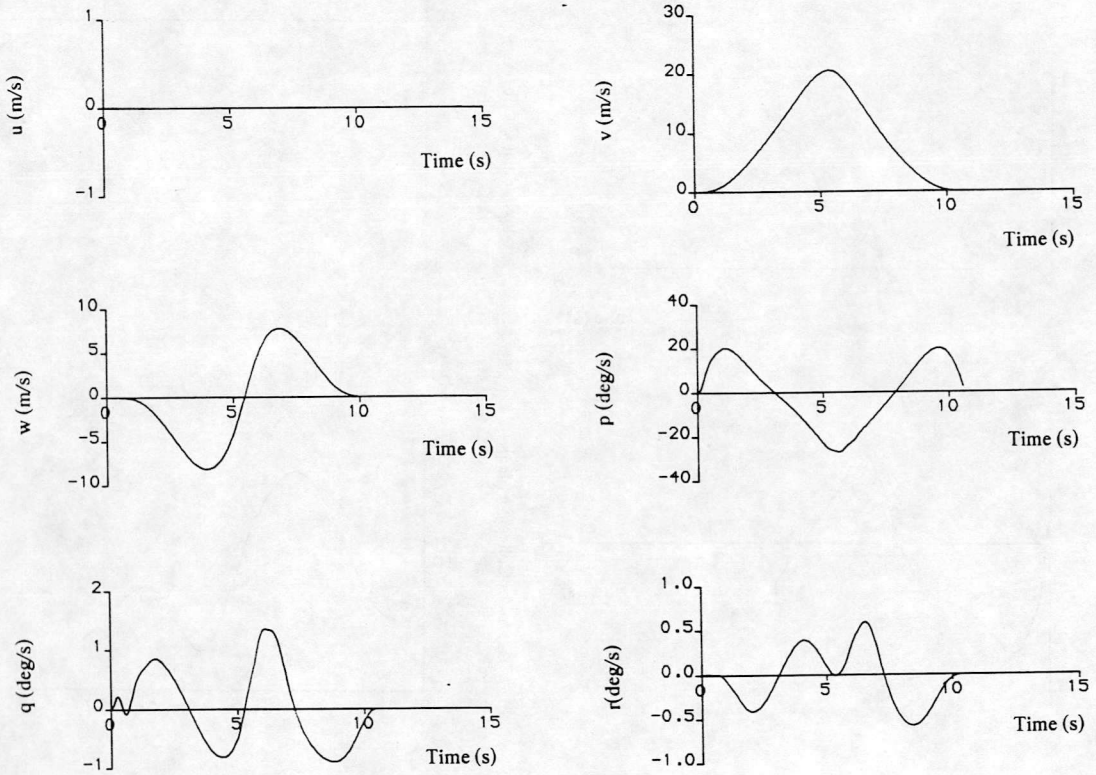

Figure 28 : Body Velocities from Inverse Simulation of Lynx Flying a Side-step Manoeuvre ($s = 100m$, $V_{max} = 40knots$)

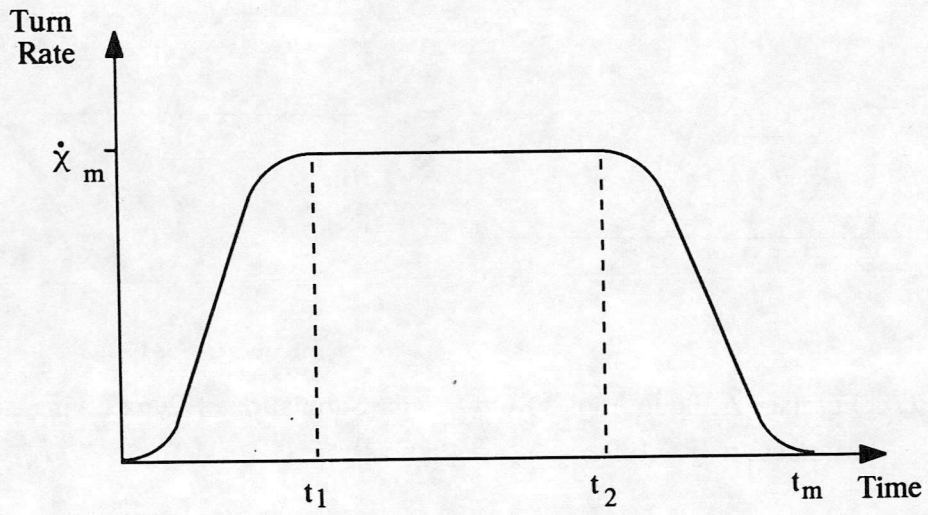

(a) Turn Rate Function

Figure 29 : The Transient Turn Manoeuvre

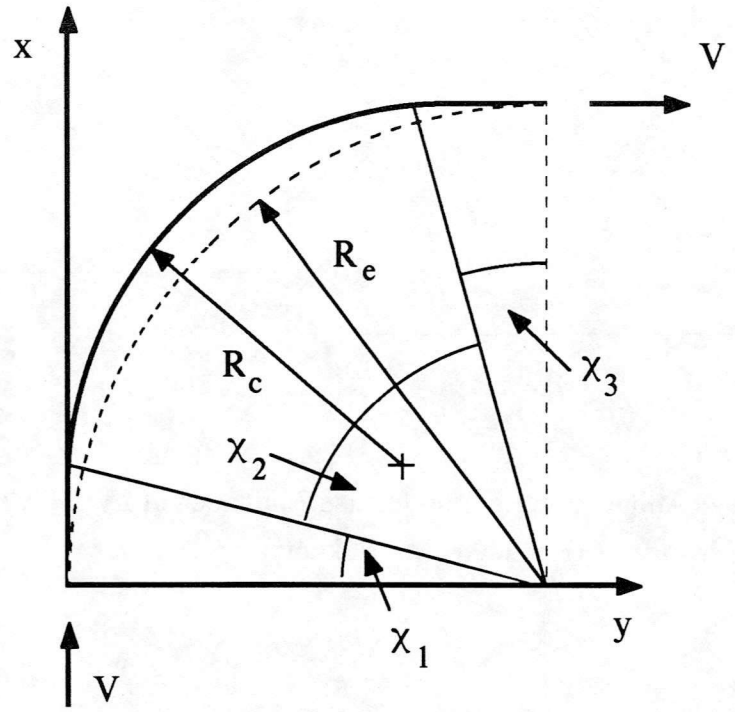

(b) Track

Figure 29 : Continued

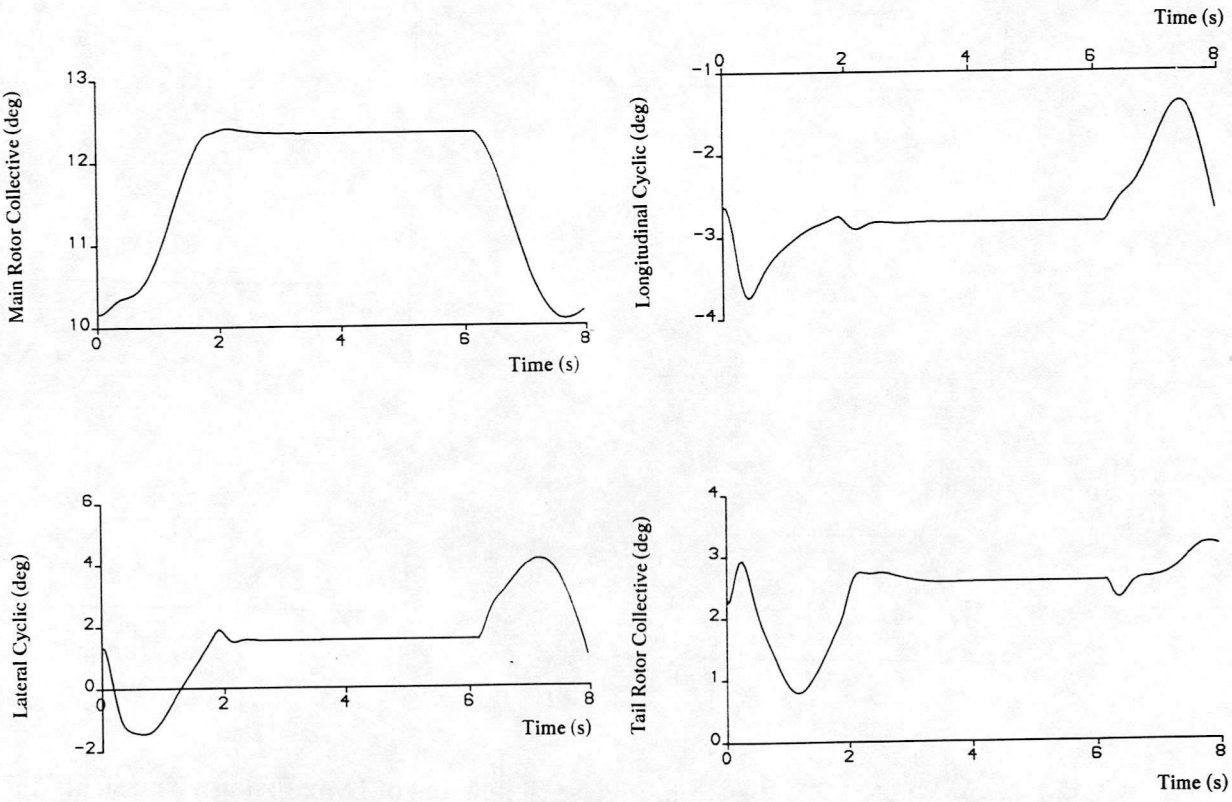

Figure 30 : Control Displacements from Inverse Simulation of Lynx Flying a Transient Turn Manoeuvre (R = 200m, V = 80knots)

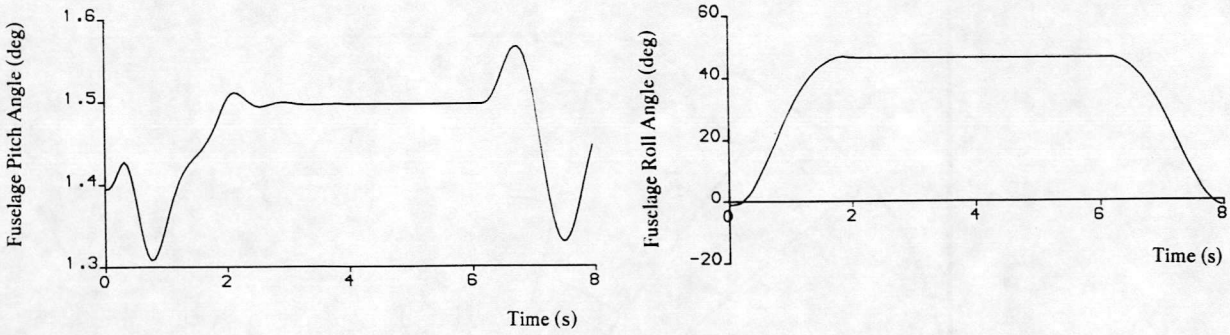

Figure 31 : Fuselage Attitude Angles from Inverse Simulation of Lynx Flying a Transient Turn Manoeuvre (R = 200m, V = 80knots)

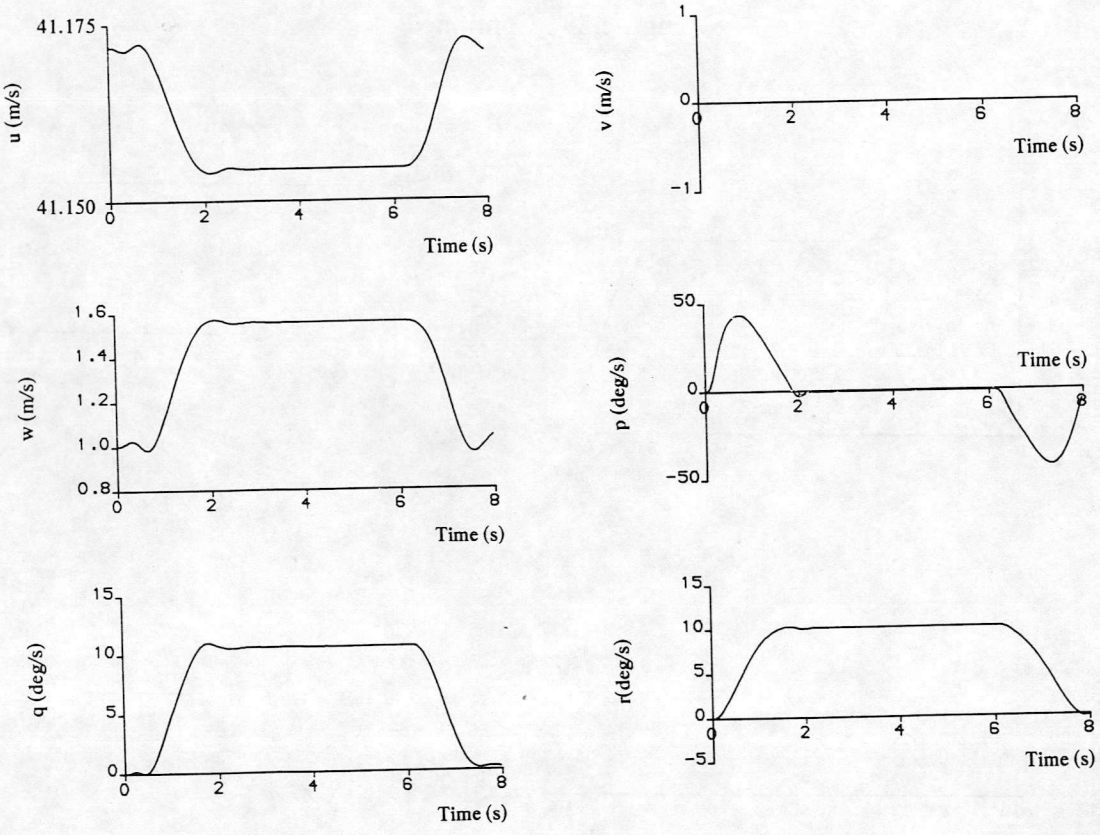

Figure 32 : Body Velocities from Inverse Simulation of Lynx Flying a Transient Turn Manoeuvre (s = 100m, V_{max} = 40knots)

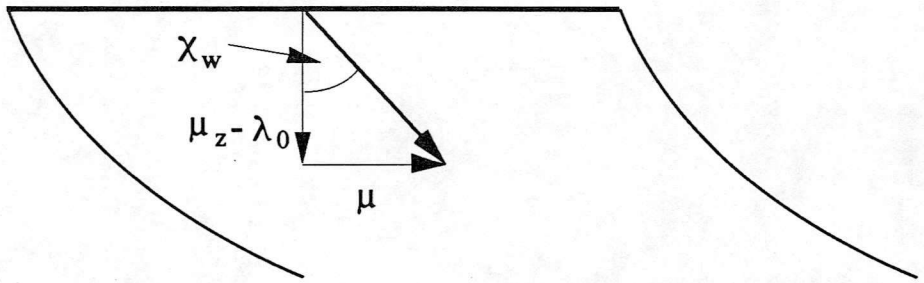

Figure A1(a) : Rotor Wake Angle

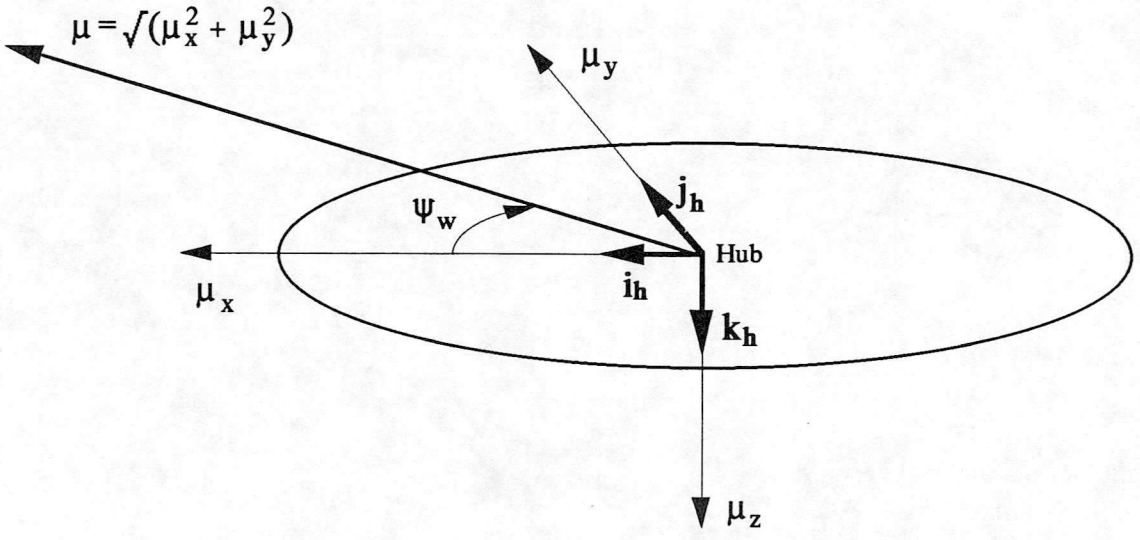

Figure A1(b) : Rotor Sideslip Angle